

Université de Montréal

Hiérarchie de fusion et systèmes T et Y
pour le modèle de boucles diluées $A_2^{(2)}$ sur le ruban

par

Florence Boileau

Département de physique
Faculté des arts et des sciences

Mémoire présenté en vue de l'obtention du grade de
Maître ès sciences (M.Sc.)
en Physique

Orientation Physique mathématique

6 février 2023

Université de Montréal

Faculté des arts et des sciences

Ce mémoire intitulé

**Hierarchie de fusion et systèmes T et Y
pour le modèle de boucles diluées $A_2^{(2)}$ sur le ruban**

présenté par

Florence Boileau

a été évalué par un jury composé des personnes suivantes :

Richard MacKenzie

(président-rapporteur)

Yvan Saint-Aubin

(directeur de recherche)

Luc Vinet

(membre du jury)

Résumé

Les modèles idéalisés, obtenus comme limite continue de modèles finis avec n degrés de liberté, jouent un rôle crucial en mécanique statistique. L'écart entre ces limites et les modèles finis avec n grand est décrit par les corrections de taille finie. Une méthode développée par Klümper et Pearce pour le calcul de telles corrections sur les plus grandes valeurs propres de la matrice de transfert fait intervenir des équations fonctionnelles nommées hiérarchie de fusion et systèmes T et Y. Cette méthode est utilisée dans la recherche de solutions analytiques de modèles intégrables sur réseau. Dans ce mémoire, le modèle de boucles diluées sur le ruban est étudié à partir de cette méthode. Ce travail est le pendant de l'étude faite par A. Morin-Duchesne et P. Pearce (J. Stat. Mech., 2019) du même modèle sur la géométrie du cylindre.

La matrice de transfert $\mathbf{D}(u)$ du modèle de boucles diluées est définie à l'aide des poids de Boltzmann introduits indépendamment par Nienhuis et par Izergin et Korepin. Le paramètre spectral u décrit l'anisotropie des interactions. La matrice de transfert dépend également du paramètre de croisement λ qui est lié au comportement critique. La hiérarchie de fusion et les systèmes T et Y sont obtenus pour λ quelconque et sont des systèmes d'équations infinis. Lorsque $e^{i\lambda}$ est une racine de l'unité, des relations supplémentaires, nommées relations de fermeture, sont obtenues et ces systèmes deviennent alors finis.

Deux familles de conditions frontières respectant l'équation de Yang-Baxter sont connues, offrant ainsi deux choix pour chaque côté du ruban. Les résultats mentionnés plus haut tiennent pour les quatre choix et sont énoncés de façon uniforme. De plus, la matrice de transfert $\mathbf{D}(u)$ de ce modèle de boucles peut être vue comme un élément de l'algèbre de Temperley-Lieb diluée $\mathbf{dTL}_N(\beta)$ et les résultats sont obtenus directement dans $\mathbf{dTL}_N(\beta)$, plutôt que dans une représentation. Finalement, la hiérarchie de fusion permet le calcul des premiers termes, dans le développement des corrections de taille finie, pour les énergies libres de *bulk* et de surface. La résolution analytique est en accord avec des résultats numériques pour de petits réseaux.

Mots-clés : modèles de boucles diluées, algèbre de Temperley-Lieb diluée, modèles intégrables sur réseau, hiérarchie de fusion, systèmes T et Y, corrections de taille finie.

Abstract

Models obtained as the continuum limit of finite models with n degrees of freedom play a crucial role in statistical mechanics. The gap between those continuum limits and the large n models is described by the finite-size corrections. Klümper and Pearce introduced an analytic method to obtain those corrections for the leading eigenvalues of the transfer matrix. This method applies to solvable lattice models and requires to establish functional equations named fusion hierarchy and T- and Y-systems. In this master's thesis, the dilute loop model on the strip is investigated with this method. This work is analogous to what was done by Morin-Duchesne and Pearce (J. Stat. Mech., 2019) for the same loop model, but defined instead on the cylinder.

The transfer matrix $\mathbf{D}(u)$ for this loop model is defined with Boltzmann weights that were introduced independently by Nienhuis and by Izergin et Korepin. The spectral parameter u describes the lattice anisotropy. The transfer matrix also depends on a crossing parameter λ which is related to the critical behaviour of the model. We obtain the fusion hierarchy and the T- and Y-systems for a general λ ; they then form an infinite systems of equations. When $e^{i\lambda}$ is instead a root of unity, additional relations, the closure relations, are derived and turn the previous results into finite systems of equations.

Two families of boundary conditions are known to satisfy the boundary Yang-Baxter equation. This produces two possible choices for each boundary of the strip. The results stated above hold for all four choices and are expressed uniformly with respect to the boundary condition. Moreover, the transfer matrix $\mathbf{D}(u)$ itself can be understood as an element of the dilute Temperley-Lieb algebra $\text{dTL}_N(\beta)$. With this interpretation, the functional equations are obtained directly in the algebra instead of in a particular representation. Finally, the fusion hierarchy allows us to compute the leading terms, in the finite-size corrections expansion, for the bulk and boundary free energies. These are found to be in agreement with numerical data obtained for small systems.

Key words: dilute loop models, dilute Temperley-Lieb algebra, solvable lattice models, fusion hierarchy, T- and Y-systems, finite-size corrections.

Table des matières

Résumé	3
Abstract	4
Table des figures	7
Table de notation	8
Remerciements	10
1 Introduction	12
1.1 Une matrice de transfert en mécanique statistique	13
1.2 La matrice de transfert du modèle de boucles denses	15
1.2.1 La définition diagrammatique de l'algèbre $\mathrm{TL}_N(\beta)$ et la représentation ρ	16
1.2.2 Modèle de boucles denses	18
1.2.3 Lien avec la mécanique statistique	19
1.3 Hiérarchie de fusion et développement en $1/N$	21
2 Fusion hierarchies, T-systems and Y-systems for the dilute $A_2^{(2)}$ loop models on a strip	24
2.1 Introduction	24
2.2 The dilute Temperley-Lieb algebra	27
2.2.1 Definition of the algebra	27
2.2.2 Standard modules	28
2.3 Integrable face and boundary operators	30
2.3.1 Definition of the operators	30
2.3.2 Diagrammatic properties of the face operator	31

2.3.3	Diagrammatic properties of the boundary operators	34
2.4	Commuting transfer matrices	39
2.4.1	Fundamental transfer tangle	40
2.4.2	Fusion hierarchy of fused transfer tangles $\mathbf{D}^{m,n}(u)$	43
2.4.3	Diagrammatic definition of $\mathbf{D}^{2,0}(u)$ and $\mathbf{D}^{1,1}(u)$	47
2.4.4	Determinantal form of the fused tangles	50
2.4.5	Reduction relations	53
2.4.6	Braid limits	56
2.4.7	T -system and Y -system	57
2.5	Polynomiality of the fused transfer matrices	59
2.5.1	Polynomiality of $\mathbf{D}^{2,0}(u)$ and $\mathbf{D}^{1,1}(u)$	59
2.5.2	Polynomiality of $\mathbf{D}^{m,0}(u)$	62
2.5.3	Polynomiality of $\mathbf{D}^{m,n}(u)$	67
2.6	Closure at roots of unity	68
2.6.1	Results and skeleton of the proof	68
2.6.2	Symmetries at roots of unity	70
2.6.3	Evaluations at finite points	72
2.6.4	Evaluation at infinity	74
2.6.5	Closure of the Y -system	78
2.7	Free energies	80
2.8	Conclusion	87
2.A	Proofs of properties of the fused transfer matrices	88
2.A.1	Proof of the crossing symmetry of $\mathbf{D}^{m,n}(u)$ and $\det(m,n)(u)$	89
2.A.2	Proof of the conjugacy of $\mathbf{D}^{m,n}(u)$ and $\det(m,n)(u)$	91
2.A.3	Proof of the T -system relations	92
2.A.4	Closure relations for $b = 2$ and $b = 3$	95
3	Conclusion	101
	Bibliographie	103

Table des figures

1.1	Diagramme de phase d'un matériau ferromagnétique.	13
1.2	Construction d'un graphe et d'un motif de boucles pour le modèle de Q -Potts.	20
2.1	Largeur du polynôme de Laurent en $z = e^{iu}$ pour les matrices fusionnées $\mathbf{D}^{m,n}(u)$ avec des conditions frontières identiques.	43
2.2	Zéros de la valeur propre fondamentale de $\mathbf{D}(u)$ et approximations de taille finie pour l'énergie libre du <i>bulk</i> et de surface avec des conditions frontières SC pour $\lambda = \frac{\pi}{10}$	83
2.3	Zéros de la valeur propre fondamentale de $\mathbf{D}(u)$ et approximations de taille finie pour l'énergie libre du <i>bulk</i> et de surface avec des conditions frontières SS pour $\lambda = \frac{\pi}{10}$	85
2.4	Zéros de la valeur propre fondamentale de $\mathbf{D}(u)$ et approximations de taille finie pour l'énergie libre du <i>bulk</i> et de surface avec des conditions frontières SC pour $\lambda = \frac{\pi}{10}$	85

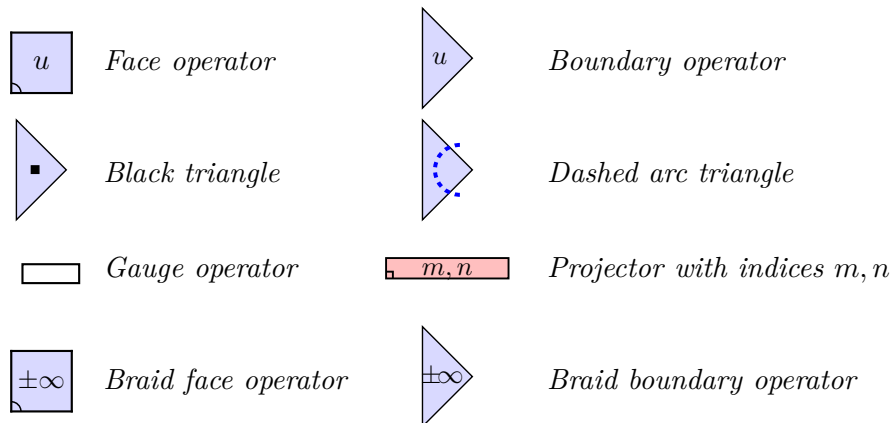
Table de notation

Cette table de notation s'applique principalement au Chapitre 2. Si certains symboles sont communs aux Chapitres 1 et 2 et y ont des significations différentes, des indications plus précises sont données. Les symboles et abréviations sont d'abord présentés et les principaux opérateurs diagrammatiques sont ensuite listés. Tous ces éléments sont ordonnés par ordre d'apparition dans le Chapitre 2.

RSOS	<i>Restricted Solid-on-Solid</i>
CFT	<i>Conformal Field Theory</i>
c, Δ	Charge centrale et poids conforme de l'algèbre de Virasoro
N	Paramètre de taille d'un réseau
$\text{TL}_N(\beta), \text{dTL}_N(\beta)$	Algèbres de Temperley-Lieb originale et diluée respectivement
\mathbf{I}	Identité de l'algèbre de Temperley-Lieb originale ou diluée selon le cas
\mathcal{W}_N^d	Module standard pour $\text{dTL}_N(\beta)$ avec d défauts
$u, z = e^{iu}$	Paramètre spectral et variable qui lui est associée pour les expressions polynomiales
$\lambda, x = e^{i\lambda}$	Paramètre de croisement et variable qui lui est associée pour les expressions polynomiales
$\rho_i(u)$	Poids de la tuile élémentaire i pour le <i>face operator</i> , voir (2.3.2)
$\beta = -2 \cos(4\lambda)$	Fugacité des boucles pour le modèle de boucles diluées
S, C	Notation indiquant une condition frontière de type sinus ou cosinus
$\delta(u), \bar{\delta}(u)$	Poids pour les tuiles élémentaires du <i>boundary operator</i> , voir (2.3.5)
u_k	Notation pour $u + k\lambda$
$s(\alpha u_k), c(\alpha u_k)$	Notation pour $\sin(\alpha(u + k\lambda))$ et $\cos(\alpha(u + k\lambda))$ respectivement
$\xi_{(j)}$	Inhomogénéité de la colonne j pour la matrice de transfert
$\tilde{\mathbf{D}}(u)$	Matrice de transfert diagrammatique, voir (2.4.1)
$\mathbf{D}(u)$	Matrice de transfert de base (et réduite s'il y a lieu, c'est-à-dire sans facteur connu), voir (2.4.3)
$f(u)$	Fonction de poids du <i>bulk</i> pour la hiérarchie de fusion, voir (2.4.6)
$\max P$	Largeur maximale d'un polynôme de Laurent en z (et centré)
$w(u), \bar{w}(u), w^{(m)}(u), \bar{w}^{(n)}(u)$	Fonctions de poids des frontières pour la hiérarchie de fusion, voir le Tableau 2.1

α^i, β^j	Coefficients de la hiérarchie de fusion usuelle (relation récursive à trois termes) pour $\mathbf{D}^{m,n}(u)$, voir (2.4.13)
$\psi = (4 - 2m - 2n)\lambda - u$	Paramètre de symétrie de croisement des matrices fusionnées
$\mathbf{D}^{m,n}(u)$	Matrice fusionnée d'indices $m, n \geq 1$, voir (2.4.15)
$Z^{2,0}(u), Z^{1,1}(u)$	Fonctions contenant les zéros connus de matrices de transfert diagrammatiques, voir (2.4.19)
$\mathcal{D}(u), \mathcal{F}(u)$	Poids utilisés dans la construction des déterminants formels, voir (2.4.26)
$\det(m, n)(u)$	Déterminant formel pour la matrice fusionnée $\mathbf{D}^{m,n}(u)$, voir Section 2.4.4
μ^i, ν^j	Coefficients pour la relation récursive à quatre termes pour $\mathbf{D}^{m,0}(u)$ ou $\mathbf{D}^{0,n}(u)$, voir (2.4.36)
$\mathbf{D}_{\infty}^{m,n}$	Limite de tresse de la matrice fusionnée $\mathbf{D}^{m,n}(u)$, voir (2.4.52)
$\mathbf{d}^m(u)$	Fonctions construites à partir de matrices fusionnées pour le système Y, voir (2.4.58)
τ^i	Coefficients pour la relation récursive à cinq termes pour $\mathbf{D}^{m,0}(u)$ ou $\mathbf{D}^{0,n}(u)$, voir (2.5.17)
η^i	Coefficients du système T après simplifications, voir (2.5.35)
$\lambda_{a,b} = \frac{(b-a)\pi}{2b}$	Paramètre λ à la racine de l'unité, pour $a, b \in \mathbb{Z}$ et $\gcd(a, b) = 1$
$U(u), V(u)$	Produits de poids frontières spécifiques à l'égalité de fermeture, voir (2.6.2)
κ	Facteur numérique spécifique à l'égalité de fermeture, voir (2.6.2)
$\mathcal{J}(u), \mathcal{P}(u)$	Polynômes avec plusieurs symétries pour l'égalité de fermeture, voir (2.6.6)
$D(u)$	Désigne une des plus grandes valeurs propres de $\mathbf{D}(u)$
$f_{\text{bulk}}(u), f_{\text{bdy}}(u)$	Premiers termes dans le développement des corrections de taille finie pour les énergie libres du <i>bulk</i> et de surface respectivement

Les principaux opérateurs diagrammatiques du Chapitre 2 sont les suivants.



Remerciements

Mille mercis vont à mon directeur de recherche Yvan Saint-Aubin. Il est difficile d'écrire ce paragraphe sans répéter ce que plusieurs ont déjà dit, tant Yvan est apprécié de ses étudiants. Sa disponibilité hors du commun et ses encouragements ont été pour moi des éléments cruciaux dans la réussite de ce projet. Cela d'autant plus que cette maîtrise s'est déroulée partiellement en temps de pandémie et a dévié de trajectoire pendant une courte incursion au doctorat. Merci Yvan d'apporter toujours autant de soin et de rigueur dans tes relectures, même lorsqu'il s'agit de premières versions de preuves cryptiques. Finalement, merci pour ta considération dans les relations humaines entourant la science, j'espère retenir un peu de ta sagesse !

Alexi Morin-Duchesne a une grande part de crédit dans la réussite de ce projet de maîtrise. C'est suite à une de ses visites à l'Université de Montréal que le sujet actuel a été fixé. Merci Alexi pour cette opportunité et pour la collaboration dans la recherche et la rédaction de l'article. Ton énergie et ton enthousiasme ont été essentiels dans les derniers mois du projet.

Je suis reconnaissante envers Éric Dupuis et Julien Gaboriaud qui toujours pris le temps de répondre à mes questions, et ce, qu'ils soient auxiliaires d'enseignement ou non. Merci pour votre enthousiasme, rigueur et grande gentillesse. Ce fut agréable de discuter de physique avec vous.

J'aimerais maintenant saluer plusieurs personnes que j'ai côtoyées avec plaisir à l'université. Je pense en particulier à ma cohorte de physique qui a aussi fait office de deuxième famille pendant les années du bac. Gabriel, ta capacité à calculer les symétries d'un solide en toutes circonstances demeure inégalée. Je me retiens de ne pas accompagner ce texte d'une preuve appropriée... Léandre, la littérature consultée en préparation à ce mémoire m'indique que le thème musical de la première saison de *The Wire* est bel et bien le meilleur. Je rajoute un théorème à ce sujet à l'instant. Lucie, merci pour la folie essentielle que tu as ajoutée au bac, surtout pendant ces innombrables soirées passées à travailler à la Planck. Finalement, je me souviens avec joie des (pas assez nombreuses) discussions sur le balcon avec Leire. À vous et à tous les autres, merci pour les bons moments !

Merci à mes parents pour leur support inconditionnel.

Merci au Département de Physique pour son financement pendant toute la durée de ce projet.

J'aimerais profiter de cette tribune encore quelques instants. Un collègue a écrit le passage suivant dans

sa thèse, qui me semble tellement juste et décrit bien ce que je souhaite améliorer s'il m'arrive de faire de la recherche dans le futur : «Pour ne pas freiner la créativité, je fais voeu de toujours trouver belle l'idée d'échouer et de changer d'avis en science.» Merci à Charles Bédard pour ces sages paroles.

Chapitre 1

Introduction

Les matrices de transfert jouent un rôle-clé en matière condensée et, en particulier, dans la résolution de modèles visant à décrire les transitions de phase. L'étude du comportement au point critique de nombreux modèles classiques peut être faite grâce à cet outil. Les matrices de transfert peuvent entre autres être utilisées pour le modèle d'Ising en une et deux dimensions (le livre de Baxter donne plusieurs exemples supplémentaires). L'idée derrière cette méthode est de réexprimer la fonction de partition comme une multiplication matricielle, faisant en sorte que son calcul revient à obtenir la trace de l'opérateur.

Une hypothèse bien acceptée est que dans la limite thermodynamique, plusieurs modèles statistiques sont invariants sous transformations conformes au point critique. Soit N un paramètre de taille d'un modèle. Une méthode développée par Klümper et Pearce permet de calculer analytiquement un développement en $1/N$ des plus grandes valeurs propres de la matrice de transfert et d'obtenir la charge centrale c et les poids conformes Δ qui caractérisent ce modèle. Cette méthode a comme point de départ plusieurs équations fonctionnelles nommées hiérarchie de fusion, systèmes T et Y et relations de fermeture.

Remarquablement, une grande classe de modèles statistiques sont aussi liés aux algèbres de Temperley-Lieb, et leurs généralisations, et aux modèles dits *de boucles*.

Cette introduction présente, sur des exemples simples, des notions et outils utilisés dans l'article du Chapitre 2. Une introduction à la matrice de transfert dans un contexte de mécanique statistique est en Section 1.1. Ensuite, un premier modèle de boucles et son lien avec les modèles statistiques sont discutés en Section 1.2. Finalement, une revue historique de la méthode de Klümper et Pearce pour obtenir le développement en $1/N$ est en Section 1.3.

1.1 Une matrice de transfert en mécanique statistique

Soit un matériau ferromagnétique dans un environnement de température T et plongé dans un champ magnétique H . Les constituants de ce matériau ont des spins et la quantité qui caractérise leur alignement est la magnétisation moyenne $M(H, T)$. La Figure 1.1 présente des résultats empiriques pour cette magnétisation moyenne avec des unités telles que $M(H, T)$ est dans l'intervalle $[-1, +1]$. Sur cette figure, la température $T < T_C$ est fixée le long de la trajectoire 1. La magnétisation y est non nulle, et ce, même en $H = 0$ où il y a une discontinuité. En effet, pour un matériau de type ferromagnétique, les spins tendent à avoir une cohérence malgré l'absence de champ (c'est la magnétisation spontanée). Lorsque la température est augmentée, la magnétisation spontanée devient de plus en plus basse, jusqu'à être nulle. Ceci est illustré le long de la trajectoire 2, où une singularité demeure tout de même présente dans la pente de la magnétisation en fonction du champ $M(H, T_C)$. La température limite de la trajectoire 2 est appelée *température critique* T_C . Finalement, si T est augmentée au-delà de T_C , la magnétisation selon le champ devient une fonction lisse. Le changement de comportement entre le fait de posséder une magnétisation spontanée, ou non, est une transition de phase.

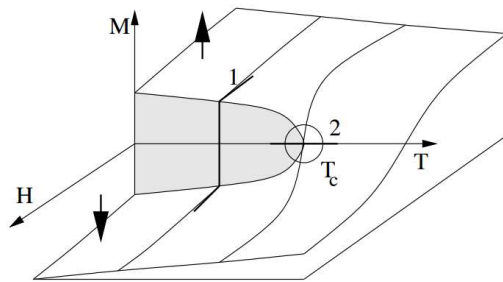


FIGURE 1.1 – Diagramme de phase de la magnétisation M d'un matériau ferromagnétique en fonction du champ H et de la température T (il est supposé que le champ magnétique appliqué est dans le même axe que M) [36].

Le modèle d'Ising est un modèle sur réseau visant à reproduire l'interaction inter-particulaire menant à une transition de phase telle que celle discutée ci-haut, tout en demeurant assez simple pour être résoluble analytiquement. Ses principales caractéristiques sont que les particules représentant les spins prennent des valeurs discrètes, et que les interactions sont limitées aux particules avoisinantes. Ce modèle a été introduit par Wilhelm Lenz en 1920, et sa version en une dimension a été résolue pour la première fois par Ernst Ising en 1925 dans sa thèse sous la supervision de Lenz [34]. Le modèle en une dimension ne possède pas de comportement critique pour $T > 0$, mais est une bonne introduction aux techniques utilisées en deux dimensions. La suite de la présente section contient une résolution sommaire du modèle en une dimension. Cette résolution suit ce qui est fait dans [35].

Soit une chaîne de N particules équidistantes. Chacune est notée comme μ_i et est contrainte de prendre une valeur dans l'ensemble $\{-1, +1\}$, ce qui représente son spin. Un état du système μ est donc un choix d'état pour chaque particule. Une condition frontière périodique est choisie pour la chaîne : $\mu_{N+1} = \mu_1$.

L'interaction entre les spins est restreinte aux proches voisins et l'énergie d'une configuration est :

$$E(\mu) = -J \sum_{i=1}^N \mu_i \mu_{i+1} - H \sum_{i=1}^N \mu_i , \quad (1.1.1)$$

où la constante J exprime le couplage entre les spins et H est le champ magnétique externe. Avec $J > 0$, la configuration de plus petite énergie est celle où tous les spins sont orientés dans une même direction, ce qui correspond à du ferromagnétisme. Le problème de mécanique statistique est d'évaluer la fonction de partition

$$Z = \sum_{\{\mu\}} \exp(-\beta E(\mu)) , \quad \beta = \frac{1}{k_B T} . \quad (1.1.2)$$

Des manipulations algébriques simples permettent d'exprimer Z comme une multiplication successive de facteurs $\Lambda(\mu_i, \mu_{i+1})$. Avec $j = J/k_B T$ et $h = H/k_B T$:

$$Z = \sum_{\{\mu\}} \prod_{i=1}^N \exp\left(j\mu_i \mu_{i+1} + \frac{h}{2}(\mu_i + \mu_{i+1})\right) = \sum_{\{\mu\}} \Lambda(\mu_1, \mu_2) \Lambda(\mu_2, \mu_3) \dots \Lambda(\mu_N, \mu_1) . \quad (1.1.3)$$

L'étape clé de la résolution est d'envisager ces facteurs $\Lambda(\mu_i, \mu_{i+1})$ comme des éléments de la matrice :

$$\Lambda = \begin{pmatrix} \exp(j+h) & \exp(-j) \\ \exp(-j) & \exp(j-h) \end{pmatrix} . \quad (1.1.4)$$

La matrice Λ est appelée la *matrice de transfert*. Puisque la somme dans (1.1.3) est sur tous les états μ , effectuer celle-ci revient à calculer

$$Z = \text{Tr}(\Lambda^N) = \sum_k \lambda_k^N , \quad (1.1.5)$$

où les λ_k sont les valeurs propres de la matrice Λ et l'indice k prend ses valeurs dans l'ensemble $\{1, 2\}$ puisque Λ est de dimension 2. Le problème d'évaluer la fonction de partition a donc été simplifié au problème de diagonaliser la matrice Λ . En une dimension, il est direct d'obtenir

$$\lambda_{1,2} = e^j \cosh(h) \pm \sqrt{e^{2j} \sinh^2(h) + e^{-2j}} . \quad (1.1.6)$$

L'énergie libre dans la limite thermodynamique est donnée par

$$f = -k_B T \lim_{N \rightarrow \infty} \frac{\log(Z_N)}{N} . \quad (1.1.7)$$

Avec $Z_N = \lambda_1^N + \lambda_2^N$ et le fait que $0 < \lambda_2/\lambda_1 < 1$ si $j > 0$, il suit

$$\lim_{N \rightarrow \infty} \frac{\log(Z_N)}{N} = \lim_{N \rightarrow \infty} \left[\log(\lambda_1) + \frac{1}{N} \log\left(1 + \left(\frac{\lambda_2}{\lambda_1}\right)^N\right) \right] = \log(\lambda_1) . \quad (1.1.8)$$

La plus grande valeur propre domine donc le comportement du modèle pour $N \rightarrow \infty$. Pour terminer, la magnétisation est obtenue à partir de l'énergie libre :

$$M(H, T) = \frac{\partial f}{\partial H} = \frac{\sinh(h)}{\sqrt{\sinh^2(h) + e^{-4j}}} . \quad (1.1.9)$$

Lorsque $h = 0$, la magnétisation est nulle pour toute température positive et finie. Le modèle ne peut donc pas donner lieu à une magnétisation spontanée.

La généralisation du formalisme de la matrice de transfert en deux dimensions est directe. Soit un réseau quadrillé apposé sur un cylindre. Les sites sont étiquetés par des indices (i, j) tels que $1 \leq i \leq M$ et $1 \leq j \leq N$ et la périodicité s'exprime par $\mu_{i, N+1} = \mu_{i, 1}$. Avec une interaction de type proche voisin et sans champ magnétique, l'énergie d'une configuration μ est :

$$E(\mu) = -J \sum_{i=1}^{M-1} \sum_{j=1}^N \mu_{i,j} \mu_{i+1,j} - J \sum_{i=1}^M \sum_{j=1}^N \mu_{i,j} \mu_{i,j+1} . \quad (1.1.10)$$

Pour retrouver une notation proche de (1.1.3), la configuration d'une colonne est exprimée :

$$\sigma_j = \{\mu_{1,j}, \mu_{2,j}, \dots, \mu_{M,j}\} . \quad (1.1.11)$$

Des manipulations similaires à ce qui a été fait en une dimension mènent ensuite à

$$Z = \sum_{\{\sigma_j\}} \Lambda(\sigma_1, \sigma_2) \Lambda(\sigma_2, \sigma_3) \dots \Lambda(\sigma_N, \sigma_1) = \text{Tr}(\Lambda^N) . \quad (1.1.12)$$

En deux dimensions, Λ est une matrice $2^M \times 2^M$ qui contient tous les poids de Boltzmann liés aux interactions entre les spins d'une colonne et entre deux colonnes successives. Puisque le modèle est étudié dans la limite $M, N \rightarrow \infty$, le problème de la diagonalisation demeure très difficile. Pour le modèle d'Ising en deux dimensions sur réseau carré, la solution a été trouvée par Onsager en 1944 et est considérée comme la première démonstration non-triviale de l'existence d'une transition de phase à partir du calcul de la fonction de partition seulement.

1.2 La matrice de transfert du modèle de boucles denses

L'appellation *modèles de boucles* réfère à une famille de modèles planaires construits à l'aide de courbes reliant certains sites déterminés. Ces modèles sont liés à plusieurs familles d'algèbres de Temperley-Lieb, un ensemble de courbes pouvant être envisagé comme un élément de l'algèbre. Cette section est une introduction aux modèles de boucles, à leur lien avec l'algèbre de Temperley-Lieb et à leur place en mécanique statistique. Afin que la discussion soit courte mais précise, seul le modèle le plus simple est présenté, soit celui de boucles denses pour la géométrie du ruban. En effet, les idées sous-jacentes

sont similaires pour les autres modèles de boucles, mais les objets mathématiques n'y sont pas aussi simples. La première étape est la définition de l'algèbre de Temperley-Lieb.

1.2.1 La définition diagrammatique de l'algèbre $\text{TL}_N(\beta)$ et la représentation ρ

Pour $N \in \mathbb{N}$ et $\beta \in \mathbb{C}$, l'algèbre de Temperley-Lieb est une algèbre associative et unitaire définie à partir des générateurs et des relations suivants :

$$\text{TL}_N(\beta) = \langle \mathbf{I}, e_j \mid j \in \{1, 2, \dots, N-1\} \rangle, \quad (1.2.1a)$$

$$e_j^2 = \beta e_j, \quad e_j e_{j\pm 1} e_j = e_j, \quad e_i e_j = e_j e_i \quad (|i-j| > 1). \quad (1.2.1b)$$

Il est possible de donner une définition diagrammatique de cette algèbre (voir [37] pour une revue pédagogique). Pour $N \in \mathbb{N}$, dessiner un rectangle avec N points sur sa bordure supérieure et N autres sur sa bordure inférieure. Une *connectivité* est un tel rectangle, où les points sont joints deux-à-deux par des courbes qui ne s'intersectent pas. Un exemple de connectivité avec $N = 6$ est

$$c_1 = \text{Diagram} \quad (1.2.2)$$

Pour N donné, le nombre de connectivités est $C_N = \frac{1}{N+1} \binom{2N}{N}$, qui est le n -ième nombre de Catalan. Un espace vectoriel E_N est défini comme toutes les combinaisons linéaires formelles sur \mathbb{C} de ces connectivités. Cet espace vectoriel est alors de dimension C_N .

Pour la structure d'algèbre, il faut aussi un produit $\circ : E_N \times E_N \rightarrow E_N$. Soit c_1 et c_2 , deux connectivités, et $\beta \in \mathbb{C}$. Le produit $c_1 \circ c_2$ est obtenu en apposant c_2 au-dessus de c_1 . Le résultat peut être lu directement comme la connectivité entre les points du dessus de c_2 et les points du bas de c_1 . Si une boucle est fermée, celle-ci est retirée et le résultat est multiplié par β . Par exemple :

$$c_2 = \text{Diagram} \quad , \quad c_1 \circ c_2 = \text{Diagram} = \beta \text{Diagram} \quad (1.2.3)$$

Le produit \circ est associatif, non-commutatif et a une unité, soit le diagramme où chaque point du haut est connecté directement au point au-dessous de lui par un trait vertical. Ce produit peut être étendu linéairement à E_N sur ses deux entrées.

Certains diagrammes peuvent être identifiés aux générateurs abstraits :

$$\mathbf{I} = \text{Diagram} \quad , \quad e_j = \text{Diagram} \quad (1.2.4)$$

Il est alors direct de vérifier les relations (1.2.1b) et il est possible de montrer que l'algèbre définie à

l'aide des diagrammes est isomorphe à celle définie de façon abstraite en (1.2.1).

Pour étudier les modèles statistiques, il est utile d'introduire la *représentation* ρ des diagrammes de $\text{TL}_N(\beta)$. Celle-ci fait intervenir une nouvelle famille de diagrammes appelés vecteurs de connectivités. Soit N points équidistants posés le long d'un segment horizontal. Un *vecteur de connectivité* est un ensemble de courbes sans intersection contraintes à demeurer au-dessus du segment. Tout point est donc connecté à un autre point, ou encore à l'infini. Les segments connectant un point à l'infini sont appelés *défauts* et leur nombre est noté d . Notons que $0 \leq d \leq N$ et que $d \equiv N \pmod{2}$ puisque les courbes n'allant pas à l'infini utilisent un nombre pair des N sites. Pour N donné, l'ensemble des vecteurs de connectivité est noté B_N (de façon analogue, le sous-ensemble des vecteurs à d défauts est noté B_N^d). Voici les vecteurs de connectivité pour $N = 4$:

$$B_4^0 = \left\{ \begin{array}{c} \text{---} \bullet \text{---} \bullet \text{---} \bullet \text{---} \bullet \text{---} \\ \text{---} \bullet \text{---} \bullet \text{---} \bullet \text{---} \bullet \text{---} \\ \text{---} \bullet \text{---} \bullet \text{---} \bullet \text{---} \bullet \text{---} \end{array} \right\}, \quad (1.2.5)$$

$$B_4^2 = \left\{ \begin{array}{c} \text{---} \bullet \text{---} \bullet \text{---} \bullet \text{---} \bullet \text{---} \\ \text{---} \bullet \text{---} \bullet \text{---} \bullet \text{---} \bullet \text{---} \\ \text{---} \bullet \text{---} \bullet \text{---} \bullet \text{---} \bullet \text{---} \end{array} \right\}, \quad B_4^4 = \left\{ \begin{array}{c} \text{---} \bullet \text{---} \bullet \text{---} \bullet \text{---} \bullet \text{---} \\ \text{---} \bullet \text{---} \bullet \text{---} \bullet \text{---} \bullet \text{---} \\ \text{---} \bullet \text{---} \bullet \text{---} \bullet \text{---} \bullet \text{---} \end{array} \right\}.$$

L'espace vectoriel engendré par les éléments de B_N (resp. B_N^d) est formé des combinaisons linéaires formelles sur \mathbb{C} des vecteurs de connectivité et est noté \mathbf{V}_N (resp. \mathbf{V}_N^d). Il suit $\mathbf{V}_N = \bigoplus_{0 \leq d \leq N} \mathbf{V}_N^d$ et il peut être montré que

$$\dim \mathbf{V}_N = \binom{N}{\lfloor N/2 \rfloor}, \quad \dim \mathbf{V}_N^d = \binom{N}{(N-d)/2} - \binom{N}{(N-d)/2 - 1}. \quad (1.2.6)$$

Pour bâtir la représentation ρ , une action des éléments de $\text{TL}_N(\beta)$ sur les vecteurs de connectivité est nécessaire. Soit $c \in \text{TL}_N(\beta)$ et $v \in \mathbf{V}_N$. L'action $c \bullet v$ est obtenue en apposant v au-dessus de c . Comme pour le produit \circ , le vecteur de connectivité résultant est lu directement comme l'ensemble de courbes liées aux points du bas du diagramme. Si une boucle est fermée, celle-ci est retirée et le résultat est multiplié par β . Par exemple :

$$c = \begin{array}{|c|} \hline \text{---} \bullet \text{---} \bullet \text{---} \bullet \text{---} \bullet \text{---} \\ \text{---} \bullet \text{---} \bullet \text{---} \bullet \text{---} \bullet \text{---} \\ \text{---} \bullet \text{---} \bullet \text{---} \bullet \text{---} \bullet \text{---} \\ \hline \end{array}, \quad v = \begin{array}{c} \text{---} \bullet \text{---} \bullet \text{---} \bullet \text{---} \bullet \text{---} \\ \text{---} \bullet \text{---} \bullet \text{---} \bullet \text{---} \bullet \text{---} \\ \text{---} \bullet \text{---} \bullet \text{---} \bullet \text{---} \bullet \text{---} \end{array}, \quad c \bullet v = \begin{array}{|c|} \hline \text{---} \bullet \text{---} \bullet \text{---} \bullet \text{---} \bullet \text{---} \\ \text{---} \bullet \text{---} \bullet \text{---} \bullet \text{---} \bullet \text{---} \\ \text{---} \bullet \text{---} \bullet \text{---} \bullet \text{---} \bullet \text{---} \\ \hline \end{array} = \beta \begin{array}{c} \text{---} \bullet \text{---} \bullet \text{---} \bullet \text{---} \bullet \text{---} \\ \text{---} \bullet \text{---} \bullet \text{---} \bullet \text{---} \bullet \text{---} \\ \text{---} \bullet \text{---} \bullet \text{---} \bullet \text{---} \bullet \text{---} \end{array}. \quad (1.2.7)$$

L'action de chaque connectivité $c \in \text{TL}_N(\beta)$ sur \mathbf{V}_N correspond à un élément de $\text{End}(\mathbf{V}_N)$ et, dans la base B_N , à une matrice notée $\rho(c)$. Par exemple, pour c plus haut :

$$\rho(c) = \begin{pmatrix} \beta & 1 & 1 & 0 & 0 & 0 \\ 0 & 0 & 0 & 0 & 0 & 0 \\ \hline 0 & 0 & 0 & 1 & \beta & 1 \\ 0 & 0 & 0 & 0 & 0 & 0 \\ 0 & 0 & 0 & 0 & 0 & 0 \\ \hline 0 & 0 & 0 & 0 & 0 & 0 \end{pmatrix}. \quad (1.2.8)$$

Pour qu'il s'agisse bien d'une représentation, il reste à vérifier que $\rho(c \circ d) = \rho(c)\rho(d)$ pour toutes connectivités $c, d \in \text{TL}_N(\beta)$, ce qui est fait dans [31].

1.2.2 Modèle de boucles denses

Le modèle de boucles denses est construit à partir d'un diagramme appelé *tuile de base*, qui est la combinaison linéaire :

$$\square^u = \sin(u) \begin{array}{|c|} \hline \bullet \\ \hline \end{array} + \sin(\lambda - u) \begin{array}{|c|} \hline \bullet \\ \hline \end{array} . \quad (1.2.9)$$

La normalisation est celle de [31]. Il existe une interprétation physique en termes de poids de Boltzmann locaux pour certains objets construits à partir des tuiles de bases. Cette interprétation n'est pas directe et demande des calculs soutenus qui sont esquissés en Section 1.2.3. Avec cette interprétation, le paramètre λ est lié au choix du modèle statistique et le paramètre u à l'anisotropie du réseau. La valeur de β est aussi fixée à $\beta = 2 \cos(\lambda)$. Les intervalles considérés sont

$$\lambda \in (0, \pi/2) , \quad u \in [0, \lambda] . \quad (1.2.10)$$

Soulignons que la tuile de base n'est pas en elle-même un élément de $\text{TL}_N(\beta)$.

La tuile de base a plusieurs propriétés de symétries énoncées en détails dans [10]. La plus importante, qui assure l'intégrabilité des modèles statistiques associés, est *l'équation de Yang-Baxter* :

$$\begin{array}{|c|} \hline \diamond \\ \hline \end{array}^{u-v} \begin{array}{|c|} \hline v \\ \hline \end{array} = \begin{array}{|c|} \hline u \\ \hline \end{array} \begin{array}{|c|} \hline \diamond \\ \hline \end{array}^{u-v} . \quad (1.2.11)$$

Pour démontrer une telle propriété, plusieurs méthodes peuvent être utilisées. La plus simple est de développer les deux côtés de l'égalité en termes de diagrammes, puis de montrer que les mêmes diagrammes ont les mêmes coefficients.

La *matrice de transfert diagrammatique* pour une géométrie de type ruban est maintenant définie :

$$D(u) = \underbrace{\begin{array}{|c|c|c|c|c|} \hline \lambda-u & \lambda-u & \dots & \dots & \lambda-u \\ \hline u & u & \dots & \dots & u \\ \hline \end{array}}_N \in \text{TL}_N(\beta) . \quad (1.2.12)$$

La dépendance en N et λ est implicite. La matrice de transfert est la somme de 2^N connectivités dans

$\text{TL}_N(\beta)$ et a les propriétés suivantes :

$$\text{symétrie de croisement} \quad \mathbf{D}(u) = \mathbf{D}(\lambda - u), \quad (1.2.13a)$$

$$\text{commutativité} \quad [\mathbf{D}(u), \mathbf{D}(v)] = 0, \quad (1.2.13b)$$

$$\text{périodicité} \quad \mathbf{D}(u) = \mathbf{D}(u + \pi), \quad (1.2.13c)$$

$$\text{polynomialité} \quad \mathbf{D}(u) \text{ est un polynôme de Laurent en } z = e^{iu}. \quad (1.2.13d)$$

Les trois premières découlent directement de propriétés diagrammatiques des tuiles de base. Des preuves présentées de façon pédagogique sont dans [38]. La polynomialité, quant à elle, est justifiée à partir de la remarque suivante. Puisque les poids dans la tuile de base (1.2.9) sont des fonctions sinus d'argument linéaire en u , la matrice de transfert est une combinaison de connectivités dont les poids sont des polynômes de Laurent en $z = e^{iu}$ et z^{-1} . Ceux-ci ont eux-mêmes des coefficients polynomiaux en $x = e^{i\lambda}$. Ces propriétés tiennent également pour les matrices de transfert d'autres modèles de boucles et jouent un rôle clé dans le calcul de plusieurs quantités.

1.2.3 Lien avec la mécanique statistique

Cette section donne un aperçu du lien entre les matrices de transfert issues de certains modèles statistiques et les matrices de transfert des modèles de boucles. Les arguments suivent ceux de [31].

Le modèle de Q -Potts est d'abord introduit. Soit un réseau $2N \times 2M$ construit comme celui de la Figure 1.2a. Chaque point noir marque l'emplacement d'un spin σ_i qui peut prendre une valeur dans l'ensemble $\{1, 2, \dots, Q\}$. L'interaction est restreinte aux proches voisins, mais peut être anisotropique : les liens en bleu sont associés à une constante d'interaction J et ceux en rouge à une constante K . La condition frontière est périodique dans la direction verticale (les points encerclés sont identifiés) et est libre pour les côtés gauche et droit du réseau. L'énergie d'une configuration σ est donc

$$E(\sigma) = -J \sum_{\langle i,j \rangle} \delta_{\sigma_i \sigma_j} - K \sum_{\langle i,j \rangle} \delta_{\sigma_i \sigma_j}, \quad (1.2.14)$$

où une somme sur $\langle i, j \rangle$ indique une somme sur les proches voisins. Le modèle de Q -Potts regroupe donc une famille de modèles statistiques qui inclut le modèle d'Ising pour $Q = 2$.

La fonction de partition à calculer est

$$Z = \sum_{\{\sigma\}} \exp \left(j \sum_{\langle i,j \rangle} \delta_{\sigma_i \sigma_j} + k \sum_{\langle i,j \rangle} \delta_{\sigma_i \sigma_j} \right), \quad j = \frac{J}{k_B T}, \quad k = \frac{K}{k_B T}. \quad (1.2.15)$$

Pour la suite de cette section, $\Lambda = \Lambda(J, K, M, N, Q)$ dénote la matrice de transfert du modèle statistique. Les grandes lignes des transformations permettant de montrer que les spectres de Λ et de $\mathbf{D}(u)$ sont liés sont maintenant présentées.

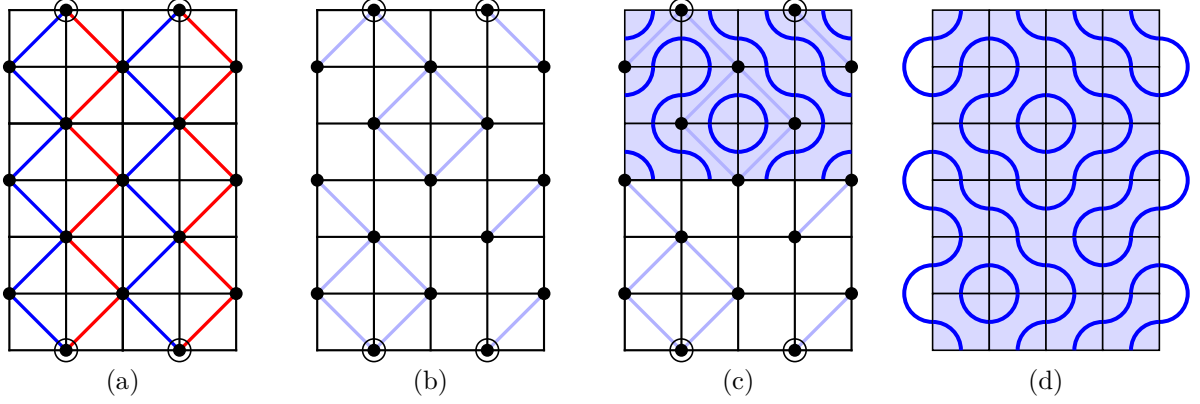


FIGURE 1.2 – En (a), un exemple du réseau du modèle de Q -Potts est présenté avec $N = 2$ et $M = 3$. Les points noirs sont des spins et les sites encadrés sont identifiés dans la direction verticale. Les traits bleus et rouges correspondent aux directions d'interaction J et K . La figure (b) contient un exemple de graphe, et les arêtes joignent des spins de même valeur. En (c) et (d), le passage au modèle de boucles est illustré.

1. La première étape est un passage vers la théorie des graphes et est illustrée à la Figure 1.2b. Pour un état σ , les liens d'énergie entre proches voisins sont exprimés à partir d'un graphe avec la prescription : (i) chaque site de spin est associé à un sommet et (ii) si deux spins proches voisins ont la même valeur, une arête est tracée entre eux. Plusieurs états de spins peuvent correspondre au même graphe. Avec N_{bJ} (resp. N_{bK}) le nombre de liens en J (resp. K) et N_c le nombre de composantes connexes d'un graphe \mathcal{G} , la fonction de partition prend la forme :

$$Z = \sum_{\{\mathcal{G}\}} (\mathbf{e}^j - 1)^{N_{bJ}} (\mathbf{e}^k - 1)^{N_{bK}} Q^{N_c} , \quad (1.2.16)$$

où $\{\mathcal{G}\}$ dénote l'ensemble de tous les graphes possibles pour le réseau.

2. La deuxième étape est la construction d'un motif de boucle $\mathcal{B}(\mathcal{G})$ pour chaque graphe tel qu'illustré aux Figure 1.2c et Figure 1.2d. Chaque case résultante du quadrillage du réseau est associée à l'une ou l'autre des tuiles de base (1.2.9) sans son poids. La règle pour sélectionner la tuile est : (i) s'il y a une arête, les boucles ne doivent pas toucher celle-ci et (ii) s'il n'y a pas d'arête, les boucles doivent croiser la diagonale où l'arête aurait été. La dernière étape est d'ajouter des demi-cercles aux frontières comme à la Figure 1.2d, ce qui nécessaire pour envisager le résultat comme un élément de $\text{TL}_N(\beta)$. Chaque graphe est associé à un unique motif de boucles¹.

Il est connu que la température critique des modèles de Q -Potts est telle que $(\mathbf{e}^j - 1)(\mathbf{e}^k - 1) = Q$ [2].

1. Lorsque plusieurs éléments de $\text{TL}_N(\beta)$ sont juxtaposés, les boucles fermées sont retirées et le résultat est multiplié par un facteur β . La remarque que chaque graphe est associé à un unique motif de boucles est valide lorsque les boucles fermées sont encore présentes.

La paramétrisation suivante est donc utilisée pour réexprimer Z :

$$\sqrt{Q} = 2 \cos(\lambda) , \quad \frac{e^j - 1}{\sqrt{Q}} = \frac{\sin(\lambda - u)}{\sin(u)} , \quad \frac{e^k - 1}{\sqrt{Q}} = \frac{\sin(u)}{\sin(\lambda - u)} . \quad (1.2.17)$$

C'est par le choix (1.2.17) que u est associé à l'anisotropie du réseau et λ au choix du modèle statistique. La fonction de partition devient

$$Z = \kappa \sum_{\{\mathcal{B}(\mathcal{G})\}} Q^{\#\mathcal{B}/2} \sin(\lambda - u)^{N_{bJ}} \sin(u)^{MN - N_{bJ}} \sin(u)^{N_{bK}} \sin(\lambda - u)^{MN - N_{bK}} , \quad (1.2.18)$$

où $\kappa = \kappa(\lambda, u, M, N)$ est un facteur multiplicatif donné dans [31], $\#\mathcal{B}$ est le nombre de boucles fermées et l'ensemble $\{\mathcal{B}(\mathcal{G})\}$ contient tous les motifs de boucles possibles pour le réseau.

3. La dernière étape est de faire le lien entre (1.2.18) et la trace de $\rho(\mathbf{D}(u)^M)$, avec M le paramètre de taille du modèle de Q -Potts. Le paramètre N doit aussi être commun à (1.2.18) et à $\mathbf{D}(u) = \mathbf{D}_N(u)$. Pour obtenir le lien recherché, une dernière définition est nécessaire. Avec N pair, nommons W la transformation linéaire qui agit comme un multiple de l'identité sur chaque \mathbf{V}_N^d avec :

$$W|_{\mathbf{V}_N^d} = \frac{\sin((d+1)\lambda)}{\sin(\lambda)} \mathbf{I} . \quad (1.2.19)$$

Le lien entre les spectres de Λ et $\rho(\mathbf{D}(u))$ est maintenant énoncé.

PROPOSITION 1.2.1. *Soit le modèle de Q -Potts avec $Q \in \{1, 2, 3\}$ sur un réseau $2N \times 2M$ comme dessiné à la Figure 1.2a. Les conditions frontières sont périodiques dans la direction verticale et libres sur les côtés gauche et droit.*

1. *La fonction de partition du modèle statistique est donnée par $Z = \kappa \text{Tr}(\rho(\mathbf{D}_N^M W))$, $\forall M \in \mathbb{N}$, avec W défini en (1.2.19).*
2. *Les valeurs propres λ de la matrice de transfert du modèle statistique Λ appartiennent au spectre de la représentation $\rho(\mathbf{D}_N)$ de la matrice de transfert du modèle de boucles.*

Les calculs justifiant ces énoncés ne sont pas présentés vu leur complexité, mais sont dans [31]. Des résultats plus complets y sont aussi.

1.3 Hiérarchie de fusion et développement en $1/N$

Dans ce qui suit, la plus grande valeur propre de la matrice de transfert est appelée valeur propre de l'état fondamental et les suivantes sont les excitations. Une valeur propre de $\mathbf{D}(u)$ est notée $D(u)$.

L'intérêt pour les modèles statistiques comme le modèle de Q -Potts réside dans la limite thermodynamique $N \rightarrow \infty$. C'est dans cette limite que des singularités apparaissent dans les fonctions thermo-

dynamiques et permettent de diagnostiquer une transition de phase². Dans cette limite, de nombreux indicateurs poussent à croire que les modèles statistiques sont invariants sous transformations conformes au point critique. Cela a même été démontré dans quelques cas précis, en particulier pour la percolation sur réseau triangulaire et pour le modèle d’Ising sur réseau carré.

L’hypothèse d’invariance conforme permet de connaître la forme des premières valeurs propres à l’aide d’un développement en $1/N$ pour certains réseaux. Ces développements ont été introduits presque simultanément en 1986 dans [41, 42]. Pour le modèle de boucles denses discuté précédemment, l’invariance conforme permet d’obtenir pour les plus grandes valeurs propres de $\mathbf{D}(u)$ [45, 4] :

$$-\log D_k(u) = 2N f_b(u) + f_s(u) + \frac{2\pi}{N} \sin\left(\frac{\pi u}{\lambda}\right) \left(-\frac{c}{24} + \Delta + k\right) + \mathcal{O}(1/N), \quad (1.3.1)$$

où f_b et f_s sont respectivement les énergies libres du *bulk* et de surface, c est la charge centrale, Δ le poids conforme et k un entier. Ces développements sont souvent appelés *corrections de taille finie*. Ainsi, s’il est possible d’obtenir une expression pour les premières valeurs propres à partir d’un modèle statistique et que cette expression est bien de la forme (1.3.1), alors la charge centrale et le poids conforme de ce modèle peuvent être obtenus.

Une méthode introduite par Klümper et Pearce permet d’obtenir ce développement en $1/N$ de manière analytique pour plusieurs modèles statistiques. Les prochains paragraphes présentent une rapide revue historique de son introduction.

Cette méthode est initiée dans [44] pour des chaînes de spins de type XXZ avec anisotropie. Cependant, seules les charges centrales sont obtenues et certaines expressions sont encore évaluées numériquement. La méthode pour obtenir les corrections de taille finie est introduite dans [24, 25] pour deux modèles spécifiques : les *tricritical hard squares* et les *critical hard hexagons*. Le point de départ est une équation fonctionnelle liant l’expression analytique d’une valeur propre de la matrice de transfert en différents points du paramètre d’anisotropie. Cette équation est alors une relation d’inversion déjà obtenue par Baxter et Pearce [39, 40]. Celle-ci est transformée en équations intégrales non-linéaires dont les solutions donnent les corrections de taille finie et les résultats sont exprimés analytiquement en termes de dilogarithmes de Rogers. Les charges centrales et poids conformes des deux modèles sont donc obtenus et concordent avec les prédictions faites en théorie conforme des champs.

Cette méthode est généralisée dans [26] pour une classe plus large de modèles, les *L-state restricted solid-on-solid (RSOS) lattice models*, à laquelle appartient les cas particuliers cités ci-dessus [24, 25]. Pour y arriver, une famille d’équations fonctionnelles liant les matrices de transfert et appelée *hiérarchie de fusion* est utilisée. Ces équations n’ont pas été obtenues en premier par Klümper et Pearce, mais par Bazhanov et Reshetikhin [43]. Cependant, afin de calculer les corrections de taille finie, des équations fonctionnelles supplémentaires sont dérivées et sont aujourd’hui connues comme les systèmes T et Y.

2. En effet, pour N fini, Z est une somme de fonctions analytiques et il suit que l’énergie libre et la magnétisation moyenne le sont aussi [2].

Les corrections de taille finie sont donc obtenues pour tous ces modèles RSOS à partir de calculs analytiques sur le spectre de la matrice de transfert et les résultats concordent avec les prédictions provenant de l’hypothèse d’invariance conforme.

C’est dans ce contexte que les premiers systèmes T sont utilisés. Des systèmes Y sont employés préalablement, entre autres dans [46, 47]. Il est aujourd’hui bien accepté que les systèmes T et Y sont des outils importants pour obtenir des solutions analytiques de modèles intégrables sur réseau.

Plus récemment, la méthode développée par Klümper et Pearce a été appliquée à certains modèles de boucles dans une série d’articles en collaboration avec Morin-Duchesne. La hiérarchie de fusion et les systèmes T et Y sont d’abord obtenus pour le modèle de boucles denses dans [10], et les résultats sont analogues à ceux de [26]. Les résultats pour les modèles de boucles *fully packed* et diluées sont respectivement dans [29] et [17]. Pour tous ces modèles, les équations fonctionnelles sont dérivées directement dans l’algèbre planaire et cela assure qu’elles tiennent pour toutes représentations matricielles de la matrice de transfert associée.

Avec les équations fonctionnelles connues, un exemple de résolution des équations intégrales non-linéaires pour le modèle de percolation a été donné dans [48]. Très récemment, ces calculs ont été généralisés aux modèles de boucles denses, *fully packed* et diluées pour la géométrie du cylindre dans [27] pour des valeurs spécifiques du paramètres λ .

Dans ce mémoire, la hiérarchie de fusion et les systèmes T et Y sont obtenus pour le modèle de boucles diluées sur le ruban. Voici les grandes lignes de l’article présenté à ce sujet en Chapitre 2. Une revue rapide de l’algèbre de Temperley-Lieb diluée est en Section 2.2. Le modèle de boucles associé est en Section 2.3, où il y a des résultats déjà connus, mais aussi de nouvelles propriétés pour les opérateurs spécifiques aux frontières. Les résultats présentés dans la suite du papier sont tous nouveaux, sauf mention contraire. La Section 2.4 contient la hiérarchie de fusion de matrices de transfert pour ce modèle, plusieurs propriétés des matrices fusionnées ainsi que les équations T et Y. La Section 2.5 est consacrée à une propriété des matrices fusionnées, la polynomialité, qui est essentielle à une preuve subséquente. Dans la Section 2.6, un des résultats principaux est énoncé et prouvé, soit que la hiérarchie de fusion et le système Y ne sont pas des systèmes d’équations infinis lorsque $e^{i\lambda}$ est une racine de l’unité. Finalement, un exemple d’application physique de ces résultats est présenté en Section 2.7, soit le calcul de plusieurs énergies libres. Le calcul de cette quantité pour le *bulk* de la matrice de transfert avait été fait préalablement, mais pas celui pour l’énergie libre de surface, $f_{bdy}(u)$. Certaines preuves techniques par rapport à $\mathbf{D}(u)$ sont reléguées en Section 2.A.

Les contributions de l’auteure sont les suivantes. Tous les nouveaux résultats ont initialement été obtenus par elle, sauf l’évaluation à l’infini pour la fermeture en Section 2.6.4, la fermeture du système Y en Section 2.6.5 et le calcul des énergies libres en Section 2.7. Un premier jet de rédaction a aussi été fait par elle pour la majorité des sections de l’article. Certaines preuves originales étaient longues ; Morin-Duchesne en a trouvé des plus courtes pour les résultats des Sections 2.A.4, 2.5.2, 2.5.3 et 2.6.3. Il en a rédigé les premières versions, ainsi que celle de la Section 2.7.

Chapitre 2

Fusion hierarchies, T -systems and Y -systems for the dilute $A_2^{(2)}$ loop models on a strip

Par Florence Boileau, Alexi Morin-Duchesne et Yvan Saint-Aubin.

Accepté dans le *Journal of Statistical Mechanics : Theory and Experiment* le 11 janvier 2023.

Abstract We study the dilute $A_2^{(2)}$ loop models on the geometry of a strip of width N . Two families of boundary conditions are known to satisfy the boundary Yang-Baxter equation. Fixing the boundary condition on the two ends of the strip leads to four models. We construct the fusion hierarchy of commuting transfer matrices for the model as well as its T - and Y -systems, for these four boundary conditions and with a generic crossing parameter λ . For λ/π rational and thus $q = -e^{4i\lambda}$ a root of unity, we prove a linear relation satisfied by the fused transfer matrices that closes the fusion hierarchy into a finite system. The fusion relations allow us to compute the two leading terms in the large- N expansion of the free energy, namely the bulk and boundary free energies. These are found to be in agreement with numerical data obtained for small N . The present work complements a previous study (A. Morin-Duchesne, P.A. Pearce, *J. Stat. Mech.* (2019)) that investigated the dilute $A_2^{(2)}$ loop models with periodic boundary conditions.

Keywords dilute loop models, dilute Temperley-Lieb algebra, fusion hierarchy, T -system, Y -system.

2.1 Introduction

Loop models have historically played a central role in deepening our understanding of critical statistical models on two-dimensional lattices [1]. The loops are random curves that typically arise in the study of models with local degrees of freedom, by considering the curves drawn on the lattice by collections of these local objects and thus elevating the model to one with non-local observables. Examples include the contour curves of percolation clusters, Ising spin domains or spanning trees. The formulation of

these problems in terms of a transfer matrix or Hamiltonian treats one of the two spatial directions as a time direction along which evolution runs in discrete steps. The various quantities of interest are then expressible in terms of the eigenvalues and eigenstates of these operators. If the model is Yang-Baxter integrable [2], then its transfer matrix and Hamiltonian are elements of larger commuting families and various techniques allow one to compute the eigenvalues and eigenstates.

Loop models are also intimately tied with vertex models, and likewise to Interaction-Round-a-Face models like the Restricted Solid-on-Solid (RSOS) models. Many interesting features of these models emerge in the continuum scaling limit, where the size N of the lattice is sent to infinity. Theoretical and numerical studies show that in this limit, the spectrum of the transfer matrix, after proper scaling, is described by characters of the Virasoro algebra. The central charge c of the underlying conformal field theory (CFT) then depends on the model considered. For instance, it depends on the loop fugacity β for the loop models, on the quantum group parameter q for the vertex models, and on the number L of allowed heights in the RSOS models. If c is a rational number, then the CFT describing the scaling limit of these models is either rational or logarithmic. The latter case is particularly interesting, with indecomposable yet reducible representations and non-trivial Jordan cells for the dilation operator [3–5]. These structures are not fully understood, so this provides in itself a good physical motivation to pursue the study of these models. But the models defined on finite lattices are also rich in algebraic structures, some of which still remain to be unraveled.

The elementary building blocks for the loops models are the face operators (or \check{R} matrices in the language of vertex models), which take the form of linear combinations of diagrams weighted by Boltzmann weights. The model is integrable if these weights are chosen so that the Yang-Baxter equation is satisfied. This in turn ensures the existence of a one-parameter family of commuting transfer matrices. Solutions to the Yang-Baxter equations are often labeled by affine Lie algebras [6, 7], with the most studied cases corresponding to the low-rank algebras $A_1^{(1)}$, $A_2^{(1)}$ and $A_2^{(2)}$. Thanks to a large body of work on the dense $A_1^{(1)}$ loop model and the related six-vertex models, it is fair to say that their $sl(2)$ integrability structures are now well understood [2, 8–11].

This article focuses on the dilute loop model in the $A_2^{(2)}$ family, a model with a richer structure also often referred to as the dilute $O(n)$ loop model. Its Boltzmann weights were obtained by Nienhuis [12], and Izergin and Korepin [13]. Some of these weights can be negative, curtailing an immediate interpretation within statistical physics, but also leading to unexpected behavior in the scaling limit [14]. Here we investigate these loop models defined on the geometry of the strip, with boundary face operators satisfying the boundary Yang-Baxter equation. Two solutions were given by Batchelor and Yung [15], and further studied by Dubail, Jacobsen and Saleur [16]. We label them by S and C (for sine and cosine). Both sides of the strip may have different boundary conditions, so a total of four models will be studied throughout, namely those with identical boundary conditions on the two sides (SS and CC), and those with mixed ones (SC and CS). We also mention that the current work complements an earlier study [17] of the dilute $A_2^{(2)}$ loop model defined with periodic boundary conditions.

The transfer matrix that we investigate for the loop model on the strip, denoted $\mathbf{D}(u)$, takes the form of a linear combination of connectivity diagrams. As such, it is an element of the dilute Temperley-Lieb algebra $\text{dTL}_N(\beta)$ [18–21], a generalisation of the Temperley-Lieb algebra [22, 23] where the loops are dilute instead of dense. The transfer matrix depends on a spectral parameter u and a crossing parameter λ , with the latter parameterizing the loop fugacity as $\beta = -2 \cos 4\lambda$. It is a Laurent polynomial in e^{iu} whose coefficients are elements of $\text{dTL}_N(\beta)$. The commutativity relation $[\mathbf{D}(u), \mathbf{D}(v)] = 0$, typical of integrable models, allows one to show that these coefficients are commuting conserved quantities.

In this paper, we construct the fusion hierarchy of transfer matrices $\mathbf{D}^{m,n}(u)$ for the $A_2^{(2)}$ loop model on the strip, with $\mathbf{D}^{1,0}(u) = \mathbf{D}(u)$. These transfer matrices satisfy relations that allow us to write each $\mathbf{D}^{m,n}(u)$ as a function of the elementary transfer matrices $\mathbf{D}(u + k\lambda)$ with $k \in \mathbb{Z}$. This directly ensures that $[\mathbf{D}^{m,n}(u), \mathbf{D}(u)] = 0$. Moreover, the construction is done in such a way that each member of the hierarchy is a Laurent polynomial in e^{iu} , which implies that its coefficients are also conserved quantities. This process might seem vacuous as the resulting fused matrices $\mathbf{D}^{m,n}(u)$ do not create new commuting quantities, since they are algebraically related to those of $\mathbf{D}(u)$. The power of the hierarchy is instead revealed for $\lambda/\pi \in \mathbb{Q}$. In this case, the fused transfer matrices satisfy a linear *closure relation* that turns the hierarchy into a finite system. Since the fused matrices of the hierarchy commute, they can be diagonalized simultaneously and the closure relation thus translates into a functional relation satisfied by the eigenvalues of these matrices. Equivalently, this system can be recast in a unique functional polynomial equation satisfied by $\mathbf{D}(u)$. This identity lives in the algebra $\text{dTL}_N(\beta)$, but is also satisfied by replacing $\mathbf{D}(u)$ by any of its eigenvalues. This is Baxter’s celebrated method [2] of functional equations, to extract physical quantities from transfer matrices. The techniques that were developed to solve these systems of equations [24–27] are intimately related to the thermodynamic Bethe ansatz.

The outline of the paper is as follows. In Section 2.2, we review the definition of the dilute Temperley-Lieb algebra and of its standard modules. Section 2.3 defines the dilute $A_2^{(2)}$ loop model in terms of its face and boundary operators and their integrable Boltzmann weights. It also gives a list of the local relations that they satisfy and reviews the definition of some projectors defined in [17]. In Section 2.4, we define first the fundamental transfer matrix $\mathbf{D}(u)$, and subsequently the fused transfer matrices $\mathbf{D}^{m,n}(u)$ using the fusion hierarchy relations that they satisfy. This longer section also discusses several key properties of the transfer matrices, in particular some alternate but equivalent definitions of these objects, the reduction relations that they satisfy at certain special values of u , and their behavior in the braid limit $u \rightarrow i\infty$. Finally, Section 2.4 also shows that the fusion hierarchy can be recast in terms of a T -system and a Y -system. The proof that the fused transfer matrices are Laurent polynomials contains new ideas not seen before for other models, and is the topic of Section 2.5. Then in Section 2.6, we set $\lambda/\pi \in \mathbb{Q}$ and prove the closure relation of the fusion hierarchy. With the polynomiality of the fused matrices established, the closure relation takes the form of an identity between Laurent polynomials in e^{iu} with coefficients in the dilute Temperley-Lieb algebra. The strategy for the proof consists in checking the identity at a finite number of points. This section also discusses the closure for the

Y-system. Some of the proofs of Sections 2.4 and 2.6 are direct whereas others are longer and are gathered in Section 2.A. Finally, Section 2.7 shows the physical relevance of the functional relations of the hierarchy by computing the bulk free energies (obtained previously by Warnaar, Batchelor and Nienhuis [28]) and the boundary free energies (which to our knowledge are new). Section 2.8 offers some concluding remarks.

2.2 The dilute Temperley-Lieb algebra

The words *planar algebras* [23] refer to a broad set of algebras whose elements are diagrams known as *tangles*. One of their main features is that tangles are multiplied by concatenation. Specific rules to be performed upon concatenation will lead to different algebras. The present section is devoted to the description of the rules defining the dilute Temperley-Lieb algebra $\text{dTL}_N(\beta)$ and its standard representations.

2.2.1 Definition of the algebra

Similarly to the dense loop model and its underlying Temperley-Lieb algebra $\text{TL}_N(\beta)$, the dilute $A_2^{(2)}$ loop model is defined using the dilute Temperley-Lieb algebra $\text{dTL}_N(\beta)$. The algebras $\text{dTL}_N(\beta)$ form a family of associative unital algebras labelled by a positive integer N and a parameter $\beta \in \mathbb{C}$. The present section introduces a diagrammatic presentation of $\text{dTL}_N(\beta)$ and some of its properties. More details and its basic representation theory are given in [21].

The construction of the basic objects, the *connectivities*, goes as follows. Let $N \in \mathbb{N}$. A rectangle with N nodes on the bottom edge and N other ones on the top edge is drawn. A set of non-intersecting planar loop segments is also drawn to connect a subset of the nodes in pairs. The loop segments are constrained to stay within the borders of the rectangle and to have each end tied to one of the $2N$ nodes. A node may be left unconnected and is then said to be *vacant*. Here are two connectivities with $N = 6$, with the loop segments depicted as solid blue lines and the vacancies as solid black circles:

$$c_1 = \text{[diagram 1]}, \quad c_2 = \text{[diagram 2]}. \quad (2.2.1)$$

The numbers of vacancies on the two sides of a connectivity always have the same parity by the requirement that loop segments have both ends connected.

As a vector space, the algebra $\text{dTL}_N(\beta)$ is the formal linear span over \mathbb{C} of connectivities. The product $c_1 c_2$ of two connectivities is defined via concatenation. To compute it, the connectivity c_2 is drawn above c_1 . The inner edges and nodes of the rectangles are identified and then removed. The resulting loop segments might have loose ends in the middle of the diagram or might be closed to form a loop. The following rules are then applied to obtain a connectivity. If a loop segment ends at a vacancy, the

result is set to zero. If loop segments join to form a loop, it is removed and the diagram is multiplied by a factor β . Otherwise, the loop segments are contracted and the resulting connectivity is read off directly. Here are two examples:

$$c_1 c_2 = \text{[Diagram: box with horizontal line, loops above]} = \beta \text{[Diagram: box with horizontal line, loops below]}, \quad c_2 c_1 = \text{[Diagram: box with horizontal line, loops above]} = 0. \quad (2.2.2)$$

The algebra $\text{dTL}_N(\beta)$ is associative and non-commutative. There is a unit element, \mathbf{I} , which is the sum of 2^N connectivities:

$$\mathbf{I} = \text{[Diagram: box with vertical dashed lines at 1, 2, 3, ..., N-1, N]}, \quad \text{[Diagram: box with vertical dashed line at 1]} = \text{[Diagram: box with vertical solid line at 1]} + \text{[Diagram: box with vertical solid line at 2]}. \quad (2.2.3)$$

The dimension of $\text{dTL}_N(\beta)$ was computed in [21] using the resemblance with the Temperley-Lieb algebra $\text{TL}_N(\beta)$:

$$\dim \text{dTL}_N(\beta) = \sum_{k=0}^N \frac{1}{k+1} \binom{2k}{k} \binom{2n}{2k} = M_{2N}, \quad (2.2.4)$$

where M_{2N} is the $2N$ -th Motzkin number. It can also be written as

$$\dim \text{dTL}_N(\beta) = \binom{2N}{0}_2 - \binom{2N}{2}_2 \quad (2.2.5)$$

where the trinomial coefficients are defined by

$$(x + 1 + x^{-1})^N = \sum_{k=-N}^N \binom{N}{k}_2 x^k. \quad (2.2.6)$$

2.2.2 Standard modules

Several key results about loop models can be obtained using the standard modules over the dilute Temperley-Lieb algebra. The set of standard modules on $\text{dTL}_N(\beta)$ is $\{\mathbf{W}_N^d, 0 \leq d \leq N\}$, where the parameters N and β are as above and d is the *defect number* introduced below.

A basis for the standard module \mathbf{W}_N^d is constituted of *link states*. To construct a link state, a horizontal line is drawn with N marked nodes. A set of non-intersecting loop segments is added above the horizontal line, each one either connecting two nodes together or connecting a node to infinity above. A loop segment of the second type is called a *defect*, and the number of defects is denoted d . Like those in a connectivity, the nodes of a link state may be left vacant. The formal linear combinations of link diagrams forms a vector space \mathbf{W}_N , and the link states with a fixed d , with $0 \leq d \leq N$, span a subspace that will be the standard module \mathbf{W}_N^d for the action to be defined below. For example, here

are the link states generating the vector spaces of the modules W_3^d with $d = 0, 1, 2, 3$:

$$\begin{aligned}
W_3^3 : & \quad \begin{array}{c} | \quad | \quad | \\ \hline \end{array}, & W_3^2 : & \quad \begin{array}{c} | \quad | \quad \bullet \\ \hline \end{array} \quad \begin{array}{c} | \quad \bullet \quad | \\ \hline \end{array} \quad \begin{array}{c} \bullet \quad | \quad | \\ \hline \end{array}, \\
W_3^1 : & \quad \begin{array}{c} | \quad \cup \\ \hline \end{array} \quad \begin{array}{c} \cup \quad | \\ \hline \end{array} \quad \begin{array}{c} | \quad \bullet \quad \bullet \\ \hline \end{array} \quad \begin{array}{c} \bullet \quad | \quad \bullet \\ \hline \end{array} \quad \begin{array}{c} \bullet \quad \bullet \quad \bullet \\ \hline \end{array}, \\
W_3^0 : & \quad \begin{array}{c} \bullet \quad \cup \\ \hline \end{array} \quad \begin{array}{c} \cup \quad \bullet \\ \hline \end{array} \quad \begin{array}{c} \cup \\ \hline \end{array} \quad \begin{array}{c} \bullet \quad \bullet \quad \bullet \\ \hline \end{array}.
\end{aligned} \tag{2.2.7}$$

There is a natural action of $dTL_N(\beta)$ on the vector space W_N^d . If c is a connectivity and w a link state, the action of c on w is computed similarly as the product of two connectivities in $dTL_N(\beta)$. The link state w is drawn above c and the nodes on the upper edge of the rectangle are identified with those of the link state and then removed. The resulting connectivity is read directly starting from the lower edge of c . Some rules apply. First, if a loop segment is connected to a vacancy, the result is zero. Second, if the concatenation reduces the number of defects, the result of the action is set to zero. Third, any closed loop created by the concatenation is removed from the diagram and the remaining link state is multiplied by the factor β^ℓ , where ℓ is the number of loops. The following are examples of the action of connectivities of $dTL_4(\beta)$ on link states in W_4^0 , W_4^3 and W_4^1 respectively:

$$\begin{array}{c} \cup \quad \cup \\ \hline \end{array} = 0, \quad \begin{array}{c} | \quad \cup \\ \hline \end{array} = 0 \quad \text{and} \quad \begin{array}{c} | \quad \cup \\ \hline \end{array} = \beta \begin{array}{c} | \quad \cup \\ \hline \end{array}. \tag{2.2.8}$$

The dimension of the module W_N^d is

$$\dim W_N^d = \binom{N}{k}_2 - \binom{N}{k+2}_2. \tag{2.2.9}$$

The standard modules W_N^d are indecomposable for all N and d with $0 \leq d \leq N$. The structure of the module W_N^d depends on the value of $\beta = q + q^{-1}$. The parameter q is said to be *generic* when it is not a root of unity. For generic values of q , each W_N^d is irreducible. When q is a root of unity, the module W_N^d is indecomposable but not always irreducible. When it is not, it is instead the quotient l_N^d of W_N^d by its radical that is irreducible. These quotients form a complete set of isomorphism classes of irreducible modules of $dTL_N(\beta)$. Let us describe the roots of unity case in more detail. For a given value of q , an integer d is said to be *critical* if $q^{2(d+1)} = 1$. For d critical, W_N^d is irreducible. Let d be non critical and d_c be the smallest critical integer larger than d . We define d^+ as the integer obtained from the reflection of d with respect to d_c , namely $d^+ = 2d_c - d$. Similarly, we define the integer d^- by a reflection of d across the largest critical integer d'_c smaller than d , that is $d^- = 2d'_c - d$. The sequence $\{\dots, d^{--}, d^-, d, d^+, d^{++}, \dots\}$ is then infinite in both directions. To study the structure of W_N^d at a root of unity, we truncate this sequence by keeping only the elements in the range $[0, N]$. This truncated sequence is called the *orbit* of d . Being in the same orbit is an equivalence relation. If both d and d_+ are in the truncated sequence, then there is a non-zero morphism $W_N^{d^+} \rightarrow W_N^d$, and W_N^d is reducible.

It has two composition factors, \mathbb{I}_N^d and $\mathbb{I}_N^{d^+}$, and its Loewy diagram is $\mathbb{I}_N^d \rightarrow \mathbb{I}_N^{d^+}$. The algebra $\mathfrak{dTL}_N(\beta)$ can be seen as a module over itself. This is the *regular* representation and it can be decomposed into a direct sum of indecomposable modules. All the elements in this direct sum that contain composition factors that arise in the set of standard modules W_N^e , with e in the orbit of a given d , are said to form a *block*. Similarly, an indecomposable \mathfrak{dTL}_N -module may only have composition factors \mathbb{I}_N^e with their labels e belonging to the same orbit. They are then naturally associated to the block labeled by this orbit. Non-trivial homomorphism and extension groups exist only between the indecomposables associated to the same block. (See [21] for more details.)

2.3 Integrable face and boundary operators

The transfer matrix of the dilute $A_2^{(2)}$ loop models is constructed out of two building blocks: the face operator and the boundary operator. The present section introduces these operators and lists some of their properties.

2.3.1 Definition of the operators

An *elementary tile* is a square with a single node on each edge. Like for a connectivity, these nodes may be connected in pairs by non-intersecting loop segments or stay vacant. There are then nine elementary tiles. The *face operator* is a linear combination of these nine tiles:

$$\begin{aligned}
 \begin{array}{|c|} \hline u \\ \hline \end{array} &= \rho_1(u) \begin{array}{|c|} \hline \bullet \\ \hline \end{array} + \rho_2(u) \begin{array}{|c|} \hline \curvearrowright \\ \hline \end{array} + \rho_3(u) \begin{array}{|c|} \hline \bullet \\ \hline \end{array} + \rho_4(u) \begin{array}{|c|} \hline \bullet \\ \hline \end{array} + \rho_5(u) \begin{array}{|c|} \hline \curvearrowleft \\ \hline \end{array} \\
 &+ \rho_6(u) \begin{array}{|c|} \hline | \\ \hline \end{array} + \rho_7(u) \begin{array}{|c|} \hline \hline \\ \hline \end{array} + \rho_8(u) \begin{array}{|c|} \hline \curvearrowright \\ \hline \end{array} + \rho_9(u) \begin{array}{|c|} \hline \curvearrowleft \\ \hline \end{array}, \tag{2.3.1}
 \end{aligned}$$

where black circles indicate vacancies, as in Section 2.2. The small quarter arc in the lower-left corner of the left-hand side indicates the orientation to be given to the diagrams. For instance, a face operator with the arc in the lower-right corner would have all the diagrams rotated counter-clockwise by 90° . The factors $\rho_i(u)$ of the elementary tiles are interpreted as local Boltzmann weights. They are parameterized by u , the *spectral parameter*, and λ , the *crossing parameter*. They are

$$\begin{aligned}
 \rho_1(u) &= \sin(2\lambda) \sin(3\lambda) + \sin(u) \sin(3\lambda - u), & \rho_{2,3}(u) &= \sin(2\lambda) \sin(3\lambda - u), \\
 \rho_{4,5}(u) &= \sin(2\lambda) \sin(u), & \rho_{6,7}(u) &= \sin(u) \sin(3\lambda - u), \\
 \rho_8(u) &= \sin(2\lambda - u) \sin(3\lambda - u), & \rho_9(u) &= -\sin(u) \sin(\lambda - u).
 \end{aligned} \tag{2.3.2}$$

The crossing parameter also parameterizes the fugacity of contractible loops as

$$\beta = -2 \cos(4\lambda). \tag{2.3.3}$$

The weights $\rho_i(u)$ are real for $u, \lambda \in \mathbb{R}$. Note however that the positivity constraint is relaxed as they can be negative. Our normalization of these local weights is different than that of [17]. The present choice removes the singularities at $\lambda = \frac{\pi}{3}, \frac{\pi}{2}, \frac{2\pi}{3}$. The crossing parameter is said to be *generic* if $\frac{\lambda}{\pi} \notin \mathbb{Q}$, whereas otherwise $\frac{\lambda}{\pi} \in \mathbb{Q}$ and thus $q = -e^{4i\lambda}$ is a root of unity.

The face operator can be seen as an element of $\mathbf{dTL}_2(\beta)$ by fixing a direction of action, that is, from two adjacent nodes that would appear at the top of the connectivities, to the remaining two adjacent nodes, that would be at the bottom [4]. The face operator can also be seen as an element of $\mathbf{dTL}_N(\beta)$ acting non-trivially on the adjacent nodes i and $i + 1$, with $1 \leq i < N$. Then for each j different from i and $i + 1$, the j -th nodes on the top and bottom of the connectivity are connected by a unit link (represented by a dashed line in (2.2.3)).

The *boundary operator* is a linear combination of two elementary triangular tiles:

$$\begin{array}{c} \text{---} \\ \text{---} \\ \text{---} \end{array} \triangleleft u = \delta\left(\frac{3\lambda}{2} - u\right) \begin{array}{c} \text{---} \\ \text{---} \\ \text{---} \end{array} \triangleleft + \delta\left(\frac{3\lambda}{2} + u\right) \begin{array}{c} \text{---} \\ \text{---} \\ \text{---} \end{array} \triangleleft . \quad (2.3.4)$$

With the triangles pointing rightward as in the equation above, the boundary operator has one node on each diagonal edge but none on the vertical one. We consider two possible choices for the function $\delta(u)$, which we refer to as the *sine* (S) and *cosine* (C) *boundary conditions*. For simplicity and to underline the links between the S and C cases, we also introduce the function $\bar{\delta}(u)$ for each case:

$$\begin{array}{ll} \text{S:} & \delta(u) = \sin(u) , \quad \bar{\delta}(u) = \cos(u) , \\ \text{C:} & \delta(u) = \cos(u) , \quad \bar{\delta}(u) = \sin(u) . \end{array} \quad (2.3.5)$$

In the following sections, when no ambiguity is possible, we use the short-hand notations

$$u_k = u + k\lambda , \quad s(\alpha u_k) = \sin(\alpha(u + k\lambda)) , \quad c(\alpha u_k) = \cos(\alpha(u + k\lambda)) . \quad (2.3.6)$$

We note that the normalisation of the function $s(\alpha u_k)$ used here differs from the one used in [17].

The weights (2.3.2) in the face operator and those (2.3.5) in the boundary one are not arbitrary. They are chosen to satisfy algebraic constraints, among them the Yang-Baxter equations, that lead to the integrability of the models defined in the next section. They were studied in [12, 13] for the weight of the face operator and in [15, 16] for the boundary ones.

2.3.2 Diagrammatic properties of the face operator

Many useful properties are satisfied by the face operator or a concatenation of a few of them. Some are valid only at given values of the spectral parameter u . Those reviewed here are well-known (see for example [17]) and thus stated without proof. These identities are derived in the planar version

of the dilute Temperley-Lieb algebra [23]. In this context, diagrammatic objects like face operators are glued together, sometimes with the dashed loop segment (2.2.3) that acts as the identity, and the outside of the diagram has a number of free nodes. These relations can then be used to simplify larger diagrams where a member of one of the identities appears. They can also be converted into identities in $dTL_N(\beta)$.

The *crossing symmetry*

$$\begin{array}{|c|} \hline u \\ \hline \end{array} = \begin{array}{|c|} \hline 3\lambda - u \\ \hline \end{array} \quad (2.3.7)$$

links the face operator evaluated at u to the one rotated by 90° and evaluated at $3\lambda - u$.

The *inversion relation*

$$\begin{array}{|c|} \hline u \\ \hline \end{array} \begin{array}{|c|} \hline -u \\ \hline \end{array} = \rho_8(u)\rho_8(-u) \begin{array}{|c|} \hline \text{---} \\ \hline \end{array} \quad (2.3.8)$$

shows that the concatenation of two face operators, evaluated at u and $-u$ respectively, is a multiple of the identity. This operator is thus invertible as long as $\rho_8(u)\rho_8(-u) \neq 0$, that is, when $u \neq \pm 2\lambda$ or $\pm 3\lambda$.

The *Yang-Baxter equation* plays a crucial role in the proof of the integrability of loop models and is given by

$$\begin{array}{|c|} \hline u-v \\ \hline \end{array} \begin{array}{|c|} \hline v \\ \hline \end{array} \begin{array}{|c|} \hline u \\ \hline \end{array} = \begin{array}{|c|} \hline u \\ \hline \end{array} \begin{array}{|c|} \hline v \\ \hline \end{array} \begin{array}{|c|} \hline u-v \\ \hline \end{array} . \quad (2.3.9)$$

At some values of the spectral parameter, the face operator factorizes into the product of two tangles. Those values are referred to as *degeneration points* in [17]. At $u = 0$ and $u = 3\lambda$, the two tangles are triangles that carry the identity arc:

$$\begin{array}{|c|} \hline 0 \\ \hline \end{array} = s(2\lambda)s(3\lambda) \begin{array}{|c|} \hline \text{---} \\ \hline \end{array}, \quad \begin{array}{|c|} \hline 3\lambda \\ \hline \end{array} = s(2\lambda)s(3\lambda) \begin{array}{|c|} \hline \text{---} \\ \hline \end{array}. \quad (2.3.10)$$

At $u = \lambda$ and $u = 2\lambda$, these tangles are

$$\begin{array}{|c|} \hline \lambda \\ \hline \end{array} = s(\lambda)s(2\lambda) \begin{array}{|c|} \hline \blacksquare \\ \hline \end{array}, \quad \begin{array}{|c|} \hline 2\lambda \\ \hline \end{array} = s(\lambda)s(2\lambda) \begin{array}{|c|} \hline \blacksquare \\ \hline \end{array}, \quad (2.3.11)$$

where the black triangle is

$$\begin{array}{|c|} \hline \blacksquare \\ \hline \end{array} = 2c(\lambda) \begin{array}{|c|} \hline \bullet \\ \hline \end{array} + \begin{array}{|c|} \hline \text{---} \\ \hline \end{array} + \begin{array}{|c|} \hline \text{---} \\ \hline \end{array} + \begin{array}{|c|} \hline \text{---} \\ \hline \end{array}. \quad (2.3.12)$$

In contrast with the boundary operator (2.3.4) that has two nodes, one on each shorter side, the black triangle tangle has three nodes, one per side. The crossing symmetry ($u \leftrightarrow 3\lambda - u$) links these degeneration points into pairs.

There are also other local relations where a collection of face operators attached together are evaluated at values of the spectral parameter that differ by 2λ or 3λ , and then have a simpler form in terms of fewer tangles. In particular, the next two relations are known as *push-through* properties, as they both involve the propagation from right to left of a triangular tile through a pair of face operators. These tangles are those defined above, namely the identity arc and the black triangle, respectively. Using the short-hand notation (2.3.6), these relations are

$$\begin{array}{c} \square \\ u_2 \\ \square \\ u_0 \end{array} \begin{array}{c} \text{---} \\ \text{---} \end{array} \triangle = -s(u_{-3})s(u_2) \triangle \begin{array}{c} \square \\ u_1 \\ \square \end{array}, \tag{2.3.13a}$$

$$\begin{array}{c} \square \\ u_3 \\ \square \\ u_0 \end{array} \text{---} = s(u_2)s(u_{-2})s(u_3)s(u_{-3}) \begin{array}{c} \square \\ \text{---} \\ \square \end{array}. \tag{2.3.13b}$$

To obtain the similar push-through properties for a propagation from left to right, one must simply rotate the whole stacks of tangles by 180° .

A last property links the face operators at u and $u + \pi$. Following [29], we define a gauge operator on one site. It is depicted as a white box:

$$\square = (-1) \begin{array}{c} \square \\ | \\ \square \end{array} + \begin{array}{c} \square \\ \bullet \\ \square \end{array}. \tag{2.3.14}$$

The following periodicity property then holds:

$$\begin{array}{c} \square \\ u + \pi \\ \square \end{array} = \begin{array}{c} \square \\ \square \\ u \\ \square \end{array} = \begin{array}{c} \square \\ \square \\ u \\ \square \end{array}. \tag{2.3.15}$$

Finally, we recall that some projectors for the dilute $A_2^{(2)}$ loop model were constructed in [17]. Here we only introduce the first two non-trivial ones, $P^{2,0}$ and $P^{1,1}$, defined as

$$\begin{array}{c} \square \\ 2,0 \\ \square \end{array} = \begin{array}{c} \square \\ \text{---} \\ \square \end{array} - \begin{array}{c} \triangle \\ \text{---} \\ \square \end{array}, \quad \begin{array}{c} \square \\ 1,1 \\ \square \end{array} = \begin{array}{c} \square \\ \text{---} \\ \square \end{array} - \begin{array}{c} \triangle \\ \text{---} \\ \square \end{array}, \tag{2.3.16}$$

where

$$\begin{array}{c} \triangleleft \square \triangleright \end{array} = \frac{s^2(2\lambda)}{s(4\lambda)s(5\lambda)} \begin{array}{c} \triangleleft \bullet \triangleright \\ \bullet \end{array} - \frac{s(2\lambda)s(3\lambda)}{s(4\lambda)s(5\lambda)} \begin{array}{c} \triangleleft \curvearrowright \triangleright \\ \bullet \end{array} - \frac{s(2\lambda)}{s(4\lambda)} \begin{array}{c} \triangleleft \bullet \triangleright \\ \diagdown \end{array} + \frac{s(2\lambda)s(3\lambda)}{s(\lambda)s(4\lambda)} \begin{array}{c} \triangleleft \diagup \triangleright \\ \bullet \end{array}, \quad (2.3.17a)$$

$$\begin{array}{c} \triangleleft \text{wavy} \triangleright \end{array} = \frac{s(2\lambda)s(3\lambda)s(7\lambda)}{s(\lambda)s(5\lambda)s(6\lambda)} \begin{array}{c} \triangleleft \bullet \triangleright \\ \bullet \end{array} + \frac{s(2\lambda)s(3\lambda)}{s(5\lambda)s(6\lambda)} \begin{array}{c} \triangleleft \curvearrowright \triangleright \\ \bullet \end{array}. \quad (2.3.17b)$$

We have the relations

$$\begin{array}{c} \triangleleft \square \triangleright \\ \bullet \end{array} = \begin{array}{c} \square \\ \text{---} \end{array}, \quad \begin{array}{c} \triangleleft \text{wavy} \triangleright \\ \bullet \end{array} = 1, \quad \begin{array}{c} \text{---} \\ \square \end{array} \begin{array}{c} \triangleleft \square \triangleright \\ \bullet \end{array} = 0, \quad \begin{array}{c} \text{---} \\ \square \end{array} \begin{array}{c} \triangleleft \text{wavy} \triangleright \\ \bullet \end{array} = 0. \quad (2.3.18)$$

The first two identities are used to show that $P^{2,0}$ and $P^{1,1}$ are indeed projectors.

2.3.3 Diagrammatic properties of the boundary operators

Similar relations involving boundary operators (2.3.4) also exist. Some of them involve only boundary operators, whereas others apply to particular combinations of boundary operators and face operators. The first relation is the *crossing symmetry at the boundary*. It is a diagrammatic relation that links boundary operators evaluated at u and $3\lambda - u$:

$$\begin{array}{c} \triangleleft \text{---} \triangleright \\ \text{---} \end{array} \begin{array}{c} \triangleleft \text{---} \triangleright \\ \text{---} \end{array} = \frac{\rho_8(2u - 3\lambda)\bar{\delta}(u - \frac{\lambda}{2})}{\bar{\delta}(\frac{5\lambda}{2} - u)} \begin{array}{c} \triangleleft \text{---} \triangleright \\ \text{---} \end{array}. \quad (2.3.19)$$

In these equations and in others below, the boundary operators are chosen to be of S or C types and the functions $\delta(u)$ and $\bar{\delta}(u)$ are set accordingly from (2.3.5). The boundary operator type S or C stays the same when an equality between tangles is presented. We also note that the function in the right-hand side in fact does not have any pole in u , as the zero in the denominator is cancelled by a zero in the numerator for both the S and C functions. The next relation is the *inversion relation at the boundary*:

$$\begin{array}{c} \triangleleft \text{---} \triangleright \\ u \end{array} \begin{array}{c} \triangleleft \text{---} \triangleright \\ -u \end{array} = \delta(\frac{3\lambda}{2} - u)\delta(\frac{3\lambda}{2} + u) \text{---}. \quad (2.3.20)$$

The boundary operators also satisfy *boundary Yang-Baxter equations*. For example, the left one is

$$(2.3.21)$$

It is by solving this equation that the expressions (2.3.4) for the boundary tile were obtained in [15, 16].

The previous identities are similar to those appearing in other models, for instance in the dense loop models (see for example [4]). In contrast, the following relations are particular to the dilute models. They are analogous to the factorization and push-through properties of the face operator. They do not apply to the boundary operator itself but to specific combinations of tangles which include boundary operators. These combinations will be interpreted as boundary conditions for the first fused transfer matrices in Section 2.4.3. The combinations are

$$(2.3.22a)$$

$$(2.3.22b)$$

The combinations are grouped in pairs linked by crossing symmetry. Starting from any member of a pair, changing the evaluation point respectively as $u \mapsto \lambda - u$ for (2.3.22a) and as $u \mapsto -u$ for (2.3.22b) and then applying a 180° rotation gives the second member. The combinations are also invariant under $u \mapsto u + \pi$. An important property of these combinations is that, similarly to (2.3.10) and (2.3.11) for the face operator, they factorize at some specific values of u into products of tangles that involve either a black triangle or an identity arc. The remarkable values of u at which this occurs depend on the type S or C of the boundary operators.

The following remarkable evaluations apply to the combinations in (2.3.22a), with these objects rewritten as a collection of operators involving black triangles. The evaluations are presented for the rightward pointing triangle, and only the tangles necessary for the factorization are drawn. There are four different values of u for each boundary operator of type S or C. The type of boundary is always specified, and SC indicates that both are allowed. These evaluations are

$$\begin{array}{cc}
 \text{S } u = \frac{\lambda}{2} : & \text{C } u = \frac{\lambda}{2} + \frac{\pi}{2} : \\
 \begin{array}{c} \text{Diagram 1: A rightward triangle with angle } \frac{\lambda}{2} \text{ and } 0 \text{ inside.} \\ \text{Diagram 2: A tangle of two triangles with angle } \frac{5\lambda}{2} \text{ and two black squares.} \end{array} & \begin{array}{c} \text{Diagram 1: A rightward triangle with angle } \frac{\lambda}{2} - \frac{\pi}{2} \text{ and } \pi \text{ inside.} \\ \text{Diagram 2: A tangle of two triangles with angle } \frac{5\lambda}{2} - \frac{\pi}{2} \text{ and two black squares.} \end{array} \\
 = p_1 & = p_1
 \end{array} \tag{2.3.23a}$$

$$\begin{array}{cc}
 \text{S } u = \frac{3\lambda}{2} : & \text{C } u = \frac{3\lambda}{2} + \frac{\pi}{2} : \\
 \begin{array}{c} \text{Diagram 1: A rightward triangle with angles } -\frac{\lambda}{2} \text{ and } 2\lambda \text{ inside.} \\ \text{Diagram 2: A rightward triangle with angle } \frac{3\lambda}{2} \text{ and a black square.} \end{array} & \begin{array}{c} \text{Diagram 1: A rightward triangle with angles } -\frac{\lambda}{2} - \frac{\pi}{2} \text{ and } 2\lambda + \pi \text{ inside.} \\ \text{Diagram 2: A rightward triangle with angle } \frac{3\lambda}{2} - \frac{\pi}{2} \text{ and a black square.} \end{array} \\
 = p_2 & = p_2
 \end{array} \tag{2.3.23b}$$

$$\begin{array}{cc}
 \text{SC } u = \lambda : & \text{SC } u = \lambda + \frac{\pi}{2} : \\
 \begin{array}{c} \text{Diagram 1: A rightward triangle with angles } 0 \text{ and } \lambda \text{ inside.} \\ \text{Diagram 2: A diamond shape with two black squares.} \end{array} & \begin{array}{c} \text{Diagram 1: A rightward triangle with angles } -\frac{\pi}{2} \text{ and } \lambda + \pi \text{ inside.} \\ \text{Diagram 2: A diamond shape with two black squares.} \end{array} \\
 = p_3 & = p_4
 \end{array} \tag{2.3.23c}$$

The weights are

$$p_1 = \frac{s(\lambda)s(2\lambda)s(3\lambda)}{2s(5\lambda)}, \quad p_2 = s(\lambda)s^2(2\lambda)s(3\lambda), \tag{2.3.24a}$$

$$p_3 = s(\lambda)s(2\lambda)\delta\left(\frac{3\lambda}{2}\right), \quad p_4 = s(\lambda)s(2\lambda)\delta\left(\frac{3\lambda}{2} - \frac{\pi}{2}\right). \tag{2.3.24b}$$

As an example, we give the steps leading to the first identity in (2.3.23a), marking each equal sign by

the identity used:

$$\begin{aligned}
 & \text{Triangle}(\lambda/2, 0) \stackrel{(2.3.10)}{=} s(2\lambda)s(3\lambda) \text{Triangle}(\lambda/2) \\
 & \stackrel{(2.3.19)}{=} \frac{s(2\lambda)s(3\lambda)\bar{\delta}(2\lambda)}{\bar{\delta}(0)\rho_8(-2\lambda)} \text{Triangle}(5\lambda/2, 2\lambda) \stackrel{(2.3.11)}{=} p_1 \text{Triangle}(5\lambda/2, \blacksquare, \blacksquare) . \quad (2.3.25)
 \end{aligned}$$

The next remarkable evaluations apply to the objects in (2.3.22b), and the resulting diagrams involve an identity arc. There are only two such values of u for each type of boundary operator. These relations are

$$\begin{aligned}
 \text{SC } u = 0 : & \quad \text{Triangle}(0, 0) = q_1 \text{Triangle}(0, 0) \\
 \text{SC } u = \frac{\pi}{2} : & \quad \text{Triangle}(-\frac{\pi}{2}, \pi) = q_2 \text{Triangle}(-\frac{\pi}{2}, \pi) \quad (2.3.26)
 \end{aligned}$$

A third evaluation point is worth mentioning even if no identity arc is factored. It cancels the combination (2.3.22b) because a loop segment connects to a vacancy:

$$\begin{aligned}
 \text{S } u = \frac{3\lambda}{2} : & \quad \text{Triangle}(-\frac{3\lambda}{2}, 3\lambda) = q_3 \text{Triangle}(-\frac{3\lambda}{2}, 3\lambda) = 0 \\
 \text{C } u = \frac{3\lambda}{2} + \frac{\pi}{2} : & \quad \text{Triangle}(-\frac{3\lambda}{2} - \frac{\pi}{2}, 3\lambda + \pi) = q_3 \text{Triangle}(-\frac{3\lambda}{2} - \frac{\pi}{2}, 3\lambda + \pi) = 0 . \quad (2.3.27)
 \end{aligned}$$

The weights in the previous identities are:

$$q_1 = s(2\lambda)s(3\lambda)\delta\left(\frac{3\lambda}{2}\right) , \quad q_2 = s(2\lambda)s(3\lambda)\delta\left(\frac{3\lambda}{2} - \frac{\pi}{2}\right) , \quad q_3 = s(2\lambda)s^3(3\lambda) . \quad (2.3.28)$$

We note that all these identities for the boundary operators of type C can be recovered from those of type S from the relation

$$\begin{array}{c} \text{(C)} \\ \triangleleft u \end{array} = \begin{array}{c} \text{(S)} \\ \triangleleft u - \frac{\pi}{2} \end{array} . \tag{2.3.29}$$

There are also push-through properties associated to the combinations (2.3.22), which we refer to as *boundary reflection properties*. Let us recall that the push-through properties (2.3.13a) and (2.3.13b) both include a pair of face operators whose evaluation points differ by 2λ or 3λ . The boundary reflection properties include similar shifts, but now in the evaluation points of the boundary operators. The first combination in (2.3.22a) contains two boundary operators shifted by 2λ and satisfies a reflection property for the black triangle for both S and C cases:

$$\begin{array}{c} \triangleleft 3\lambda - u_2 \\ \triangleleft 2u - \lambda \\ \triangleleft 3\lambda - u_0 \end{array} = 2s(2u_{-3})\delta(u_{-5/2})\bar{\delta}(\frac{\lambda}{2} - u)\delta(u_{1/2}) \begin{array}{c} \triangleleft 3\lambda - u_1 \\ \blacksquare \end{array} . \tag{2.3.30}$$

The second reflection property applies to the first object (2.3.22b), to which an identity arc factor is attached. Similarly to (2.3.13b), this combination contains two boundary operators shifted by 3λ and holds for both S and C cases:

$$\begin{array}{c} \triangleleft 3\lambda - u_3 \\ \triangleleft 2u \\ \triangleleft 3\lambda - u_0 \end{array} = -2s(2u_{-3})\delta(u_{-5/2})\delta(u_{-3/2})\bar{\delta}(u_{-1/2})\delta(u_{3/2}) \begin{array}{c} \triangleleft \text{arc} \end{array} . \tag{2.3.31}$$

A straightforward method to prove (2.3.30) and (2.3.31) is to expand each operator in terms of its elementary tiles, and then compute the resulting connectivities using the rules stated in Section 2.2 for the concatenation of diagrams. The coefficients of identical connectivities are added together and simplified. Then the proof consists of checking that identical connectivities on the two sides of the equation have equal coefficients. This method is direct but cumbersome and cannot be easily applied to calculations implying a large number of tangles.

A second method to prove the previous properties will also play an important role in the following sections. A quick presentation is in order. The weights appearing in the face and boundary operators are trigonometric functions, and the spectral parameter u always appears linearly in their arguments. Seen as functions of the new variable $z = e^{iu}$, these operators are thus Laurent polynomials of the form $\sum_{-m \leq i \leq m} C_i z^i$ for some linear combination of tangles C_i and some integer m . Since the weights in the boundary operator contain a single trigonometric function, the boundary triangles in the tangles on the left-hand side of (2.3.30) and (2.3.31) account for polynomials in z of maximal degree $m = 1$. The weights ρ_i have either one or two trigonometric functions whose arguments are linear in u . The face operator in the two tangles is evaluated at $2u - \lambda$ or $2u$ and its coefficients will be polynomials of maximal degree up to $m = 4$. The other faces in the tangles, namely the black triangles and the triangles containing the identity strand, do not depend on u (or z). The tangles in the boundary reflection properties are thus polynomials of the form $\sum_{-m \leq i \leq m} C_i z^i$ with $m = 6$. To determine the coefficients C_i , it is sufficient to check the equality at $2m + 1$ distinct values of z .

As stated earlier, the combinations (2.3.22) are invariant under $u \mapsto u + \pi$. Because the black triangle and the identity arc do not depend on u , the left-hand side of (2.3.30) and (2.3.31) are also invariant under this transformation. However, u and $u + \pi$ respectively lead to $z_1 = e^{iu}$ and $z_2 = e^{i(u+\pi)} = -z_1$, which are not equal. Each evaluation in u with $\text{Re}(u) \in [0, \pi)$ thus gives us two values of z , and it is sufficient to check $m + 1$ values of u in this domain.

Combinations of tangles are easier to compute if the value of the spectral parameter u is such that (i) one of the sides of the identity vanishes trivially or (ii) diagrammatic properties can be used. As an example, one can consider the following evaluation points for (2.3.30) for the boundary of type S:

$$(i): \quad -\frac{\lambda}{2}, \frac{\lambda}{2} + \frac{\pi}{2}, \frac{5\lambda}{2}, 3\lambda, 3\lambda + \frac{\pi}{2}, \quad (ii): \quad \frac{\lambda}{2}, \frac{3\lambda}{2}, \lambda, \lambda + \frac{\pi}{2}. \quad (2.3.32)$$

The right hand side of (2.3.30) vanishes when evaluated at the points (i), and the identities (2.3.23a), (2.3.23b) and (2.3.23c) can be used for the evaluations at points (ii). We do not present the remaining explicit computations. All those points are distinct for λ generic and thus give more than the seven verifications needed. The push-through property (2.3.30) then extends to all λ by continuity.

This technique for proving tangle identities is based on a *polynomial argument* and was introduced in [17], replacing the usual diagrammatic method that consists in expanding all the diagrams and verifying the identity for all u .

2.4 Commuting transfer matrices

The previous sections prepared the ground for introducing the family of commuting transfer matrices of the $A_2^{(2)}$ loop models on the geometry of the strip. In Section 2.4.1, we introduce the fundamental transfer matrix of the model $D(u) = D^{1,0}(u)$. In Section 2.4.2, we give a recursive definition of the

fused transfer matrices $\mathbf{D}^{m,n}(u)$, based on the fusion hierarchy relations and valid for all m, n . Then Section 2.4.3 gives a second equivalent definition for $\mathbf{D}^{2,0}(u)$ and $\mathbf{D}^{1,1}(u)$ that is diagrammatic. In Section 2.4.4, we discuss a formulation of $\mathbf{D}^{m,n}(u)$ in terms of the determinant of a matrix of size $m + n$ whose entries are proportional to \mathbf{I} or $\mathbf{D}(u + k\lambda)$, with $k \in \mathbb{Z}$. In Section 2.4.5, we show that the fused transfer matrices $\mathbf{D}^{m,0}(u)$ with the spectral parameter u specialized to certain special values satisfy reduction relations. In Section 2.4.6, we discuss the braid limits $u \rightarrow \pm i\infty$ of the face and boundary operators and of the fused transfer matrices. Finally, Section 2.4.7 derives the T -systems and Y -systems of equations for this integrable hierarchy of commuting transfer matrices. The technical proofs of some properties of the fused transfer matrices are relegated to Section 2.A. In the proofs here and in the appendix, we assume when needed that the parameter λ is generic, that is, $e^{i\lambda}$ is not a root of unity. The results then extend to roots of unity as the identities under study are between Laurent polynomials in both the variables e^{iu} and $e^{i\lambda}$.

2.4.1 Fundamental transfer tangle

In this section, we define the fundamental transfer matrix $\mathbf{D}(u)$ and discuss some of its important properties. As a first step towards this goal, let us define the following tangle built from $2N$ face operators and two boundary operators:

$$\tilde{\mathbf{D}}(u) = \begin{array}{c} \text{Diagram of the fundamental transfer tangle } \tilde{\mathbf{D}}(u) \end{array} \quad (2.4.1)$$

The tangle $\tilde{\mathbf{D}}(u)$ is an element of $\text{dTL}_N(\beta)$: there are N nodes on its upper edge and N on its lower edge. The tangle depends on the crossing parameter λ , the spectral parameter u and the number of sites N . These parameters λ and N will be fixed throughout, so we only write the dependence on the spectral parameter u explicitly. Each column is assigned an arbitrary inhomogeneity $\xi_{(j)}$. We note that the subscript j in parenthesis is a column label and not a shift in the evaluation of the spectrum parameter. Note that, using crossing symmetry, the arcs in the upper tiles can be moved to the left lower corners at the expense of changing the evaluation points from $u + \xi_{(j)}$ to $3\lambda - u - \xi_{(j)}$. The proofs of certain results below will assume that $\xi_{(j_1)} \neq \xi_{(j_2)}$, however by continuity these results will also hold when two inhomogeneities (or more) coincide. The homogeneous transfer tangle is obtained from $\tilde{\mathbf{D}}(u)$ by setting $\xi_{(j)} \rightarrow 0$ for all j .

The boundary operators are chosen in (2.3.5) to be either of S or C type, and this choice can be different for the two boundaries. This leads to four possible boundary conditions for the transfer tangles, that we gather in two groups: (i) *identical*, for SS and CC, and (ii) *mixed*, for SC and CS. For instance, SC refers to the choice S for the left boundary and to C for the right boundary.

The diagrammatic properties introduced in Section 2.3 result in important properties satisfied by $\tilde{\mathbf{D}}(u)$.

The first one is a crossing symmetry which ties the evaluations of the spectral parameter at u and $3\lambda - u$. The proof follows closely the similar proof given in [30] for Interaction-Round-a-Face models and is a direct consequence of (2.3.7), (2.3.8) and (2.3.19). The crossing symmetry takes different forms depending on the choice of boundaries:

$$\text{SS and CC} \quad \tilde{D}(u) = \tilde{D}(3\lambda - u) , \quad (2.4.2a)$$

$$\text{SC} \quad s\left(u - \frac{\lambda}{2}\right) c\left(\frac{5\lambda}{2} - u\right) \tilde{D}(u) = c\left(u - \frac{\lambda}{2}\right) s\left(\frac{5\lambda}{2} - u\right) \tilde{D}(3\lambda - u) , \quad (2.4.2b)$$

$$\text{CS} \quad c\left(u - \frac{\lambda}{2}\right) s\left(\frac{5\lambda}{2} - u\right) \tilde{D}(u) = s\left(u - \frac{\lambda}{2}\right) c\left(\frac{5\lambda}{2} - u\right) \tilde{D}(3\lambda - u) . \quad (2.4.2c)$$

Note that the pairs of trigonometric factors on the left and right sides of (2.4.2b) and (2.4.2c) are themselves tied by the crossing symmetry $u \mapsto 3\lambda - u$.

Because $\tilde{D}(u)$ is a Laurent polynomial in $z = e^{iu}$, it has no poles for $z \in \mathbb{C}^\times$. We then deduce from (2.4.2b) and (2.4.2c) that $\tilde{D}(u)$ has overall trigonometric factors in the mixed cases. It is convenient to define a renormalized tangle where these factors are removed. The reduced matrices $D(u)$ are defined in the four cases as ¹

$$\text{SS:} \quad D(u) = -\tilde{D}(u) , \quad \text{CC:} \quad D(u) = -\tilde{D}(u) , \quad (2.4.3a)$$

$$\text{SC:} \quad D(u) = \frac{\tilde{D}(u)}{c\left(u - \frac{\lambda}{2}\right) s\left(\frac{5\lambda}{2} - u\right)} , \quad \text{CS:} \quad D(u) = \frac{\tilde{D}(u)}{s\left(u - \frac{\lambda}{2}\right) c\left(\frac{5\lambda}{2} - u\right)} . \quad (2.4.3b)$$

We shall refer to $D(u)$ as the *fundamental transfer tangle* (or transfer matrix). Its symmetry properties can be expressed uniformly for all choices of boundary conditions:

$$\text{crossing symmetry} \quad D(u) = D(3\lambda - u) , \quad (2.4.4a)$$

$$\text{commutativity} \quad [D(u), D(v)] = 0 , \quad (2.4.4b)$$

$$\text{periodicity} \quad D(u) = D(u + \pi) . \quad (2.4.4c)$$

The relation (2.4.4b) is the commutation of two transfer tangles with different spectral parameters. It embodies the integrability of the model and can be proved diagrammatically with (2.3.8) and the Yang-Baxter equations (2.3.9) and (2.3.21). The arguments follow those in section 3.4 of [30]. The periodicity property (2.4.4c) is a consequence of the gauge transformation (2.3.15).

Another feature of the fundamental transfer matrix is that it evaluates to a multiple of the identity at

1. The minus sign for SS and CC is included for convenience, so that the fusion hierarchy relations of Section 2.4.2 are written in a uniform way.

certain special values of u :

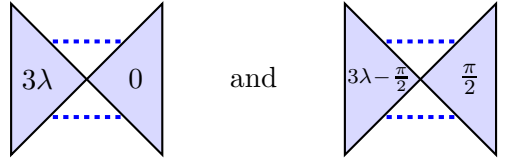
$$\mathbf{D}(0) = f(2\lambda)f(3\lambda)\mathbf{I} \times \frac{s(6\lambda)}{s(2\lambda)} \times \begin{cases} -\frac{s(3\lambda/2)c(\lambda/2)s(5\lambda/2)}{c(3\lambda/2)} & \text{SS,} \\ \frac{c(3\lambda/2)s(\lambda/2)c(5\lambda/2)}{s(3\lambda/2)} & \text{CC,} \\ 1 & \text{SC and CS,} \end{cases} \quad (2.4.5a)$$

$$\mathbf{D}\left(\frac{\pi}{2}\right) = f\left(2\lambda + \frac{\pi}{2}\right)f\left(3\lambda + \frac{\pi}{2}\right)\mathbf{I} \times \frac{s(6\lambda)}{s(2\lambda)} \times \begin{cases} \frac{c(3\lambda/2)s(\lambda/2)c(5\lambda/2)}{s(3\lambda/2)} & \text{SS,} \\ -\frac{s(3\lambda/2)c(\lambda/2)s(5\lambda/2)}{c(3\lambda/2)} & \text{CC,} \\ 1 & \text{SC and CS,} \end{cases} \quad (2.4.5b)$$

where

$$f(u) = \prod_{j=1}^N s(u - \xi_{(j)}) s(u + \xi_{(j)}) . \quad (2.4.6)$$

To obtain these results, one applies the push-through property (2.3.13b) subsequently N times to (2.4.1) specified at $u = 0, \frac{\pi}{2}$, and then evaluates the constant diagrams



$$\quad (2.4.7)$$

Of course, because of the crossing symmetry and periodicity, $\mathbf{D}(u)$ also evaluates to a multiple of the identity at $u = 3\lambda, \pi, 3\lambda + \frac{\pi}{2}$, etc.

It directly follows from the definition (2.4.1) that $\tilde{\mathbf{D}}(u)$ is a Laurent polynomial in $z = e^{iu}$:

$$\tilde{\mathbf{D}}(u) = \sum_{j=-(4N+2)}^{4N+2} C_j z^j , \quad (2.4.8)$$

with coefficients C_j that are elements of $\text{dTL}_N(\beta)$ that depend on λ . As discussed in Section 2.3.3, the degree is fixed by the number of tiles used in the diagrammatic definition. A centered Laurent polynomial such as the one in (2.4.8) is said to have *maximal power* $\max P = 4N + 2$. A consequence of the definitions (2.4.3) is that the maximal power of $\mathbf{D}(u)$ depends on the type of boundary:

$$\text{identical:} \quad \max P(\mathbf{D}(u)) = 4N + 2, \quad \text{mixed:} \quad \max P(\mathbf{D}(u)) = 4N. \quad (2.4.9)$$

We also remark that, because $\max P(s(u_k - \xi_{(j)})) = 1$ for all j , the maximal power of the function $f(u)$ is $2N$. Moreover, all zeros of $f(u)$ are distinct for generic inhomogeneities, an observation that will be useful in the following.

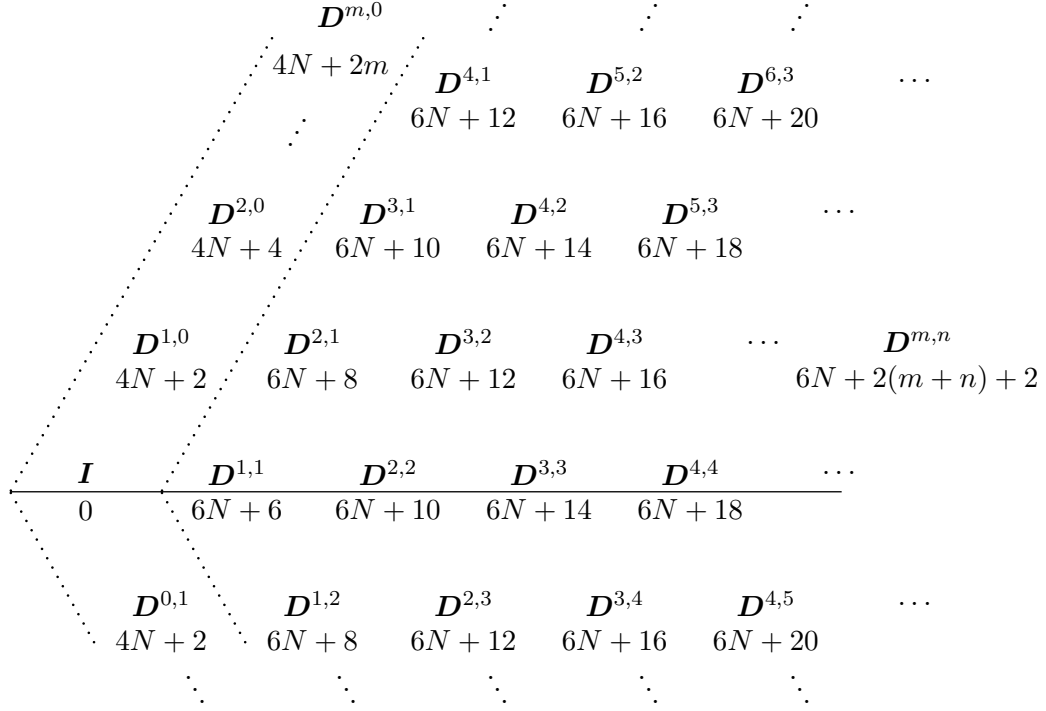


FIGURE 2.1 – The fused transfer matrices and their maximal power (maxP) for identical boundary conditions (SS and CC). The elements near the boundary of the wedge, between the dotted lines, are the fused transfer tangles $D^{m,0}(u)$ and $D^{0,n}(u)$ and their maxP behaves differently to those of the elements $D^{m,n}(u)$, for $m, n > 1$. For mixed boundary conditions (SC and CS), the maximal powers are $4N$ for the fused tangles $D^{m,0}(u)$ or $D^{0,n}(u)$ and $6N$ for $D^{m,n}(u)$ with $m, n \geq 1$. The index of the tangles $D^{m,n}(u)$ are exchanged upon reflection with respect to the horizontal line.

2.4.2 Fusion hierarchy of fused transfer tangles $D^{m,n}(u)$

The *fused transfer tangles* $D^{m,n}(u)$ for the $A_2^{(2)}$ loop models form a commuting family of $d\text{TL}_N(\beta)$ elements. The fused tangles are labelled by pairs of integers (m, n) and depicted on a lattice in Figure 2.1. The fundamental transfer matrix considered as an element of this larger set is labelled as

$$D(u) = D^{1,0}(u) . \quad (2.4.10)$$

The *conjugate fundamental transfer tangle* is defined by

$$D^{0,1}(u) = D^{1,0}(u + \lambda) . \quad (2.4.11)$$

Let us introduce the additional short-hand notations

$$D_k^{m,n} = D^{m,n}(u + k\lambda) , \quad f_k = f(u_k) . \quad (2.4.12)$$

Two techniques were previously used to introduce transfer tangles of loop models with higher fusion indices. For some models, a diagrammatic definition is possible in terms of the appropriate projectors. The recursive relations can then be directly derived by diagrammatic manipulations that use the recursive definition of these projectors. This was achieved for the $A_1^{(1)}$ and $A_2^{(1)}$ loop models, in [10] and [29] respectively.

For the $A_2^{(2)}$ loop models, the appropriate projectors are not all known. An alternative technique was used in [17]: a set of fusion hierarchy relations are written down, these are used as a recursive definition of the fused transfer tangles, and then the desired properties are shown to hold. In this section, we employ the second technique to define the transfer matrices $\mathbf{D}^{m,n}(u)$, with the desired properties given in (2.4.17a) – (2.4.17d).

The fused matrices depend on the choice of boundary conditions for $\mathbf{D}^{1,0}(u)$ and therefore on the corresponding functions defined in (2.3.5). To express the upcoming equations (2.4.15) in a unified manner for all boundary conditions, we introduce four functions in Table 2.1, namely $w(u)$, $\bar{w}(u)$, $w^{(m)}(u_k)$ and $\bar{w}^{(n)}(u_k)$, that differ according to the boundary conditions chosen for $\mathbf{D}^{1,0}(u)$. We stress in particular that the functions $\delta(u)$ and $w(u)$ are not the same. Indeed, the transfer matrix contains two boundary operators, which may or may not be assigned the same choice of $\delta(u)$. In contrast, the functions $w(u)$ and $\bar{w}(u)$ are associated to a pair of boundary conditions for $\mathbf{D}(u)$.

	$w(u)$	$\bar{w}(u)$	$w^{(m)}(u)$	$\bar{w}^{(n)}(u)$
SS	$s(u)$	$c(u)$	$s(u + m\frac{\pi}{2})$	$c(u + n\frac{\pi}{2})$
CC	$c(u)$	$s(u)$	$c(u + m\frac{\pi}{2})$	$s(u + n\frac{\pi}{2})$
SC	1	1	1	1
CS	1	1	1	1

TABLE 2.1 – The weights for the four choices of boundary conditions.

The structure of the fusion hierarchy for the strip geometry is analogous to that of the periodic one (see the set of equations (5.11) in [17]): the shifts in the f functions are identical and the recursion formula for the transfer tangle $\mathbf{D}^{m,n}(u)$ involves the same tangles obtained at a previous step. However, a large number of boundary weights need to be included for the present case with a double-row transfer matrix with boundary operators. Here are the coefficients appearing in the recursive formulas:

$$\begin{aligned}
\alpha^0(u) &= w(u_{-3/2})\bar{w}(u_{1/2})f(u_{-2}) \\
\alpha^1(m, u) &= s(2u_{m-2})s(2u_{2m-5})w^{(m)}(u_{m-5/2})\bar{w}^{(-1)}(u_{2m-9/2})f(u_{2m-5})f(u_{2m-4}) \\
\alpha^2(m, u) &= s(2u_{m-4})s(2u_{2m-3})w^{(m-1)}(u_{m-7/2})\bar{w}(u_{2m-7/2}) \\
\alpha^3(m, u) &= s(2u_{m-5})s(2u_{2m-2})\bar{w}(u_{2m-9/2})w(u_{2m-5/2})f(u_{2m-2})
\end{aligned} \tag{2.4.13a}$$

$$\begin{aligned}
\beta^0(m, u) &= f(u_{2m})f(u_{2m+1}) \\
\beta^1(m, n, u) &= s(2u_{m+n-2})s(2\psi_{2n-2})f(u_{2m-2}) \\
\beta^2(m, n, u) &= s(2u_{m-2})s(2\psi_{n-2})w^{(m)}(u_{m-5/2})w^{(n)}(\psi_{n-5/2}) \\
\beta^3(m, n, u) &= s(2u_{m-4})s(2\psi_{n-4})\bar{w}^{(m)}(u_{m-7/2})\bar{w}^{(n)}(\psi_{n-7/2}) \\
&\quad \times \bar{w}(u_{2m-3/2})\bar{w}(\psi_{2n-3/2})w(u_{2m-1/2})w(\psi_{2n-1/2}).
\end{aligned} \tag{2.4.13b}$$

Equation (2.4.4a) states the crossing symmetry of the fundamental tangle $\mathbf{D}^{1,0}(u)$. As will be seen below, the fused tangles $\mathbf{D}^{m,n}(u)$ satisfy a crossing symmetry extending (2.4.17a), with a shift that depends on the fusion indices. This symmetry will describe how $\mathbf{D}^{m,n}(u)$ behaves under

$$u \mapsto \psi = (4 - 2m - 2n)\lambda - u. \tag{2.4.14}$$

This new variable ψ already appears in several of the functions β^j . The fusion hierarchy relations defining $\mathbf{D}^{m,n}(u)$ are expressed in terms of the functions α^i and the β^j , and their form depends crucially on the position of the label (m, n) in Figure 2.1, namely:

(i) for the elements near the wedge of the region:

$$\alpha^1(2, u)\mathbf{D}_0^{2,0} = \alpha^2(2, u)\mathbf{D}_0^{1,0}\mathbf{D}_2^{1,0} - \alpha^3(2, u)\alpha^0(u_{-1})\mathbf{D}_0^{0,1}, \tag{2.4.15a}$$

$$\beta^1(1, 1, u)\mathbf{D}_0^{1,1} = \beta^2(1, 1, u)\mathbf{D}_0^{1,0}\mathbf{D}_2^{0,1} - \beta^3(1, 1, u)\beta^0(1, u)\beta^0(1, \psi)\mathbf{I}, \tag{2.4.15b}$$

$$\alpha^1(2, \psi)\mathbf{D}_0^{0,2} = \alpha^2(2, \psi)\mathbf{D}_0^{0,1}\mathbf{D}_2^{0,1} - \alpha^3(2, \psi)\alpha^0(\psi_{-1})\mathbf{D}_2^{1,0}, \tag{2.4.15c}$$

(ii) for the elements at the boundary of the region:

$$\alpha^1(m, u)\mathbf{D}_0^{m,0} = \alpha^2(m, u)\mathbf{D}_0^{m-1,0}\mathbf{D}_{2m-2}^{1,0} - \alpha^3(m, u)\mathbf{D}_0^{m-2,1}, \quad m > 2, \tag{2.4.15d}$$

$$\alpha^1(n, \psi)\mathbf{D}_0^{0,n} = \alpha^2(n, \psi)\mathbf{D}_0^{0,1}\mathbf{D}_2^{0,n-1} - \alpha^3(n, \psi)\mathbf{D}_2^{1,n-2}, \quad n > 2, \tag{2.4.15e}$$

(iii) for the elements adjacent to a boundary elements:

$$\beta^1(m, 1, u)\mathbf{D}_0^{m,1} = \beta^2(m, 1, u)\mathbf{D}_0^{m,0}\mathbf{D}_{2m}^{0,1} - \beta^3(m, 1, u)\beta^0(m, u)\mathbf{D}_0^{m-1,0}, \quad m > 1, \tag{2.4.15f}$$

$$\beta^1(n, 1, \psi)\mathbf{D}_0^{1,n} = \beta^2(n, 1, \psi)\mathbf{D}_0^{1,0}\mathbf{D}_2^{0,n} - \beta^3(n, 1, \psi)\beta^0(n, \psi)\mathbf{D}_4^{0,n-1}, \quad n > 1, \tag{2.4.15g}$$

(iv) elsewhere:

$$\beta^1(m, n, u)\mathbf{D}_0^{m,n} = \beta^2(m, n, u)\mathbf{D}_0^{m,0}\mathbf{D}_{2m}^{0,n} - \beta^3(m, n, u)\mathbf{D}_0^{m-1,0}\mathbf{D}_{2m+2}^{0,n-1}, \quad m, n > 1. \tag{2.4.15h}$$

All matrices are evaluated at u in (2.4.15). The coefficients α^i apply to the boundary segments of the region shown in Figure 2.1 and the coefficients β^i are for every other fused tangles (anywhere inside

the region). We note that the fusion hierarchy relations are divided in these many cases because of the different maximal degrees of the transfer tangles $\mathbf{D}^{m,0}(u)$ and $\mathbf{D}^{0,n}(u)$ compared to $\mathbf{D}^{m,n}(u)$ with $m, n \geq 1$. The functions α^i and β^j then compensate for these degrees accordingly: $\alpha^1, \alpha^2, \alpha^3$ and β^0 for the relations labeled by pairs (m, n) near the boundary of the wedge in Figure 2.1, and α^0 and β^0 near the corner.

In (2.4.15), ψ sometimes appears as the evaluation point for some functions α^i . The integers m and n needed to compute ψ are then the ones of the fused tangle created by the fusion hierarchy, that is, the one appearing on the left-hand side of each equation. The m and n in the definition of ψ are thus the same throughout a given equation. The notation ψ is handy, but somewhat dangerous as the operation $u \mapsto \psi$ does not commute with that of shifting $u \mapsto u_k = u + k\lambda$. Unless stated otherwise, the operation $u \mapsto \psi$ in these expressions is the last to be performed. For example, the function $\alpha^0(\psi_{-1})$ appears in (2.4.15c) where $m = 0$ and $n = 2$ and thus $\psi = -u$. This function for SS boundary conditions is

$$\begin{aligned}
\alpha^0(\psi_{-1}) &= \alpha^0(u_{-1})|_{u \mapsto \psi = -u} \\
&= \left(w(u_{-3/2}) \bar{w}(u_{1/2}) f(u_{-2}) \right)_{-1} |_{u \mapsto \psi = -u} \\
&= s\left(u - \frac{5\lambda}{2}\right) c\left(u - \frac{\lambda}{2}\right) f(u - 3\lambda) |_{u \mapsto \psi = -u} \\
&= -s\left(u + \frac{5\lambda}{2}\right) c\left(u + \frac{\lambda}{2}\right) f(u + 3\lambda) ,
\end{aligned} \tag{2.4.16}$$

where we used $f(-u) = f(u)$.

The weights β^j appear in pairs invariant under $u \mapsto (4 - 2m + 2n)\lambda - u$ and $m \leftrightarrow n$. For this reason, a relation between $\mathbf{D}^{m,n}(u)$ and $\mathbf{D}^{n,m}(\psi)$ becomes apparent, at least for the pair of equations (2.4.15f) and (2.4.15g), and for the fused tangles defined with (2.4.15h). This property, the generalization of the crossing symmetry (2.4.4a), is proved in Section 2.A.1. Thus, any two tangles $\mathbf{D}^{m,n}(u)$ and $\mathbf{D}^{n,m}(u)$ that appear in Figure 2.1 as mirror images through the horizontal line are related by crossing-symmetry.

Figure 2.1 also gives the maximal power $\max P$ of the fused tangles for identical boundary conditions (SS or CC) in the variable $z = e^{iu}$ introduced earlier. These maximal degrees should be contrasted with those of the periodic case obtained in [17]. In the latter case, fused matrices have different polynomial degrees: the ones with labels on a boundary of the region have $\max P = 2N$, and all the others have $\max P = 3N$. For the strip geometry, the cases of identical and mixed boundaries need to be distinguished. The mixed cases behave in a way similar to the periodic geometry: the maximal powers of the fused transfer matrices are respectively $4N$ and $6N$ on the boundary and inside the region. The identical cases do not behave as nicely, and the maximal power of $\mathbf{D}^{m,n}(u)$ increases linearly with the fusion indices, as $4N + 2m$ for the cases $(m, 0)$ and $(0, m)$, and as $6N + 2(m + n) + 2$ for (m, n) with $m, n \geq 1$.

The fused matrices satisfy the following properties for all fusion indices m, n :

$$\text{crossing symmetry} \quad \mathbf{D}^{m,n}(u) = \mathbf{D}^{n,m}((4 - 2m - 2n)\lambda - u), \quad (2.4.17a)$$

$$\text{commutativity} \quad [\mathbf{D}^{m,n}(u), \mathbf{D}^{m',n'}(v)] = 0, \quad (2.4.17b)$$

$$\text{periodicity} \quad \mathbf{D}^{m,n}(u) = \mathbf{D}^{m,n}(u + \pi), \quad (2.4.17c)$$

$$\text{conjugacy} \quad \mathbf{D}^{0,n}(u) = \mathbf{D}^{n,0}(u + \lambda), \quad (2.4.17d)$$

$$\text{polynomiality} \quad \text{The coefficients of } \mathbf{D}^{m,n}(u) \text{ are Laurent polynomials in } z. \quad (2.4.17e)$$

These equations generalize the properties (2.4.4a) to (2.4.4c) of the tangle $\mathbf{D}^{1,0}(u)$. The first one is the crossing symmetry discussed above and its proof is given in Section 2.A.1. The second is the commutation that holds for any integers m, n, m', n' and spectral parameters u, v . This property follows directly from (2.4.4b), since the fused transfer tangles are all expressible in terms of the fundamental transfer tangle evaluated at different values of u . The third one, the periodicity, follows similarly from (2.4.4c). The proof of the conjugacy linking $\mathbf{D}^{0,n}(u)$ and $\mathbf{D}^{n,0}(u + \lambda)$ is non-trivial and relegated to Section 2.A.2. Likewise, the polynomial properties $\mathbf{D}^{m,n}(u)$ are not obvious and will be the topic of Section 2.5.

2.4.3 Diagrammatic definition of $\mathbf{D}^{2,0}(u)$ and $\mathbf{D}^{1,1}(u)$

In this section, we focus on the first fused transfer matrices $\mathbf{D}^{2,0}(u)$ and $\mathbf{D}^{1,1}(u)$, for which the projectors $P^{2,0}$ and $P^{1,1}$ are known [17]. This allows us to give a diagrammatic definition for these two transfer matrices:

$$\mathbf{D}^{2,0}(u) = \frac{1}{Z^{2,0}(u)} \left(\begin{array}{c} \text{Diagrammatic representation of } \mathbf{D}^{2,0}(u) \end{array} \right), \quad (2.4.18a)$$

$$D^{1,1}(u) = \frac{1}{Z^{1,1}(u)} \left(\begin{array}{c} \text{Diagram with triangles and a grid of boxes} \end{array} \right), \quad (2.4.18b)$$

The diagram shows a central grid of boxes with four rows and four columns. The top row contains boxes with labels $u_3 + \xi_{(1)}, u_3 + \xi_{(2)}, \dots, u_3 + \xi_{(N)}$. The second row contains $u_0 + \xi_{(1)}, u_0 + \xi_{(2)}, \dots, u_0 + \xi_{(N)}$. The third row contains $u_3 - \xi_{(1)}, u_3 - \xi_{(2)}, \dots, u_3 - \xi_{(N)}$. The bottom row contains $u_0 - \xi_{(1)}, u_0 - \xi_{(2)}, \dots, u_0 - \xi_{(N)}$. To the left of the grid is a triangle with vertices labeled $3\lambda - u_3$, $2u$, and $3\lambda - u_0$. To the right is a triangle with vertices labeled u_3 , $-2u$, and u_0 . Dotted blue lines connect the vertices of the triangles to the boxes in the grid. A small red rectangle is positioned below the first column of the grid.

where

$$Z^{2,0}(u) = 4s(2u_{-1})s(2u_0)\delta_L(u_{-3/2})\delta_L(u_{-1/2})\delta_R(u_{-1/2})\delta_R(u_{1/2})f(u_{-1})f(u_0) \times \begin{cases} -1 & \text{SS and CC,} \\ \delta_L(u_{-5/2})\delta_L(u_{1/2})\delta_R(u_{-3/2})\delta_R(u_{3/2}) & \text{SC and CS,} \end{cases} \quad (2.4.19a)$$

$$Z^{1,1}(u) = 4s(2u_0)^2\delta_L(\frac{3\lambda}{2} - u)\delta_R(\frac{3\lambda}{2} + u)f(u_0) \times \begin{cases} -1 & \text{SS and CC,} \\ \delta_L(\frac{\lambda}{2} + u)\delta_R(\frac{\lambda}{2} - u)\delta_L(\frac{3\lambda}{2} + u)\delta_R(\frac{3\lambda}{2} - u)\delta_L(\frac{5\lambda}{2} - u)\delta_R(\frac{5\lambda}{2} + u) & \text{SC and CS.} \end{cases} \quad (2.4.19b)$$

Here we add subscripts L and R to the functions $\delta(u)$ to distinguish contributions coming from the left and right boundaries, thus allowing us to treat all four choices of boundary conditions simultaneously.

We now show that these definitions are equivalent to those presented in Section 2.4.2. In each case, expanding the projector as in (2.3.16) produces two terms:

$$Z^{2,0}(u)D^{2,0}(u) = A_I - A_{II}, \quad Z^{1,1}(u)D^{1,1}(u) = B_I - B_{II}. \quad (2.4.20)$$

Using the notation

$$\boxed{u - \xi} = \boxed{u - \xi_{(1)}} \boxed{u - \xi_{(2)}} \cdots \boxed{u - \xi_{(N)}}, \quad \boxed{u + \xi} = \boxed{u + \xi_{(1)}} \boxed{u + \xi_{(2)}} \cdots \boxed{u + \xi_{(N)}}, \quad (2.4.21)$$

we rewrite A_I as

$$A_I = \left(\begin{array}{c} \text{Diagram with triangles and a grid of boxes} \end{array} \right) = \left(\begin{array}{c} \text{Diagram with triangles and a grid of boxes} \end{array} \right)$$

The diagram shows two equivalent representations of A_I . The left representation features a central grid of four boxes with labels $u_2 + \xi$, $u_0 + \xi$, $u_2 - \xi$, and $u_0 - \xi$. To the left is a triangle with vertices $3\lambda - u_2$, $2u - \lambda$, and $3\lambda - u_0$. To the right is a triangle with vertices u_2 , $\lambda - 2u$, and u_0 . Dotted blue lines connect the vertices to the boxes. The right representation is identical but the central grid is replaced by a diamond shape with vertices $2u - \lambda$ and $\lambda - 2u$.

$$\begin{aligned}
&= \rho_8(2u - \lambda)\rho_8(\lambda - 2u) \begin{array}{c} \text{Diagram with four rows of boxes: } \\ \text{Top row: } u_2 + \xi, \text{ right triangle } u_2, \text{ left triangle } 3\lambda - u_2 \\ \text{Second row: } u_2 - \xi \\ \text{Third row: } u_0 + \xi, \text{ right triangle } u_0, \text{ left triangle } 3\lambda - u_0 \\ \text{Bottom row: } u_0 - \xi \end{array} = \rho_8(2u - \lambda)\rho_8(\lambda - 2u)\tilde{D}_0^{1,0}\tilde{D}_2^{1,0}, \quad (2.4.22)
\end{aligned}$$

where we first applied the Yang-Baxter equation and then the inversion identity. For \mathbf{A}_{II} , we write

$$\begin{aligned}
\mathbf{A}_{\text{II}} &= \begin{array}{c} \text{Diagram with four rows of boxes: } \\ \text{Top row: } u_2 + \xi, \text{ right triangle } u_2, \text{ left triangle } 3\lambda - u_2 \\ \text{Second row: } u_0 + \xi, \text{ right triangle } \lambda - 2u, \text{ left triangle } 2u - \lambda \\ \text{Third row: } u_2 - \xi \\ \text{Bottom row: } u_0 - \xi, \text{ right triangle } u_0, \text{ left triangle } 3\lambda - u_0 \end{array} = \ell(u) \begin{array}{c} \text{Diagram with four rows of boxes: } \\ \text{Top row: } u_2 + \xi, \text{ right triangle } u_2, \text{ left triangle } 3\lambda - u_1 \\ \text{Second row: } u_0 + \xi, \text{ right triangle } \lambda - 2u, \text{ left triangle } 1 \\ \text{Third row: } u_2 - \xi \\ \text{Bottom row: } u_0 - \xi, \text{ right triangle } u_0, \text{ left triangle } 1 \end{array} \\
&= \ell(u)t(u) \begin{array}{c} \text{Diagram with four rows of boxes: } \\ \text{Top row: } u_1 + \xi, \text{ right triangle } u_2, \text{ left triangle } 3\lambda - u_1 \\ \text{Second row: } u_2 - \xi, \text{ right triangle } \lambda - 2u, \text{ left triangle } 1 \\ \text{Third row: } u_0 - \xi \\ \text{Bottom row: } u_0 - \xi, \text{ right triangle } u_0, \text{ left triangle } 1 \end{array} = \ell(u)t(u)r(u) \begin{array}{c} \text{Diagram with four rows of boxes: } \\ \text{Top row: } u_1 + \xi, \text{ right triangle } u_1, \text{ left triangle } 3\lambda - u_1 \\ \text{Second row: } u_2 - \xi, \text{ right triangle } \lambda - 2u, \text{ left triangle } 1 \\ \text{Third row: } u_0 - \xi \\ \text{Bottom row: } u_0 - \xi, \text{ right triangle } u_1, \text{ left triangle } 1 \end{array} \\
&= \ell(u)t(u)r(u)b(u) \begin{array}{c} \text{Diagram with four rows of boxes: } \\ \text{Top row: } u_1 + \xi, \text{ right triangle } u_1, \text{ left triangle } 3\lambda - u_1 \\ \text{Second row: } u_1 - \xi, \text{ right triangle } u_1, \text{ left triangle } 1 \\ \text{Third row: } u_1 - \xi \\ \text{Bottom row: } u_1 - \xi, \text{ right triangle } u_1, \text{ left triangle } 1 \end{array} = \ell(u)t(u)r(u)b(u)\tilde{D}_0^{0,1}. \quad (2.4.23)
\end{aligned}$$

Here we applied the push-through property N times on the top and bottom of the diagram, at the third and fifth equality. The resulting functions $t(u)$ and $b(u)$ are obtained from (2.3.13a) and satisfy $t(u)b(u) = f(u_{-3})f(u_2)$. Similarly, the factors $\ell(u)$ and $r(u)$ arose at the second and fourth equality from the application of the boundary reflection property on the left and right boundary, respectively, and are read off from (2.3.30):

$$\ell(u) = 2s(2u_{-3})\delta_L(u_{-5/2})\bar{\delta}_L(\frac{\lambda}{2} - u)\delta_L(u_{1/2}), \quad r(u) = \ell(\lambda - u)|_{\delta_L \rightarrow \delta_R}. \quad (2.4.24)$$

Finally, we used (2.3.18) at the last step and obtained $\tilde{D}_1^{1,0} = \tilde{D}_0^{0,1}$. The final result is an iden-

tity relating $D_0^{2,0}$, $D_0^{1,0}D_2^{1,0}$ and $D_0^{0,1}$ which precisely reproduces (2.4.15a) after simplification of the trigonometric prefactors.

The same arguments can be applied to compute B_I and B_{II} , leading to

$$B_I = \rho_8(2u)\rho_8(-2u)\tilde{D}_0^{1,0}\tilde{D}_3^{1,0}, \quad B_{II} = \tilde{\ell}(u)\tilde{t}(u)\tilde{r}(u)\tilde{b}(u)\mathbf{I}, \quad (2.4.25)$$

with $\tilde{t}(u)\tilde{b}(u) = f(u_{-3})f(u_{-2})f(u_2)f(u_3)$ and the functions $\tilde{\ell}(u)$ and $\tilde{r}(u) = \tilde{\ell}(-u)|_{\delta_L \rightarrow \delta_R}$ read off from (2.3.31). After simplification of the prefactors, the resulting relation is found to be exactly (2.4.15b). This then confirms that the recursive and diagrammatic definitions are equivalent, for both $D^{2,0}(u)$ and $D^{1,1}(u)$.

We stress that we still have not proven that $D^{2,0}(u)$ and $D^{1,1}(u)$ are Laurent polynomials in $z = e^{iu}$. Indeed, both the recursive and diagrammatic definitions involve denominators written in terms of trigonometric functions of u that could potentially lead to singularities. Showing the polynomiality of the fused transfer matrices is a non-trivial task which is addressed in Section 2.5. Finally, we note that it is also possible to give diagrammatic definitions of $D^{m,0}(u)$ for $m > 2$ using the projectors in the Appendix A of [17], however these expressions are not needed in this paper.

2.4.4 Determinantal form of the fused tangles

The fusion relations define recursively the fused transfer tangles as polynomials in the elementary transfer tangles $D^{1,0}(u)$. In this section, we write $D^{m,n}(u)$ in terms of a formal determinant and use it to rewrite the fusion hierarchy (2.4.15). The proof of these determinant formulas is sketched at the end the section.

The determinants are expressed in terms of the following quantities:

$$\mathcal{D}(u) = s(2u_{-4})s(2u_1)\bar{w}(u_{-3/2})w^{(1)}(u_{-3/2})D_0^{1,0}(u) = \det(1,0)(u), \quad (2.4.26a)$$

$$\mathcal{F}(u) = s(2u_{-4})s(2u_3)w(u_{-5/2})w(u_{3/2})\bar{w}(u_{-3/2})\bar{w}(u_{1/2})f(u_{-3})f(u_2)\mathbf{I}. \quad (2.4.26b)$$

We often use the shorthand notation $\mathcal{D}_k = \mathcal{D}(u_k)$ and $\mathcal{F}_k = \mathcal{F}(u_k)$. These new functions satisfy

$$\mathcal{D}(u) = \mathcal{D}(3\lambda - u), \quad \mathcal{D}(u) = \mathcal{D}(u + \pi), \quad (2.4.26c)$$

$$\mathcal{F}(u) = \mathcal{F}(\lambda - u), \quad \mathcal{F}(u) = \mathcal{F}(u + \pi). \quad (2.4.26d)$$

The fused transfer matrices will be written in terms of two families of determinants. The first is for fused tangles with indices $(m,0)$ and $(0,n)$ corresponding to the boundary of the domain depicted

in Figure 2.1:

$$\det(m, 0)(u) = \begin{vmatrix} \mathcal{D}_{2m-2} & \mathcal{D}_{2m-3} & \mathcal{F}_{2m-5} & 0 & 0 & 0 \\ \mathcal{F}_{2m-4} & \mathcal{D}_{2m-4} & \mathcal{D}_{2m-5} & \mathcal{F}_{2m-7} & 0 & 0 \\ 0 & \mathcal{F}_{2m-6} & \mathcal{D}_{2m-6} & \mathcal{D}_{2m-7} & \ddots & 0 \\ 0 & 0 & \ddots & \ddots & \ddots & \mathcal{F}_1 \\ 0 & 0 & 0 & \mathcal{F}_2 & \mathcal{D}_2 & \mathcal{D}_1 \\ 0 & 0 & 0 & 0 & \mathcal{F}_0 & \mathcal{D}_0 \end{vmatrix}, \quad (2.4.27a)$$

$$\det(0, n)(u) = \det(n, 0)(4\lambda - 2n\lambda - u). \quad (2.4.27b)$$

The matrix in the determinant $\det(m, 0)_0$ has size $m \times m$. Like for the functions $\mathcal{F}(u)$ and $\mathcal{D}(u)$, we will use the notation $\det(m, 0)_k = \det(m, 0)(u_k)$.

The first determinant is tied to the fused matrix $\mathbf{D}^{m,0}(u)$ by

$$\begin{aligned} \det(m, 0)_0 &= s(2u_{-4})s(2u_{2m-1})w^{(m)}(u_{m-5/2})\mathbf{D}^{m,0}(u) \\ &\times \left(\prod_{j=0}^{m-2} s(2u_j) \right) \left(\prod_{j=m-3}^{2m-5} s(2u_j) \right) \left(\prod_{l=-1}^{2m-4} f(u_l) \right) \left(\prod_{k=0}^{m-1} \bar{w}(u_{2k-3/2}) \right) \left(\prod_{k=0}^{m-2} w(u_{2k-1/2}) \right). \end{aligned} \quad (2.4.28)$$

We postpone the (sketch of the) proof of this statement until the end of the section.

The definition $\det(0, n)(u)$ as $\det(n, 0)(\psi)$, with $\psi = 4\lambda - 2n\lambda - u$, ensures that the crossing symmetry (2.4.17a) is realized. Moreover, this first family of determinants has the property

$$\det(0, n)_0 = \det(n, 0)_1. \quad (2.4.29)$$

The proof is given in Section 2.A.2. The property $\mathbf{D}_0^{0,n} = \mathbf{D}_1^{n,0}$ for $n > 1$ is also proved in Section 2.A.2.

The second family of determinants is

$$\det(m, n)(u) = \begin{vmatrix} \ddots & \ddots & \mathcal{F}_{2m+2} & 0 & 0 & 0 & 0 \\ \ddots & \ddots & \mathcal{D}_{2m+2} & 0 & 0 & 0 & 0 \\ 0 & \mathcal{F}_{2m+1} & \mathcal{D}_{2m+1} & \mathcal{F}_{2m-1} & 0 & 0 & 0 \\ \hline 0 & 0 & \mathcal{F}_{2m-2} & \mathcal{D}_{2m-2} & \mathcal{D}_{2m-3} & \mathcal{F}_{2m-5} & 0 \\ 0 & 0 & 0 & \mathcal{F}_{2m-4} & \ddots & \ddots & \ddots \end{vmatrix} \quad (2.4.30a)$$

$$= \begin{vmatrix} \boxed{\det(n, 0)_{2m+1}} & 0 & 0 & 0 \\ 0 & 0 & 0 & 0 \\ 0 & 0 & \mathcal{F}_{2m-2} & 0 \\ 0 & 0 & 0 & \boxed{\det(m, 0)_0} \end{vmatrix}. \quad (2.4.30b)$$

It applies to all fusion pairs (m, n) with $m, n > 1$, corresponding to the positions in Figure 2.1 that do not touch the edge of the wedge. The bottom-right and the top-left blocks are of size $m \times m$ and $n \times n$ respectively. The determinant (2.4.30a) and the fused matrix $\mathbf{D}^{m,n}(u)$ are related by

$$\begin{aligned} s(2u_{2m-4})s(2\psi_{2n-4}) \det(m, n)(u) = & \quad (2.4.31) \\ & s(2u_{-4})s(2\psi_{-4})s(2u_{m-3})s(2\psi_{n-3})s(2u_{m+n-2})s(2\psi_{2n-2})f(u_{2m-2})\mathbf{D}^{m,n}(u) \\ & \times \left(\prod_{j=0}^{2m-3} s(2u_j) \right) \left(\prod_{k=0}^{m-1} \bar{w}(u_{2k-3/2}) \right) \left(\prod_{k=0}^{m-2} w(u_{2k-1/2}) \right) \left(\prod_{l=-1}^{2m-4} f(u_l) \right) \\ & \times \left(\prod_{j=0}^{2n-3} s(2\psi_j) \right) \left(\prod_{k=0}^{n-1} \bar{w}(\psi_{2k-3/2}) \right) \left(\prod_{k=0}^{n-2} w(\psi_{2k-1/2}) \right) \left(\prod_{l=-1}^{2n-4} f(\psi_l) \right), \end{aligned}$$

with $\psi = (4 - 2m - 2n)\lambda - u$. We note that the right-hand side of (2.4.31) always contains factors $s(2u_{2m-4})s(2\psi_{2n-4})$, even for $m = 1$ or $n = 1$. It is however easier to leave them as prefactors on the left-hand side instead of identifying in which factor they appear in the right-hand side, as this depends on m and n .

These determinants satisfy a number of recurrence relations. The following ones express the fusion hierarchies in a unified manner, namely for all four choices of boundary conditions and independently of the position of the label (m, n) in Figure 2.1:

$$\det(m, 0)_0 = \mathcal{D}_{2m-2} \det(m-1, 0)_0 - \mathcal{F}_{2m-4} \det(m-2, 1)_0, \quad (2.4.32a)$$

$$\det(0, n)_0 = \mathcal{D}_1 \det(0, n-1)_2 - \mathcal{F}_1 \det(1, n-2)_2, \quad (2.4.32b)$$

$$\begin{aligned} \det(m, n)_0 = & \det(m, 0)_0 \det(0, n)_{2m} \\ & - \mathcal{F}_{2m-2} \mathcal{F}_{2m-1} \det(m-1, 0)_0 \det(0, n-1)_{2m+2}. \end{aligned} \quad (2.4.32c)$$

These relations are valid for $m, n \geq 1$, with the convention

$$\det(0, 0)_k = 1, \quad \det(m, -1)_k = \det(-1, n)_k = 0. \quad (2.4.33)$$

The relations (2.4.32a) and (2.4.32b) are respectively obtained by expanding $\det(m, 0)_0$ and $\det(0, n)_0$ along the first row and the last column. Expanding with respect to the first column after the dashed

line leads to (2.4.32c). Two additional useful recurrence relations are

$$\begin{aligned} \det(m, 0)_0 &= \mathcal{D}_{2m-2} \det(m-1, 0)_0 \\ &\quad - \mathcal{F}_{2m-4} (\mathcal{D}_{2m-3} \det(m-2, 0)_0 - \mathcal{F}_{2m-6} \mathcal{F}_{2m-5} \det(m-3, 0)_0), \end{aligned} \quad (2.4.34a)$$

$$\det(m, 0)_0 = \mathcal{D}_0 \det(m-1, 0)_2 - \mathcal{F}_0 (\mathcal{D}_1 \det(m-2, 0)_4 - \mathcal{F}_1 \mathcal{F}_2 \det(m-3, 0)_6), \quad (2.4.34b)$$

with $m \geq 2$. The first is a rewriting of (2.4.32a) and the second is obtained from the determinant (2.4.27a) by an expansion along the last column.

The symmetry properties of the determinants are analogous to those satisfied by the fused transfer matrices. These are expressed in a form that is independent of the choice of boundary conditions:

$$\text{crossing symmetry} \quad \det(m, n)(u) = \det(n, m)((4 - 2m - 2n)\lambda - u), \quad (2.4.35a)$$

$$\text{commutativity} \quad [\det(m, n)(u), \det(m', n')(v)] = 0, \quad (2.4.35b)$$

$$\text{periodicity} \quad \det(m, n)(u) = \det(m, n)(u + \pi), \quad (2.4.35c)$$

$$\text{conjugacy} \quad \det(0, n)(u) = \det(n, 0)(u + \lambda). \quad (2.4.35d)$$

We end this section by sketching the proof of the relations (2.4.28) and (2.4.31) that relate the formal determinants and the fused transfer matrices. For (2.4.28), the proof is done by induction on m using (2.4.34a). The seed cases $m = 1$ and $m = 2$ are first checked separately. For $m = 1$, (2.4.28) follows directly from the definition of $\mathcal{D}(u)$. For $m = 2$, we check that (2.4.32a) reduces to (2.4.15a) using (2.4.28). For $m \geq 3$, the proof proceeds using the induction hypothesis (2.4.28) for $m' < m$. With (2.4.15d) and (2.4.15f), one first derives a new relation that ties $\mathbf{D}^{m,0}(u)$, $\mathbf{D}^{m-1,0}(u)$, $\mathbf{D}^{m-2,0}(u)$ and $\mathbf{D}^{m-3,0}(u)$. Then we must show that (2.4.34a) reduces to this relation upon applying (2.4.28). Each step is straightforward and tedious, and amounts to writing the prefactors for each fused transfer matrix, cancelling the common terms, and then checking that the remaining ones precisely match those in the new relation. We omit the details of this calculation, which in the end proves (2.4.28). The similar result for $m, n \geq 1$, namely the relation (2.4.31), is proved using the same idea. We use (2.4.32c) to expand $\det(m, n)_0$, and then (2.4.28) to express all the determinants in terms of the fused transfer matrices. After the cancellation of many common terms, one obtains (2.4.15f), (2.4.15g) or (2.4.15h) depending on the fusion indices (m, n) .

2.4.5 Reduction relations

In this subsection, we study properties of the fused transfer matrices $\mathbf{D}^{m,0}(u)$ at specific values $u = \hat{u}$ of the spectral parameter. We find that $\mathbf{D}^{m,0}(\hat{u})$ is proportional to a fused transfer matrix with the index m reduced by 3. We refer to these identities as *reduction relations*. Applying these relations repeatedly, we find that $\mathbf{D}^{m,0}(\hat{u})$ is proportional to the unit \mathbf{I} . To proceed, we first write down the

functional relations

$$\mu^1(m, u) \mathbf{D}_0^{m,0} = \mu^2(m, u) \mathbf{D}_0^{m-1,0} \mathbf{D}_{2m-2}^{1,0} - \mu^3(m, u) \mathbf{D}_0^{m-2,0} \mathbf{D}_{2m-3}^{1,0} + \mu^4(m, u) \mathbf{D}_0^{m-3,0}, \quad (2.4.36a)$$

$$\nu^1(m, u) \mathbf{D}_0^{m,0} = \nu^2(m, u) \mathbf{D}_0^{1,0} \mathbf{D}_2^{m-1,0} - \nu^3(m, u) \mathbf{D}_1^{1,0} \mathbf{D}_4^{m-2,0} + \nu^4(m, u) \mathbf{D}_6^{m-3,0}, \quad (2.4.36b)$$

where

$$\mu^1(m, u) = w(u_{2m-9/2}) w^{(m)}(u_{m-5/2}) s(2u_{m-3}) s(2u_{m-2}) s(2u_{2m-6}) s(2u_{2m-5}) f_{2m-6} f_{2m-5} f_{2m-4}, \quad (2.4.37a)$$

$$\mu^2(m, u) = w^{(1)}(u_{2m-7/2}) w^{(m-1)}(u_{m-7/2}) s(2u_{m-4}) s(2u_{m-3}) s(2u_{2m-6}) s(2u_{2m-3}) f_{2m-6}, \quad (2.4.37b)$$

$$\begin{aligned} \mu^3(m, u) &= w(u_{2m-5/2}) \bar{w}(u_{2m-9/2}) w^{(1)}(u_{2m-9/2}) w^{(m-2)}(u_{m-9/2}) s(2u_{m-5}) s(2u_{m-4}) \\ &\quad s(2u_{2m-5}) s(2u_{2m-2}) f_{2m-2}, \end{aligned} \quad (2.4.37c)$$

$$\begin{aligned} \mu^4(m, u) &= w(u_{2m-15/2}) w(u_{2m-9/2}) w(u_{2m-7/2}) w(u_{2m-5/2}) \bar{w}(u_{2m-13/2}) \bar{w}(u_{2m-11/2}) \bar{w}(u_{2m-9/2}) \\ &\quad w^{(m-3)}(u_{m-11/2}) s(2u_{m-6}) s(2u_{m-5}) s(2u_{2m-3}) s(2u_{2m-2}) f_{2m-4} f_{2m-3} f_{2m-2}, \end{aligned} \quad (2.4.37d)$$

and

$$\nu^1(m, u) = w(u_{-1/2}) w^{(m)}(u_{m-5/2}) s(2u_0) s(2u_1) s(2u_{m-3}) s(2u_{m-2}) f_{-1} f_0 f_1, \quad (2.4.38a)$$

$$\nu^2(m, u) = w^{(1)}(u_{-3/2}) w^{(m-1)}(u_{m-3/2}) s(2u_{-2}) s(2u_1) s(2u_{m-2}) s(2u_{m-1}) f_1, \quad (2.4.38b)$$

$$\nu^3(m, u) = w(u_{-5/2}) \bar{w}(u_{-1/2}) w^{(1)}(u_{-1/2}) w^{(m-2)}(u_{m-1/2}) s(2u_{-3}) s(2u_0) s(2u_{m-1}) s(2u_m) f_{-3}, \quad (2.4.38c)$$

$$\begin{aligned} \nu^4(m, u) &= w(u_{-5/2}) w(u_{-3/2}) w(u_{-1/2}) w(u_{5/2}) \bar{w}(u_{-1/2}) \bar{w}(u_{1/2}) \bar{w}(u_{3/2}) w^{(m-3)}(u_{m+1/2}) \\ &\quad s(2u_{-3}) s(2u_{-2}) s(2u_m) s(2u_{m+1}) f_{-3} f_{-2} f_{-1}. \end{aligned} \quad (2.4.38d)$$

These are obtained by two possible methods: (i) by combining the fusion hierarchy relations for $\mathbf{D}^{m,0}(u)$, $\mathbf{D}^{m-2,1}(u)$ and $\mathbf{D}^{1,m-2}(u)$, or (ii) by simplifying the common prefactors in (2.4.34). The above equations hold for $m \geq 4$, but also for $m = 2, 3$ with the identifications $\mathbf{D}_k^{0,0} \mapsto f_{k-2} f_{k-3} \mathbf{I}$ and $\mathbf{D}_k^{-1,0} \mapsto 0$. Moreover, we remark that the relations (2.4.36a) and (2.4.36b) are related by a crossing symmetry linking the evaluations at u and $(5 - 2m)\lambda - u$.

These relations allow us to derive *reduction relations* for the fused transfer tangles. For instance, we note that

$$\begin{aligned} \mu^2(m, \hat{u}) = \mu^3(m, \hat{u}) = 0 &\quad \text{for } \hat{u} = (4 - m)\lambda + \frac{r\pi}{2}, \\ \nu^2(m, \hat{v}) = \nu^3(m, \hat{v}) = 0 &\quad \text{for } \hat{v} = (1 - m)\lambda + \frac{r\pi}{2}, \end{aligned} \quad r \in \mathbb{Z}. \quad (2.4.39)$$

Moreover, for $m \geq 3$, $\mu^1(m, \hat{u})$ and $\mu^4(m, \hat{u})$ are non-zero for generic values of λ , and likewise for

$\nu^1(m, \hat{v})$ and $\nu^4(m, \hat{v})$. We therefore have

$$\mathbf{D}_0^{m,0}(\hat{u}) = \frac{\mu^4(m, \hat{u})}{\mu^1(m, \hat{u})} \mathbf{D}_0^{m-3,0}(\hat{u}) = \frac{\mu^4(m, \hat{u})}{\mu^1(m, \hat{u})} \mathbf{D}_0^{m-3,0}((7-m)\lambda + \frac{r\pi}{2}) = \frac{\mu^4(m, \hat{u})}{\mu^1(m, \hat{u})} [\mathbf{D}_0^{m,0}(\hat{u})|_{m \rightarrow m-3}], \quad (2.4.40a)$$

$$\mathbf{D}_0^{m,0}(\hat{v}) = \frac{\nu^4(m, \hat{v})}{\nu^1(m, \hat{v})} \mathbf{D}_6^{m-3,0}(\hat{v}) = \frac{\nu^4(m, \hat{v})}{\nu^1(m, \hat{v})} \mathbf{D}_0^{m-3,0}((4-m)\lambda + \frac{r\pi}{2}) = \frac{\nu^4(m, \hat{v})}{\nu^1(m, \hat{v})} [\mathbf{D}_0^{m,0}(\hat{v})|_{m \rightarrow m-3}], \quad (2.4.40b)$$

where we used crossing symmetry at the second equalities. Writing $m = x + 3y$ with $x \in \{0, 1, 2\}$ and $y \in \mathbb{N}$, we apply the first reduction relation repeatedly to write

$$\mathbf{D}^{m,0}(\hat{u}) = \mathbf{D}^{x,0}((4-x)\lambda + \frac{r\pi}{2}) \prod_{k=0}^{y-1} g^r(m-3k), \quad g^r(m) = \frac{\mu^4(m, (4-m)\lambda + \frac{r\pi}{2})}{\mu^1(m, (4-m)\lambda + \frac{r\pi}{2})}. \quad (2.4.41)$$

This relation also holds for $y = 0$ provided that the product is replaced by the factor 1. Crucially, one can write each of the tangles for $m = 0, 1, 2$ in terms of one of the following objects:

$$\mathbf{D}^{0,0}(4\lambda + \frac{r\pi}{2}) \mapsto f(2\lambda + \frac{r\pi}{2})f(\lambda + \frac{r\pi}{2})\mathbf{I}, \quad (2.4.42a)$$

$$\mathbf{D}^{1,0}(3\lambda + \frac{r\pi}{2}) = \mathbf{D}^{1,0}(\frac{r\pi}{2}) = f(2\lambda + \frac{r\pi}{2})f(3\lambda + \frac{r\pi}{2}) \frac{s(6\lambda)}{s(2\lambda)} \frac{w(\frac{5\lambda}{2} + \frac{r\pi}{2})w(-\frac{3\lambda}{2} + \frac{r\pi}{2})\bar{w}(-\frac{\lambda}{2} + \frac{r\pi}{2})}{w^{(1)}(\frac{3\lambda}{2} + \frac{r\pi}{2})} \mathbf{I}, \quad (2.4.42b)$$

$$\mathbf{D}^{2,0}(2\lambda + \frac{r\pi}{2}) = -\frac{\alpha^3(2, 2\lambda + \frac{r\pi}{2})\alpha^0(\lambda + \frac{r\pi}{2})}{\alpha^1(2, 2\lambda + \frac{r\pi}{2})} \mathbf{D}^{1,0}(3\lambda + \frac{r\pi}{2}). \quad (2.4.42c)$$

The relation (2.4.42a) follows directly from our convention for $\mathbf{D}^{0,0}(u)$ used in (2.4.36), and (2.4.42b) was given in (2.4.5). Finally for (2.4.42c), we used the fact that $\alpha^2(2, u)$ in (2.4.15a) has a factor $s(2u_{-2})$.

This proves that $\mathbf{D}^{m,0}(\hat{u})$ is proportional to the identity element \mathbf{I} , for all $m \geq 0$. The overall prefactor is a non-trivial product of trigonometric factors, which can be simplified to

$$\mathbf{D}^{m,0}(\hat{u}) = \mathbf{I} \times f(\hat{u}_{2m-3})f(\hat{u}_{2m-2}) \frac{s(2\hat{u}_{2m-3})s(2\hat{u}_{2m-2})}{s(2\hat{u}_{m-3})s(2\hat{u}_{m-2})} \frac{w(\hat{u}_{2m-5/2})}{w^{(m)}(\hat{u}_{m-5/2})} \prod_{j=0}^{m-1} w(-\hat{u}_{2j-3/2})\bar{w}(-\hat{u}_{2j-5/2}). \quad (2.4.43)$$

This formula is valid for all four boundary conditions. It can be checked first for $m = 0, 1, 2$ and then proved inductively on m by steps of 3 using (2.4.40a).

2.4.6 Braid limits

The *bulk braid operators* are defined as the following limits of the face operator:

$$\boxed{\pm\infty} = \lim_{u \rightarrow \pm i\infty} \frac{e^{\mp i(\pi-2\lambda)}}{\rho_8(u)} \boxed{u} = \boxed{} + \boxed{} + \boxed{} - e^{\pm 2i\lambda} \boxed{} - e^{\mp 2i\lambda} \boxed{}. \quad (2.4.44)$$

Diagrammatic properties then follow from the ones of the face operator:

$$\boxed{\pm\infty} = \boxed{\mp\infty}, \quad \diamond_{\pm\infty} \diamond_{\mp\infty} = \diamond_{\pm\infty}, \quad \diamond_{\pm\infty} \begin{matrix} \boxed{\mp\infty} \\ \boxed{\pm\infty} \end{matrix} = \begin{matrix} \boxed{\pm\infty} \\ \boxed{\mp\infty} \end{matrix} \diamond_{\mp\infty}. \quad (2.4.45)$$

The bulk braid operators also have push-through properties for the arc and the vacancies:

$$\begin{matrix} \boxed{\pm\infty} \\ \boxed{\pm\infty} \end{matrix} = \begin{matrix} \boxed{} \\ \boxed{} \end{matrix}, \quad \boxed{\pm\infty} = \begin{matrix} \boxed{} \\ \bullet \\ \bullet \end{matrix}. \quad (2.4.46)$$

The *boundary braid operators* are defined as

$$\triangleleft_{\pm\infty} = \lim_{u \rightarrow \pm i\infty} \frac{1}{\delta(u)} \triangleleft_u = \vartheta e^{\pm 3i\lambda/2} \triangleleft_{\pm\infty} + e^{\mp 3i\lambda/2} \triangleleft_{\mp\infty}, \quad \vartheta = \begin{cases} -1 & S \\ 1 & C \end{cases}. \quad (2.4.47)$$

These satisfy the crossing symmetry relation

$$\triangleleft_{\pm\infty} \diamond_{\pm\infty} = e^{\mp 3i\lambda} \triangleleft_{\mp\infty}. \quad (2.4.48)$$

The *fundamental braid transfer tangle* is defined from the limits of the operators composing $\mathbf{D}^{1,0}(u)$:

$$\mathbf{D}_{\infty} = \mathbf{D}_{\infty}^{1,0} = \begin{matrix} \triangleleft_{\mp\infty} & \boxed{\mp\infty} & \boxed{\mp\infty} & \cdots & \cdots & \boxed{\mp\infty} & \triangleleft_{\pm\infty} \\ \boxed{\pm\infty} & \boxed{\pm\infty} & \cdots & \cdots & \boxed{\pm\infty} & \end{matrix} = \lim_{u \rightarrow \pm i\infty} \frac{e^{\pm 4i\lambda N} \mathbf{D}^{1,0}(u)}{\gamma(u) f_{-3} f_{-2}}, \quad (2.4.49)$$

where $\gamma(u)$ depends on the choice of boundary condition:

$$\text{identical: } \gamma(u) = -w(u)w(3\lambda - u), \quad \text{mixed: } \gamma(u) = 1. \quad (2.4.50)$$

Using the braid inversion relation, the Yang-Baxter equation and the crossing symmetry at the bound-

ary, one can show that

$$(2.4.51)$$

It thus follows that $D_\infty^{1,0}$ does not depend on the choice of limit $u \rightarrow \pm i\infty$ in its definition.

The *fused braid transfer tangles* are defined as

$$D_\infty^{m,0} = \lim_{u \rightarrow \pm i\infty} \frac{e^{\pm 4i\lambda m N} D^{m,0}(u)}{f(u_{-3})f(u_{-2}) \prod_{j=0}^{m-1} \gamma(u_{2j})}, \quad (2.4.52a)$$

$$D_\infty^{0,n} = D_\infty^{n,0}, \quad (2.4.52b)$$

$$D_\infty^{m,n} = \lim_{u \rightarrow \pm i\infty} \frac{e^{\pm 4i\lambda(m+n)N} D^{m,n}(u)}{w^{(m)}(u_{m-5/2})w^{(n)}(\psi_{n-5/2})f(u_{-3})f(u_{-2})f(u_{2m-1}) \prod_{j=0}^{m-1} \gamma(u_{2j}) \prod_{j=0}^{n-1} \gamma(\psi_{2j})}, \quad (2.4.52c)$$

for $m, n > 1$. The definition (2.4.52) is completed with $D_\infty^{0,0} = I$. For the mixed boundary cases, these definitions are similar to those used for the periodic geometry [17]. For all choices of boundary condition, the fusion hierarchy relations in the limit $u \rightarrow \pm i\infty$ become:

$$D_\infty^{m,0} = D_\infty^{m-1,0} D_\infty^{1,0} - D_\infty^{m-2,1}, \quad (2.4.53a)$$

$$D_\infty^{m,n} = D_\infty^{m,0} D_\infty^{0,n} - D_\infty^{m-1,0} D_\infty^{0,n-1}. \quad (2.4.53b)$$

It immediately follows that each fused braid tangle is a polynomial in D_∞ that can be expressed as a determinant:

$$D_\infty^{m,0} = \begin{vmatrix} D_\infty & D_\infty & I & 0 & 0 & 0 \\ I & D_\infty & D_\infty & I & 0 & 0 \\ 0 & \ddots & \ddots & \ddots & \ddots & 0 \\ 0 & 0 & I & D_\infty & D_\infty & I \\ 0 & 0 & 0 & I & D_\infty & D_\infty \\ 0 & 0 & 0 & 0 & I & D_\infty \end{vmatrix}, \quad D_\infty^{m,n} = \begin{vmatrix} \boxed{n \times n} & 0 & 0 & 0 \\ \boxed{n \times n} & 0 & 0 & 0 \\ 0 & 0 & I & 0 & 0 \\ 0 & 0 & 0 & \boxed{m \times m} & 0 \\ 0 & 0 & 0 & \boxed{m \times m} & 0 \end{vmatrix}. \quad (2.4.54)$$

As previously in (2.4.30a), the upper block is associated to $D_\infty^{0,n}$ and the lower block to $D_\infty^{m,0}$.

2.4.7 T -system and Y -system

The T -system is a set of quadratic equations satisfied by the fused transfer matrices, that follows from the fusion hierarchy relations. For the $A_2^{(2)}$ model on the strip, it can be written in a uniform way using

the determinantal forms given in Section 2.4.4, namely

$$\det(m, 0)_0 \det(m-k, 0)_{2k+2} = \left(\prod_{j=k}^{m-1} \mathcal{F}_{2j} \right) \det(k, m-k)_0 + \det(m+1, 0)_0 \det(m-k-1, 0)_{2k+2} \quad (2.4.55)$$

where $0 \leq k < m$ and $\det(0, 0) = \mathbf{I}$. The proof, given in Section 2.A.3, is completely analogous to the one given for the periodic case in [17]. Of course, the T -system can be written directly in terms of the fused transfer matrices $\mathbf{D}^{m,n}(u)$. For all boundary conditions, the T -system equation reads

$$\begin{aligned} & s(2u_{m-3})s(2u_{m+k})w^{(m)}(u_{m-5/2})w^{(m-k)}(u_{m+k-1/2})\mathbf{D}_0^{m,0}\mathbf{D}_{2k+2}^{m-k,0} \\ &= \left(\prod_{j=k}^{m-1} \bar{w}(-u_{2j-1/2}) \right) \left(\prod_{j=k}^{m-2} w(-u_{2j+1/2}) \right) s(2u_{k-3})s(2u_{2m})w(u_{2m-1/2})f_{2m}\mathbf{D}_0^{k,m-k} \\ &+ s(2u_{m-1})s(2u_{m+k-2})w^{(m+1)}(u_{m-3/2})w^{(m-k-1)}(u_{m+k-3/2})\mathbf{D}_0^{m+1,0}\mathbf{D}_{2k+2}^{m-k-1,0} \end{aligned} \quad (2.4.56)$$

for $0 < k < m$, with $\mathbf{D}_\ell^{0,0} = f_{\ell-3}f_{\ell-2}\mathbf{I}$ used for the case $k = m - 1$. A similar result holds for $k = 0$ with the first term of the right-hand side replaced by

$$\begin{aligned} & \left(\prod_{j=0}^{m-1} \bar{w}(-u_{2j-1/2}) \right) \left(\prod_{j=0}^{m-2} w(-u_{2j+1/2}) \right) \\ & \times s(2u_{-3})s(2u_{2m})w(u_{-5/2})w(u_{2m-1/2})w^{(m)}(-u_{m-3/2})f_{-3}f_{2m}\mathbf{D}_0^{0,m}. \end{aligned} \quad (2.4.57)$$

It is clearly more convenient to work with the determinantal expressions. To express this in terms of a Y -system, we first define the functions $\mathbf{d}^m(u)$ as

$$\mathbf{d}^m(u) = \frac{\det(m+1, 0)_0 \det(m-1, 0)_2}{\left(\prod_{j=0}^{m-1} \mathcal{F}_{2j} \right) \det(m, 0)_1}, \quad m \geq 0, \quad (2.4.58)$$

with $\mathbf{d}^0(u) = 0$. It then directly follows from (2.4.55) that

$$\mathbf{I} + \mathbf{d}_0^m = \frac{\det(m, 0)_0 \det(m, 0)_2}{\left(\prod_{j=0}^{m-1} \mathcal{F}_{2j} \right) \det(m, 0)_1}. \quad (2.4.59)$$

The starting point to derive the Y -system equation is to compute the product $\mathbf{d}_0^m \mathbf{d}_2^m$:

$$\begin{aligned} \mathbf{d}_0^m \mathbf{d}_2^m &= \frac{\det(m-1, 0)_2 \det(m-1, 0)_4 \det(m+1, 0)_0 \det(m+1, 0)_2}{\prod_{j=0}^{m-1} \mathcal{F}_{2j} \prod_{j=1}^m \mathcal{F}_{2j} \det(m, 0)_1 \det(m, 0)_3} \\ &= \frac{\prod_{j=0}^m \mathcal{F}_{2j} \prod_{j=1}^{m-1} \mathcal{F}_{2j} (\mathbf{I} + \mathbf{d}_2^{m-1})(\mathbf{I} + \mathbf{d}_0^{m+1}) \det(m+1, 0)_1 \det(m-1, 0)_3}{\prod_{j=0}^{m-1} \mathcal{F}_{2j} \prod_{j=1}^m \mathcal{F}_{2j} (\mathbf{I} + \mathbf{d}_1^m) \det(m, 0)_2 \prod_{j=0}^{m-1} \mathcal{F}_{2j+1}} \\ &= \frac{(\mathbf{I} + \mathbf{d}_2^{m-1})(\mathbf{I} + \mathbf{d}_0^{m+1})}{(\mathbf{I} + \mathbf{d}_1^m)} \mathbf{d}_1^m. \end{aligned} \quad (2.4.60)$$

The Y -system is therefore identical to the one obtained for periodic boundary conditions:

$$\frac{\mathbf{d}_0^m \mathbf{d}_2^m}{\mathbf{d}_1^m} = \frac{(\mathbf{I} + \mathbf{d}_2^{m-1})(\mathbf{I} + \mathbf{d}_0^{m+1})}{\mathbf{I} + \mathbf{d}_1^m}, \quad m \geq 1. \quad (2.4.61)$$

2.5 Polynomiality of the fused transfer matrices

In this section, we prove an important property of the fused transfer matrices $\mathbf{D}^{m,n}(u)$, namely that they are Laurent polynomials in $z = e^{iu}$. The proof is divided in three cases. In Section 2.5.1, the polynomiality of $\mathbf{D}^{2,0}(u)$ and $\mathbf{D}^{1,1}(u)$ is established using the diagrammatic definitions of these transfer matrices given in Section 2.4.3. Then in Sections 2.5.2 and 2.5.3, we respectively prove the polynomiality of $\mathbf{D}^{m,0}(u)$ and $\mathbf{D}^{m,n}(u)$ for $m, n > 1$, by cleverly using the fusion hierarchy relations. Throughout the section, the arguments are done for generic values of λ . By continuity, they then hold at all values of λ , including those for which q is a root of unity. A reader uninterested in these technical proofs may wish to accept this result and skip forward to Section 2.6.

2.5.1 Polynomiality of $\mathbf{D}^{2,0}(u)$ and $\mathbf{D}^{1,1}(u)$

In this section, we prove that $\mathbf{D}^{2,0}(u)$ and $\mathbf{D}^{1,1}(u)$ are Laurent polynomials in $z = e^{iu}$. Let us first recall that we have two equivalent definitions for these objects. The first definitions in (2.4.15) express $\mathbf{D}^{2,0}(u)$ and $\mathbf{D}^{1,1}(u)$ as functions of $\mathbf{D}^{1,0}(u)$ and its shifts, whereas the second definitions in (2.4.18) are diagrammatic and written in terms of projectors. For $\mathbf{D}^{2,0}(u)$, the potential poles are the zeros of the functions $\alpha^1(2, u)$ and $Z^{2,0}(u)$, or more precisely the common zeros of these two functions:

$$\begin{aligned} \text{(i)} \quad u = \frac{r\pi}{2}, & \quad \text{(ii)} \quad u = \lambda + \frac{r\pi}{2}, & \quad \text{(iii)} \quad u = \frac{\lambda}{2} + \begin{cases} r\pi & \text{SS,} \\ (r + \frac{1}{2})\pi & \text{CC,} \end{cases} \\ \text{(iv)} \quad u = \lambda \pm \xi_{(j)} + r\pi, & \quad \text{(v)} \quad u = \pm \xi_{(j)} + r\pi, & \quad \text{for } j = 1, \dots, N, \quad r \in \mathbb{Z}. \end{aligned} \quad (2.5.1)$$

For the mixed cases, there are no potential poles of types (iii). We also note that the functions $\alpha^1(2, u)$ and $Z^{2,0}(u)$ have simple zeros for (i), (ii), (iv) and (v), and double zeros for (iii) for the boundary conditions SS and CC. Likewise the potential poles of $\mathbf{D}^{1,1}(u)$ are the common zeros of $\beta^1(1, 1, u)$ and $Z^{1,1}(u)$, which are the values of u in (i) and (v). In this case, the zeros are double for (i) and simple for (v), and this holds for all boundary conditions.

To prove that $\mathbf{D}^{2,0}(u)$ and $\mathbf{D}^{1,1}(u)$ are regular at the points, we note that their diagrammatic definitions

can be rewritten as

$$\mathbf{D}^{2,0}(u) = \frac{1}{Z^{2,0}(u)}$$
(2.5.2a)

$$\mathbf{D}^{1,1}(u) = \frac{1}{Z^{1,1}(u)}$$
(2.5.2b)

We justify this claim as follows. For $\mathbf{D}^{2,0}(u)$, let us choose any of the projectors $P^{2,0}$ in (2.5.2a) and expand it using (2.3.16). The black triangle of the second term in this decomposition points leftwards if we selected a projector in the bottom part of the diagram, and to the right if it belongs to the top part. This triangle is then either pushed through a pair of face operators using (2.3.13a), or it reflects on the boundary using (2.3.30). In all cases, this black triangle then connects with another $P^{2,0}$ projector, yielding a zero result due to the third identity in (2.3.18). Only the first term of the decomposition (2.3.16) survives, and the final result is a diagram identical to the original one, but with this projector now absent. This argument is repeated until all projectors are removed except for one. The same argument applies for $\mathbf{D}^{1,1}(u)$ and its $P^{1,1}$ projectors.

These expressions with many projectors allow us to investigate the polynomiality of $\mathbf{D}^{2,0}(u)$ and $\mathbf{D}^{1,1}(u)$ in terms of some of their constituting parts. First, let us consider the combinations

$$\frac{1}{s(u_{-1} - \xi_{(j)})s(u_0 - \xi_{(j)})}$$
,

$$\frac{1}{s(u_0 - \xi_{(j)})}$$
(2.5.3)

Each of these combinations is a Laurent polynomial in $z = e^{iu}$. To show this, we note that

$$\begin{array}{c} \text{2,0} \\ \hline u_2 - \xi_{(j)} \\ \hline u_0 - \xi_{(j)} \\ \hline \end{array} \Big|_{u=\xi_{(j)}} = s(\lambda)s^2(2\lambda)s(3\lambda) \begin{array}{c} \text{2,0} \\ \hline \text{---} \\ \hline \text{---} \\ \hline \end{array} = 0, \quad (2.5.4a)$$

$$\begin{array}{c} \text{1,1} \\ \hline u_3 - \xi_{(j)} \\ \hline u_0 - \xi_{(j)} \\ \hline \end{array} \Big|_{u=\xi_{(j)}} = s^2(2\lambda)s^2(3\lambda) \begin{array}{c} \text{1,1} \\ \hline \text{---} \\ \hline \text{---} \\ \hline \end{array} = 0, \quad (2.5.4b)$$

where we used (2.3.10), (2.3.11) and (2.3.18). Similar identities holds with u shifted by π , and likewise for (2.5.4a) with $u = \lambda + \xi_{(j)} + r\pi$. The combinations (2.5.3) appear in the bottom bulk sections of the diagrams in (2.5.2), which are now understood to be Laurent polynomials. The same holds for the top bulk parts of these diagrams, as this follows from repeating the argument with $\xi_{(j)} \mapsto -\xi_{(j)}$, using combinations similar to those in (2.5.3) but with projectors attached to the right. This ends the proof that $\mathbf{D}^{2,0}(u)$ is regular at the points (iv) and (v), and likewise that $\mathbf{D}^{1,1}(u)$ is regular at the points (v).

The proofs of the regularity at the point (i), (ii) and (iii) are instead related to the operators on the boundaries. In this case, we consider the combinations

$$\frac{1}{s(2u_{-1})\delta_L(u_{-3/2})\delta_L(u_{-1/2})} \begin{array}{c} \text{2,0} \\ \hline 3\lambda - u_2 \\ \hline 2u - \lambda \\ \hline 3\lambda - u_0 \end{array}, \quad \frac{1}{s(2u_0)\delta_L(u_{-3/2})} \begin{array}{c} \text{1,1} \\ \hline 3\lambda - u_3 \\ \hline 2u \\ \hline 3\lambda - u_0 \end{array}. \quad (2.5.5)$$

These are also Laurent polynomials. The proof uses the same arguments, namely one shows using (2.3.23), (2.3.26) and (2.3.27) that the diagrams evaluate to zero if u is specified to a value where the denominator vanishes. Similar identities hold on the right boundary. The relevant combinations are obtained from (2.5.5) by rotating the diagram, replacing δ_L by δ_R , and changing $u \mapsto \lambda - u$ and $u \mapsto -u$ for the first and second combinations, respectively. This allows us to conclude that the expressions (2.5.2) for $\mathbf{D}^{2,0}(u)$ and $\mathbf{D}^{1,1}(u)$ are regular at a number of values of u that includes all the points of type (i), (ii) and (iii). This is also true in the cases of double zeros, as in these cases, one zero is accounted for in the combination corresponding to the left boundary and the second for the one in the right boundary. This ends the proof of the polynomiality of $\mathbf{D}^{2,0}(u)$ and $\mathbf{D}^{1,1}(u)$.

2.5.2 Polynomiality of $D^{m,0}(u)$

Idea of the inductive proof. The polynomiality of $D^{m,0}(u)$ is already established for $m = 1$ and $m = 2$. This section proves that this also holds for $m \geq 3$, using induction on m . Dividing (2.4.36a) and (2.4.36b) by $\mu^1(m, u)$ and $\nu^1(m, u)$ respectively gives two different expressions for $D^{m,0}(u)$ in terms of fused transfer matrices $D^{m',0}(u)$ with $m' < m$. By the inductive hypothesis, these transfer matrices with lower fusion indices are assumed to be Laurent polynomials in $z = e^{iu}$. Therefore the only potential poles for $D^{m,0}(u)$ are the zeros of $\mu^1(m, u)$ and $\nu^1(m, u)$, or more precisely the common zeros of these two functions. Upon inspection, we see that they share the factor $s(2u_{m-3})s(2u_{m-2})w^{(m)}(u_{m-5/2})$. Therefore $D^{m,0}(u)$ potentially has poles at the following values of u :

$$(i) u = (2-m)\lambda + \frac{r\pi}{2}, \quad (ii) u = (3-m)\lambda + \frac{r\pi}{2}, \quad (iii) u = \left(\frac{5}{2}-m\right)\lambda + r\pi + \begin{cases} m\frac{\pi}{2} & \text{SS,} \\ (m+1)\frac{\pi}{2} & \text{CC,} \end{cases} \quad (2.5.6)$$

with $r \in \mathbb{Z}$. Of course, there is no potential pole of type (iii) for the mixed cases SC and CS. For $m \geq 4$, all the other zeros of $\mu^1(m, u)$ are not zeros of $\nu^1(m, u)$, so the above list exhausts all the possible problematic values of u . Let us thus first consider $m \geq 4$. (The case $m = 3$ is discussed at the end of the section). Below we prove that $D^{m,0}(u)$ is regular at each of these points.

Proof for (i) and (ii). From the periodicity and crossing symmetry, we have

$$D^{m,0}\left((2-m)\lambda + \frac{r\pi}{2}\right) = D^{m,0}\left((3-m)\lambda + \frac{r\pi}{2}\right). \quad (2.5.7)$$

As a result, the proof of regularity for (i) will imply the same result for (ii). We thus focus on (i) and define $\hat{u} = (2-m)\lambda + \frac{r\pi}{2}$. The function $\nu^1(m, u)$ has a zero of degree one at $u = \hat{u}$. To show that $D^{m,0}(\hat{u})$ is non-singular, we must show that

$$K(m) = \lim_{u \rightarrow \hat{u}} \left(\nu^2(m, u) D_0^{1,0} D_2^{m-1,0} - \nu^3(m, u) D_1^{1,0} D_4^{m-2,0} + \nu^4(m, u) D_6^{m-3,0} \right) = 0. \quad (2.5.8)$$

We readily observe that $\nu^2(m, u) = 0$ at $u = \hat{u}$ because it has a factor of $s(2u_{m-2})$. In contrast, $\nu^3(m, \hat{u})$ and $\nu^4(m, \hat{u})$ are non-zero. We thus have

$$K(m) = -\nu^3(m, \hat{u}) D_1^{1,0}(\hat{u}) D_4^{m-2,0}(\hat{u}) + \nu^4(m, \hat{u}) D_6^{m-3,0}(\hat{u}). \quad (2.5.9)$$

As a first step, we note that

$$D_6^{m-3,0}(\hat{u}) = \frac{\mu^2(m-3, \hat{u}_6)}{\mu^1(m-3, \hat{u}_6)} D_6^{m-4,0}(\hat{u}) D_{2m-2}^{1,0}(\hat{u}), \quad (2.5.10)$$

with the other two terms absent due to zeros of $\mu^3(m-3, \hat{u}_6)$ and $\mu^4(m-3, \hat{u}_6)$. This holds for $m \geq 4$.² From crossing symmetry and periodicity, we have $\mathbf{D}_{2m-2}^{1,0}(\hat{u}) = \mathbf{D}_1^{1,0}(\hat{u})$ and

$$\mathbf{K}(m) = -\nu^3(m, \hat{u}) \mathbf{D}_1^{1,0}(\hat{u}) \underbrace{\left(\mathbf{D}_4^{m-2,0}(\hat{u}) - \frac{\nu^4(m, \hat{u}) \mu^2(m-3, \hat{u}_6)}{\nu^3(m, \hat{u}) \mu^1(m-3, \hat{u}_6)} \mathbf{D}_6^{m-4,0}(\hat{u}) \right)}_{=\mathbf{J}(m)}. \quad (2.5.11)$$

The factor in front of the parenthesis is non-zero leaving us to show that the content of the parenthesis, $\mathbf{J}(m)$, vanishes. We check the cases $m = 4, 5, 6$ explicitly:

$$\mathbf{J}(4) = \mathbf{D}_4^{2,0}(\hat{u}) - \frac{\nu^4(4, \hat{u}) \mu^2(1, \hat{u}_6)}{\nu^3(4, \hat{u}) \mu^1(1, \hat{u}_6)} \mathbf{D}_6^{0,0}(\hat{u}), \quad \hat{u} = -2\lambda + \frac{r\pi}{2}, \quad (2.5.12a)$$

$$\mathbf{J}(5) = \mathbf{D}_4^{3,0}(\hat{u}) - \frac{\nu^4(5, \hat{u}) \mu^2(2, \hat{u}_6)}{\nu^3(5, \hat{u}) \mu^1(2, \hat{u}_6)} \mathbf{D}_6^{1,0}(\hat{u}), \quad \hat{u} = -3\lambda + \frac{r\pi}{2}, \quad (2.5.12b)$$

$$\mathbf{J}(6) = \mathbf{D}_4^{4,0}(\hat{u}) - \frac{\nu^4(6, \hat{u}) \mu^2(3, \hat{u}_6)}{\nu^3(6, \hat{u}) \mu^1(3, \hat{u}_6)} \mathbf{D}_6^{2,0}(\hat{u}), \quad \hat{u} = -4\lambda + \frac{r\pi}{2}. \quad (2.5.12c)$$

All six transfer tangles in (2.5.12) turn out to be proportional to the identity \mathbf{I} . Indeed, using the crossing symmetry, periodicity and conjugacy of the transfer matrices as well as the reduction relations (2.4.40), one can write each of these tangles in terms of the objects in (2.4.42). Verifying that $\mathbf{J}(4)$, $\mathbf{J}(5)$ and $\mathbf{J}(6)$ vanish is then straightforward, as it amounts to checking three equalities satisfied by finite products of trigonometric factors.

Returning to the cases $m \geq 7$ with $\hat{u} = (2-m)\lambda + \frac{r\pi}{2}$, we apply (2.4.40) to both transfer matrices in $\mathbf{J}(m)$ and find

$$\begin{aligned} \mathbf{J}(m) &= \frac{\mu_4(m-2, \hat{u}_4)}{\mu_1(m-2, \hat{u}_4)} \mathbf{D}_4^{m-5,0}(\hat{u}) - \frac{\nu^4(m, \hat{u}) \mu^2(m-3, \hat{u}_6) \mu^4(m-4, \hat{u}_6)}{\nu^3(m, \hat{u}) \mu^1(m-3, \hat{u}_6) \mu^1(m-4, \hat{u}_6)} \mathbf{D}_6^{m-7,0}(\hat{u}) \\ &= \frac{\mu_4(m-2, \hat{u}_4)}{\mu_1(m-2, \hat{u}_4)} \mathbf{J}(m-3). \end{aligned} \quad (2.5.13)$$

The last equality stems from the definition (2.5.11) of $\mathbf{J}(m-3)$ and the relations

$$\frac{\nu^4(m, \hat{u}) \mu^1(m-2, \hat{u}_4) \mu^2(m-3, \hat{u}_6) \mu^4(m-4, \hat{u}_6)}{\nu^3(m, \hat{u}) \mu^4(m-2, \hat{u}_4) \mu^1(m-3, \hat{u}_6) \mu^1(m-4, \hat{u}_6)} = \frac{\nu^4(m-3, \hat{v}) \mu^2(m-6, \hat{v}_6)}{\nu^3(m-3, \hat{v}) \mu^1(m-6, \hat{v}_6)}, \quad (2.5.14a)$$

$$\mathbf{D}_4^{m-5,0}(\hat{u}) = \mathbf{D}_4^{m-5,0}(\hat{v}), \quad \mathbf{D}_6^{m-7,0}(\hat{u}) = \mathbf{D}_6^{m-7,0}(\hat{v}), \quad \hat{v} = \hat{u}|_{m \rightarrow m-3} = (5-m)\lambda + \frac{r\pi}{2}, \quad (2.5.14b)$$

valid for $m \geq 7$.³ By the induction hypothesis, $\mathbf{D}^{m-3,0}((5-m)\lambda + \frac{r\pi}{2})$ is finite and therefore $\mathbf{J}(m-3) =$

2. For $m = 4$, $\mathbf{D}_6^{m-3,0}(\hat{u}) = \mathbf{D}_6^{1,0}(\hat{u})$. The relation (2.4.36a) holds trivially as $\mu^1(1, u) \mathbf{D}^{1,0}(u) = \mu^2(1, u) \mathbf{D}^{0,0}(u) \mathbf{D}^{1,0}(u)$ and all other terms vanish due to negative fusion indices. In (2.5.10), each $\mu^i(m-3, \hat{u}_6)$ vanishes, but one can check that the equality still holds by using a limit and understanding $\frac{\mu^2(m-3, \hat{u}_6)}{\mu^1(m-3, \hat{u}_6)}$ as $\lim_{u \rightarrow \hat{u}} \frac{\mu^2(m-3, u_6)}{\mu^1(m-3, u_6)}$.

3. This also works in the case $m = 7$, in which case the functions $\mu^1(m-6, \hat{v}_6)$ and $\mu^2(m-6, \hat{v}_6)$ both vanish and

0. Because $\mu_1(m-2, \widehat{u}_4) \neq 0$ we deduce that $\mathbf{J}(m) = 0$. This ends the proof that $\mathbf{D}^{m,0}(u)$ is regular at $u = (2-m)\lambda + \frac{r\pi}{2}$ and $(3-m)\lambda + \frac{r\pi}{2}$.

Proof for (iii). This case applies only to SS and CC boundary conditions. We start by deriving a new functional equation. Recall that a section of the matrix used to defined $\det(m, 0)(u)$ takes the form

$$\det(m, 0)(u) = \begin{vmatrix} \ddots & & \ddots & & \ddots & & & & & & 0 \\ \ddots & \mathcal{D}_{2k+4} & \mathcal{D}_{2k+3} & \mathcal{F}_{2k+1} & & & & & 0 & & \\ 0 & \mathcal{F}_{2k+2} & \mathcal{D}_{2k+2} & \mathcal{D}_{2k+1} & \mathcal{F}_{2k-1} & & & & 0 & & \\ & 0 & \mathcal{F}_{2k} & \mathcal{D}_{2k} & \mathcal{D}_{2k-1} & \mathcal{F}_{2k-3} & & & 0 & & \\ \text{---} & & 0 & \mathcal{F}_{2k-2} & \mathcal{D}_{2k-2} & \mathcal{D}_{2k-3} & \mathcal{F}_{2k-5} & & & & 0 \\ & & & 0 & \mathcal{F}_{2k-4} & \mathcal{D}_{2k-4} & \mathcal{D}_{2k-5} & \ddots & & & \\ & & & & 0 & \mathcal{F}_{2k-6} & \mathcal{D}_{2k-6} & \ddots & & & \\ & & & & & 0 & \ddots & \ddots & & & \end{vmatrix}. \quad (2.5.15)$$

Using the determinant minor expansion, we obtain the five-term relation

$$\begin{aligned} \det(m, 0)_0 &= \det(m-k, 0)_{2k} \det(k, 0)_0 + \mathcal{F}_{2k-2} \mathcal{F}_{2k-1} \mathcal{F}_{2k} \det(m-k-2, 0)_{2k+4} \det(k-1, 0)_0 \\ &\quad - \mathcal{F}_{2k-2} \mathcal{D}_{2k-1} \det(m-k-1, 0)_{2k+2} \det(k-1, 0)_0 \\ &\quad + \mathcal{F}_{2k-4} \mathcal{F}_{2k-3} \mathcal{F}_{2k-2} \det(m-k-1, 0)_{2k+2} \det(k-2, 0)_0, \quad k = 1, \dots, m-1. \end{aligned} \quad (2.5.16)$$

Rewriting this equation in terms of the fused transfer tangles, we find

$$\begin{aligned} \tau^1(m, k, u) \mathbf{D}_0^{m,0} &= \tau^2(m, k, u) \mathbf{D}_{2k}^{m-k,0} \mathbf{D}_0^{k,0} + \tau^3(m, k, u) \mathbf{D}_{2k+4}^{m-k-2,0} \mathbf{D}_0^{k-1,0} \\ &\quad + \tau^4(m, k, u) \mathbf{D}_{2k+2}^{m-k-1,0} \mathbf{D}_{2k-1}^{1,0} \mathbf{D}_0^{k-1,0} + \tau^5(m, k, u) \mathbf{D}_{2k+2}^{m-k-1,0} \mathbf{D}_0^{k-2,0}, \end{aligned} \quad (2.5.17)$$

where $k = 2, \dots, m-2$ and

$$\begin{aligned} \tau^1(m, k, u) &= s(2u_{m-2})s(2u_{m-3})s(2u_{2k-4})s(2u_{2k-3})s(2u_{2k-2})s(2u_{2k-1})w(u_{2k-5/2})w^{(m)}(u_{m-5/2}) \\ &\quad \times f(u_{2k-4})f(u_{2k-3})f(u_{2k-2})f(u_{2k-1}), \end{aligned} \quad (2.5.18a)$$

$$\begin{aligned} \tau^2(m, k, u) &= s(2u_{k-3})s(2u_{k-2})s(2u_{2k-4})s(2u_{2k-1})s(2u_{m+k-3})s(2u_{m+k-2})w^{(m-k)}(u_{m+k-5/2}) \\ &\quad \times w^{(k)}(u_{k-5/2})f(u_{2k-4})f(u_{2k-1}), \end{aligned} \quad (2.5.18b)$$

$$\begin{aligned} \tau^3(m, k, u) &= s(2u_{k-4})s(2u_{k-3})s(2u_{2k-4})s(2u_{2k-3})s(2u_{m+k-1})s(2u_{m+k})w(u_{2k-7/2})w(u_{2k-5/2}) \\ &\quad \times w(u_{2k+1/2})\bar{w}(u_{2k-5/2})\bar{w}(u_{2k-3/2})\bar{w}(u_{2k-1/2})w^{(m-k-2)}(u_{m+k-1/2})w^{(k-1)}(u_{k-7/2}) \end{aligned}$$

their ratio in (2.5.14a) should be interpreted as $\lim_{v \rightarrow v} \widehat{\frac{\mu^2(m-6, v_6)}{\mu^1(m-6, v_6)}}$.

$$\times f(u_{2k-4})f(u_{2k-3}), \quad (2.5.18c)$$

$$\begin{aligned} \tau^4(m, k, u) &= -s(2u_{k-4})s(2u_{k-3})s(2u_{2k-3})s(2u_{2k-2})s(2u_{m+k-2})s(2u_{m+k-1})\bar{w}(u_{2k-5/2}) \\ &\times w^{(m-k-1)}(u_{m+k-3/2})w^{(1)}(u_{2k-5/2})w^{(k-1)}(u_{k-7/2}), \end{aligned} \quad (2.5.18d)$$

$$\begin{aligned} \tau^5(m, k, u) &= s(2u_{k-5})s(2u_{k-4})s(2u_{2k-2})s(2u_{2k-1})s(2u_{m+k-2})s(2u_{m+k-1})w(u_{2k-11/2})w(u_{2k-5/2}) \\ &\times w(u_{2k-3/2})\bar{w}(u_{2k-9/2})\bar{w}(u_{2k-7/2})\bar{w}(u_{2k-5/2})w^{(m-k-1)}(u_{m+k-3/2})w^{(k-2)}(u_{k-9/2}) \\ &\times f(u_{2k-2})f(u_{2k-1}). \end{aligned} \quad (2.5.18e)$$

The determinant relations (2.5.16) for $k = 1$ and $k = m - 1$ correspond to (2.4.36a) and (2.4.36b). For all values of k , the function $\tau^1(m, k, u)$ contains the problematic factor $w^{(m)}(u_{m-5/2})$, which may produce potential poles for $\mathbf{D}^{m,0}(u)$ for SS and CC boundary conditions. To show that this is not the case, we treat separately the cases of m odd and even.

Starting with m odd, we set $\hat{u} = (\frac{5}{2} - m)\lambda + (r + \frac{1}{2})\pi$ for SS boundary conditions and $\hat{u} = (\frac{5}{2} - m)\lambda + r\pi$ for CC boundary conditions. We use the relation (2.5.17) with $k = \frac{m+1}{2}$, noting that $\tau^5(m, \frac{m+1}{2}, \hat{u}) = 0$ and that the degree of the zero of $\tau^1(m, \frac{m+1}{2}, u)$ at $u = \hat{u}$ is one. Thus to prove that $\mathbf{D}^{m,0}(\hat{u})$ is non-singular, we must show that

$$\begin{aligned} &\tau^2(m, \frac{m+1}{2}, \hat{u})\mathbf{D}_{m+1}^{(m-1)/2,0}(\hat{u})\mathbf{D}_0^{(m+1)/2,0}(\hat{u}) + \tau^3(m, \frac{m+1}{2}, \hat{u})\mathbf{D}_{m+5}^{(m-5)/2,0}(\hat{u})\mathbf{D}_0^{(m-1)/2,0}(\hat{u}) \\ &+ \tau^4(m, \frac{m+1}{2}, \hat{u})\mathbf{D}_{m+3}^{(m-3)/2,0}(\hat{u})\mathbf{D}_m^{1,0}(\hat{u})\mathbf{D}_0^{(m-1)/2,0}(\hat{u}) = 0. \end{aligned} \quad (2.5.19)$$

With the function $\mu^1(\frac{m+1}{2}, \hat{u})$ non-zero, we rewrite $\mathbf{D}^{(m+1)/2,0}(\hat{u})$ as

$$\mathbf{D}_0^{(m+1)/2,0}(\hat{u}) = -\frac{\mu^3(\frac{m+1}{2}, \hat{u})}{\mu^1(\frac{m+1}{2}, \hat{u})}\mathbf{D}_0^{(m-3)/2,0}(\hat{u})\mathbf{D}_{m-2}^{1,0}(\hat{u}) + \frac{\mu^4(\frac{m+1}{2}, \hat{u})}{\mu^1(\frac{m+1}{2}, \hat{u})}\mathbf{D}_0^{(m-5)/2,0}(\hat{u}). \quad (2.5.20)$$

This expresses the left side of (2.5.19) as a sum of four terms. With crossing symmetry, we find that two of them are proportional to $\mathbf{D}_{m+5}^{(m-5)/2,0}(\hat{u})\mathbf{D}_0^{(m-1)/2,0}(\hat{u})$, whereas the other two are proportional to $\mathbf{D}_{m+3}^{(m-3)/2,0}(\hat{u})\mathbf{D}_m^{1,0}(\hat{u})\mathbf{D}_0^{(m-1)/2,0}(\hat{u})$. It is then straightforward to check that the sum of their coefficients vanishes. This also holds for the special case $m = 5$ where $\mathbf{D}_0^{(m-5)/2,0}(\hat{u}) \mapsto f_{-3}f_{-2}(\hat{u})$, and using $f_{-3}(5\lambda - u)f_{-2}(5\lambda - u) = f_{-3}(u)f_{-2}(u)$. This ends the proof for m odd.

For m even, we define $\hat{u} = (\frac{5}{2} - m)\lambda + r\pi$ for SS boundary conditions and $\hat{u} = (\frac{5}{2} - m)\lambda + (r + \frac{1}{2})\pi$ for CC boundary conditions. In this case, we use the relation (2.5.17) with $k = \frac{m}{2}$. We note that $\tau^j(m, \frac{m}{2}, u)$ vanishes at $u = \hat{u}$ for $j = 1, 3, 5$, and that $\tau^1(m, \frac{m}{2}, u)$ has a double zero whereas $\tau^3(m, \frac{m}{2}, u)$ and $\tau^5(m, \frac{m}{2}, u)$ have simple zeros. To show that $\mathbf{D}^{m,0}(u)$ is regular at $u = \hat{u}$, we show that

$$\mathbf{L} = \lim_{u \rightarrow \hat{u}} \frac{\tau^1(m, \frac{m}{2}, u)\mathbf{D}^{m,0}(u)}{w^{(m)}(u_{m-5/2})} = 0, \quad (2.5.21)$$

or equivalently

$$\begin{aligned} \mathbf{L} = \lim_{u \rightarrow \hat{u}} \frac{1}{w^{(m)}(u_{m-5/2})} & \left[\tau^2(m, \frac{m}{2}, u) \mathbf{D}_m^{m/2,0} \mathbf{D}_0^{m/2,0} + \tau^3(m, \frac{m}{2}, u) \mathbf{D}_{m+4}^{m/2-2,0} \mathbf{D}_0^{m/2-1,0} \right. \\ & \left. + \tau^4(m, \frac{m}{2}, u) \mathbf{D}_{m+2}^{m/2-1,0} \mathbf{D}_{m-1}^{1,0} \mathbf{D}_0^{m/2-1,0} + \tau^5(m, \frac{m}{2}, u) \mathbf{D}_{m+2}^{m/2-1,0} \mathbf{D}_0^{m/2-2,0} \right] = 0. \end{aligned} \quad (2.5.22)$$

Because $\tau^3(m, \frac{m}{2}, \hat{u}) = \tau^5(m, \frac{m}{2}, \hat{u}) = 0$, the limits of the second and fourth terms are evaluated directly and their sum is found to vanish due to the relations

$$\mathbf{D}_{m+2j}^{m/2-j,0}(\hat{u}) = \mathbf{D}_0^{m/2-j,0}(\hat{u}), \quad \lim_{u \rightarrow \hat{u}} \frac{\tau^3(m, \frac{m}{2}, u)}{w^{(m)}(u_{m-5/2})} = - \lim_{u \rightarrow \hat{u}} \frac{\tau^5(m, \frac{m}{2}, u)}{w^{(m)}(u_{m-5/2})}, \quad (2.5.23)$$

the first of which is obtained by crossing symmetry. For the remaining terms, we expand $\mathbf{D}_m^{m/2,0}$ and $\mathbf{D}_0^{m/2,0}$ as

$$\mathbf{D}_0^{m/2,0} = \frac{\mu^2(\frac{m}{2}, u)}{\mu^1(\frac{m}{2}, u)} \mathbf{D}_0^{m/2-1,0} \mathbf{D}_{m-2}^{1,0} - \frac{\mu^3(\frac{m}{2}, u)}{\mu^1(\frac{m}{2}, u)} \mathbf{D}_0^{m/2-2,0} \mathbf{D}_{m-3}^{1,0} + \frac{\mu^4(\frac{m}{2}, u)}{\mu^1(\frac{m}{2}, u)} \mathbf{D}_0^{m/2-3,0}, \quad (2.5.24a)$$

$$\mathbf{D}_m^{m/2,0} = \frac{\nu^2(\frac{m}{2}, u_m)}{\nu^1(\frac{m}{2}, u_m)} \mathbf{D}_m^{1,0} \mathbf{D}_{m+2}^{m/2-1,0} - \frac{\nu^3(\frac{m}{2}, u_m)}{\nu^1(\frac{m}{2}, u_m)} \mathbf{D}_{m+1}^{1,0} \mathbf{D}_{m+4}^{m/2-2,0} + \frac{\nu^4(\frac{m}{2}, u_m)}{\nu^1(\frac{m}{2}, u_m)} \mathbf{D}_{m+6}^{m/2-3,0}. \quad (2.5.24b)$$

The functions $\mu^3(\frac{m}{2}, u)$, $\mu^4(\frac{m}{2}, u)$, $\nu^3(\frac{m}{2}, u_m)$ and $\nu^4(\frac{m}{2}, u_m)$ vanish at $u = \hat{u}$ with simple zeros. Expanding $\mathbf{D}_m^{m/2,0} \mathbf{D}_0^{m/2,0}$ with (2.5.24) yields nine terms, four of which contain two of these functions. Dividing by $w^{(m)}(u_{m-5/2})$ and taking the limit $u \rightarrow \hat{u}$, these four terms vanish. Four more terms contain exactly one of the functions $\mu^3(\frac{m}{2}, u)$, $\mu^4(\frac{m}{2}, u)$, $\nu^3(\frac{m}{2}, u_m)$ and $\nu^4(\frac{m}{2}, u_m)$. After the division by $w^{(m)}(u_{m-5/2})$, the limit of each term is well-defined and nonzero, and involves fused transfer matrices evaluated at $u = \hat{u}$ and shifts thereof. These four terms then cancel pairwise due to the crossing-symmetry relations in (2.5.23) and

$$\mu^2(\frac{m}{2}, \hat{u}) = (-1)^{m/2} \nu^2(\frac{m}{2}, \hat{u}_m), \quad \lim_{u \rightarrow \hat{u}} \frac{\mu^j(\frac{m}{2}, u)}{w^{(m)}(u_{m-5/2})} = (-1)^{m/2-1} \lim_{u \rightarrow \hat{u}} \frac{\nu^j(\frac{m}{2}, u_m)}{w^{(m)}(u_{m-5/2})}, \quad j = 3, 4. \quad (2.5.25)$$

The remaining terms combine to

$$\begin{aligned} \mathbf{L} = \lim_{u \rightarrow \hat{u}} \frac{1}{w^{(m)}(u_{m-5/2})} & \left[\tau^2(m, \frac{m}{2}, u) \frac{\mu^2(\frac{m}{2}, u)}{\mu^1(\frac{m}{2}, u)} \frac{\nu^2(\frac{m}{2}, u_m)}{\nu^1(\frac{m}{2}, u_m)} \mathbf{D}_m^{1,0} \mathbf{D}_{m-2}^{1,0} \right. \\ & \left. + \tau^4(m, \frac{m}{2}, u) \mathbf{D}_{m-1}^{1,0} \right] \mathbf{D}_0^{m/2-1,0} \mathbf{D}_{m+2}^{m/2-1,0}. \end{aligned} \quad (2.5.26)$$

With

$$\gamma = \frac{\tau^2(m, \frac{m}{2}, u) \mu^2(\frac{m}{2}, u) \nu^2(\frac{m}{2}, u_m)}{\mu^1(\frac{m}{2}, u) \nu^1(\frac{m}{2}, u_m) \alpha^2(2, u_{m-2})} = - \frac{\tau^4(m, \frac{m}{2}, u)}{\alpha^3(2, u_{m-2}) \alpha^0(u_{m-3})}, \quad (2.5.27)$$

it follows that

$$\mathbf{L} = \lim_{u \rightarrow \hat{u}} \frac{\gamma}{w^{(m)}(u_{m-5/2})} \left[\alpha^1(2, u_{m-2}) \mathbf{D}_{m-2}^{2,0} \right] \mathbf{D}_0^{m/2-1,0} \mathbf{D}_{m+2}^{m/2-1,0}. \quad (2.5.28)$$

The function $\alpha^1(2, u_{m-2})$ has a double zero at $u = \hat{u}$, so after dividing by $w^{(m)}(u_{m-5/2})$, we find that \mathbf{L} vanishes, ending the proof that $\mathbf{D}^{m,0}(u)$ is regular at $u = \hat{u}$ for m even.

The special case $m = 3$. For $m = 3$, (2.4.15d) and (2.4.15e) provide two equations for $\mathbf{D}^{3,0}(u)$. The results of Section 2.5.1 confirm that the right-hand sides of these equations are Laurent polynomials in $z = e^{iu}$. The coefficients of $\mathbf{D}^{3,0}(u)$ in these equations are respectively

$$\alpha^1(3, u) = s(2u_1)^2 w^{(3)}(u_{1/2}) \bar{w}^{(-1)}(u_{3/2}) f_1 f_2, \quad (2.5.29a)$$

$$\alpha^1(3, \psi - \lambda) = s(2u_0)^2 w^{(3)}(-u_{1/2}) \bar{w}^{(-1)}(-u_{-1/2}) f_0 f_{-1}. \quad (2.5.29b)$$

For the mixed boundary conditions, these two have no common zeroes for generic inhomogeneities $\xi_{(j)}$ and $\mathbf{D}^{3,0}(u)$ is thus a polynomial. For the boundary conditions SS and CC, the only common zeroes are those arising from $w^{(3)}(u_{1/2})$ which is equal up to a possible sign to $w^{(3)}(-u_{1/2})$. Thus the only zeroes to be studied are

$$\hat{u} = -\frac{\lambda}{2} + \begin{cases} (r + \frac{1}{2})\pi & \text{SS,} \\ r\pi & \text{CC.} \end{cases} \quad (2.5.30)$$

To show that $\mathbf{D}^{3,0}(u)$ is regular at this value, we use (2.4.36a) and note that $\mu^1(3, u)$ and $\mu^4(3, u)$ have simple zeros at $u = \hat{u}$. We must then show that

$$\mu^2(3, \hat{u}) \mathbf{D}_0^{2,0}(\hat{u}) \mathbf{D}_4^{1,0}(\hat{u}) - \mu^3(3, \hat{u}) \mathbf{D}_0^{1,0}(\hat{u}) \mathbf{D}_3^{1,0}(\hat{u}) = 0. \quad (2.5.31)$$

This follows directly from the crossing symmetry of $\mathbf{D}^{1,0}(u)$ and the relation

$$\mathbf{D}^{2,0}(\hat{u}) = -\frac{\alpha^3(2, \hat{u}) \alpha^0(\hat{u}_{-1})}{\alpha^1(2, \hat{u})} \mathbf{D}_1^{1,0}(\hat{u}). \quad (2.5.32)$$

This ends the proof of the polynomiality of $\mathbf{D}^{3,0}(u)$, and of $\mathbf{D}^{m,0}(u)$ by the inductive argument.

2.5.3 Polynomiality of $\mathbf{D}^{m,n}(u)$

In this section, we show the polynomiality of $\mathbf{D}^{m,n}(u)$ for $m, n \geq 1$, assuming that it holds for $\mathbf{D}^{m,0}(u)$. Recall also that this property was already established for $\mathbf{D}^{1,1}(u)$ in Section 2.5.1. From (2.4.15h), the potential poles of $\mathbf{D}^{m,n}(u)$ are at the values of u where

$$\beta^1(m, n, u) = -s(2u_{m+n-2}) s(2u_{2m-2}) f(u_{2m-2}) = 0. \quad (2.5.33)$$

We write down a second formula for $\mathbf{D}^{m,n}(u)$ starting from the T -system relation (2.4.55) with

$(m, k) \mapsto (m + n, m)$:

$$\left(\prod_{j=m}^{m+n-1} \mathcal{F}_{2j} \right) \det(m, n)_0 = \det(m+n, 0)_0 \det(n, 0)_{2m+2} - \det(m+n+1, 0)_0 \det(n-1, 0)_{2m+2} . \quad (2.5.34)$$

Reformulated in terms of fused transfer matrices, it reads

$$\eta^1(m, n, u) \mathbf{D}_0^{m,n} = \eta^2(m, n, u) \mathbf{D}_0^{m+n,0} \mathbf{D}_{2m+2}^{n,0} - \eta^3(m, n, u) \mathbf{D}_0^{m+n+1,0} \mathbf{D}_{2m+2}^{n-1,0} , \quad (2.5.35)$$

with

$$\eta^1(m, n, u) = \left(\prod_{j=0}^{n-1} \bar{w}(\psi_{2j-3/2}) \right) \left(\prod_{j=0}^{n-2} w(\psi_{2j-1/2}) \right) s(2u_{m-3}) s(2u_{2m+2n}) w(u_{2m+2n-1/2}) f_{2m+2n} , \quad (2.5.36a)$$

$$\eta^2(m, n, u) = s(2u_{m+n-3}) s(2u_{2m+n}) w^{(m+n)}(u_{m+n-5/2}) w^{(n)}(u_{2m+n-1/2}) , \quad (2.5.36b)$$

$$\eta^3(m, n, u) = s(2u_{m+n-1}) s(2u_{2m+n-2}) w^{(m+n+1)}(u_{m+n-3/2}) w^{(n-1)}(u_{2m+n-3/2}) . \quad (2.5.36c)$$

This relation holds for $m, n \geq 1$ with the convention $\mathbf{D}_k^{0,0} \mapsto f_{k-3} f_{k-2} \mathbf{I}$ used for the special case $n = 1$. Having established in Section 2.5.2 the polynomiality of the transfer matrices $\mathbf{D}^{m,0}(u)$ with $m \geq 1$, we conclude that the right side of (2.5.35) is also a Laurent polynomial. It can then be checked that the intersection of the zeros of $\beta^1(m, n, u)$ and $\eta^1(m, n, u)$ is empty for generic values of λ , for all $m, n \geq 1$. This ends the proof that $\mathbf{D}^{m,n}(u)$ is a Laurent polynomial in $z = e^{iu}$.

2.6 Closure at roots of unity

For generic values of λ , the fusion hierarchy, T -system and Y -system are infinite systems of equations. In this section, we fix the crossing parameter to rational multiples of π

$$\lambda = \lambda_{a,b} = \frac{\pi(b-a)}{2b} , \quad \gcd(a, b) = 1 , \quad (2.6.1)$$

for which these systems close finitely. The main result of this section, stated in Section 2.6.1, is the closure relation for the fusion hierarchy. There, we also give the strategy of the proof, which is then the topic of Sections 2.6.2 to 2.6.4. Finally, Section 2.6.5 shows that the Y -system also closes finitely at roots of unity.

2.6.1 Results and skeleton of the proof

A closure relation for the fusion hierarchy is a linear relation between fused transfer matrices. The following theorem gives these relations for the $A_2^{(2)}$ loop model on the strip.

THEOREM 2.6.1. For $\lambda = \lambda_{a,b}$ with $b \geq 2$, the fusion hierarchy is finite, namely $\mathbf{D}^{b,0}(u)$ can be expressed as a linear combination of $\mathbf{D}^{m,n}(u)$ with $m + n < b$. For $b > 2$, the closure relation reads

$$\begin{aligned} & w^{(a)}(u_{-5/2})f_{-1}\mathbf{D}_0^{b,0} - w^{(1)}(u_{-5/2})\mathbf{D}_2^{b-2,1} \\ & + w(u_{-7/2})w(u_{-5/2})\bar{w}(u_{-5/2})\bar{w}(u_{-3/2})\bar{w}(u_{-1/2})\bar{w}^{(a)}(u_{-3/2})\bar{w}^{(-1)}(u_{1/2})f_{-3}\mathbf{D}_4^{b-3,0} \\ & = w(u_{-5/2})(U - 2V)f_{-3}f_{-2}f_{-1}\kappa\mathbf{I}, \end{aligned} \quad (2.6.2a)$$

and for $b = 2$

$$w^{(a)}(u_{-5/2})\mathbf{D}_0^{2,0} - w^{(1)}(u_{-5/2})w^{(1)}(-u_{3/2})w(u_{-1/2})\mathbf{D}_2^{0,1} = w(u_{-5/2})(U - 2V)f_{-3}f_{-2}\kappa\mathbf{I}, \quad (2.6.2b)$$

where

$$U(u) = \prod_{j=0}^{b-1} \bar{w}(u_{2j+1/2})w(u_{2j+3/2}), \quad V(u) = \prod_{j=0}^{b-1} \bar{w}(u_{2j+3/2})w(u_{2j+1/2}), \quad (2.6.2c)$$

and

$$\kappa = \begin{cases} (-1)^{a-1}(2 + (-1)^b) & \text{identical,} \\ -3 & \text{mixed.} \end{cases} \quad (2.6.2d)$$

The relation (2.6.2) holds for $b = 3$ with $\mathbf{D}_4^{0,0} \mapsto f_1f_2\mathbf{I}$.

This result thus holds for all four choices of boundary conditions. A proof of the theorem follows in Sections 2.6.2 to 2.6.4. The rest of this section presents the skeleton of this proof.

First we note that (2.6.2a) is an equality between centered Laurent polynomials in $z = e^{iu}$ of maximal degree $6N + 2b + 1$ and $6N$, for identical and mixed boundary conditions respectively. Using the strategy outlined at the end of Section 2.3.3, it thus suffices to check that the identity holds for $12N + 4b + 3$ and $12N + 1$ values of z , respectively.

An important simplification arises from the fact that the closure relation can be written in terms of the determinants as

$$\det(b, 0)_0 - \mathcal{F}_{-2} \det(b - 2, 1)_2 + \mathcal{F}_{-2}\mathcal{F}_{-1}\mathcal{F}_0 \det(b - 3, 0)_4 = \Lambda(U - 2V)\kappa\mathbf{I} \quad (2.6.3)$$

with

$$\Lambda(u) = \prod_{j=0}^{2b-1} s(2u_j)f_j \prod_{\ell=0}^{b-1} \bar{w}(u_{2\ell+1/2})w(u_{2\ell+3/2}). \quad (2.6.4)$$

We then define

$$\mathcal{P}_0 = \det(b, 0)_0 - \mathcal{F}_{-2} \det(b - 2, 1)_2 + \mathcal{F}_{-2}\mathcal{F}_{-1}\mathcal{F}_0 \det(b - 3, 0)_4, \quad \mathcal{J}_0 = \Lambda(U - 2V)\kappa\mathbf{I}, \quad (2.6.5)$$

so that the closure equation reads $\mathcal{P}_0 = \mathcal{J}_0$. This equation is also an equality between Laurent polynomials, whose degrees are however larger than the ones given above for (2.6.2a). We will show in

Section 2.6.2 that for $\lambda = \lambda_{a,b}$, $\mathcal{P}(u)$ and $\mathcal{J}(u)$ satisfy the periodicity and crossing symmetries

$$\mathcal{P}(u) = \mathcal{P}(u + 2\lambda) = \mathcal{P}(5\lambda - 2b\lambda - u), \quad \mathcal{J}(u) = \mathcal{J}(u + 2\lambda) = \mathcal{J}(5\lambda - 2b\lambda - u). \quad (2.6.6)$$

These symmetries turn out to be useful to reduce the number of points where (2.6.2a) needs to be evaluated. Indeed, dividing both sides of (2.6.2a) by $w(u_{-5/2})f_{-3}f_{-2}f_{-1}$, we see that the equation we want to prove reduces to

$$\begin{aligned} & \frac{1}{w(u_{-5/2})f_{-3}f_{-2}f_{-1}} \left[w^{(a)}(u_{-5/2})f_{-1}\mathbf{D}_0^{b,0} - w^{(1)}(u_{-5/2})\mathbf{D}_2^{b-2,1} \right. \\ & \left. + w(u_{-7/2})w(u_{-5/2})\bar{w}(u_{-5/2})\bar{w}(u_{-3/2})\bar{w}(u_{-1/2})\bar{w}^{(a)}(u_{-3/2})\bar{w}^{(-1)}(u_{1/2})f_{-3}\mathbf{D}_4^{b-3,0} \right] \\ & = (U - 2V)\kappa \mathbf{I}. \end{aligned} \quad (2.6.7)$$

We readily observe that the right-hand side is invariant under shifts of 2λ . The same applies to the left-hand side, as it can be expressed as $\mathcal{P}(u)/\Lambda(u)$, with both factors individually invariant under shifts of 2λ .

The left-hand side of (2.6.7) has a non-trivial denominator, letting us believe that it may have poles at values of u where $w(u_{-5/2})f_{-3}f_{-2}f_{-1} = 0$. But it is clear that it has no poles at values of u where $w(u_{-1/2})f_0f_1 = 0$. Once (2.6.6) is established, we know that the left-hand side is periodic in u with period 2λ , and thus deduce that it has no poles at all, including at the zeros of the denominator $w(u_{-5/2})f_{-3}f_{-2}f_{-1}$. This equivalently implies that (2.6.2a) holds at all values where $w(u_{-5/2})f_{-3}f_{-2}f_{-1} = 0$. We conclude that (2.6.7) is an equality of Laurent polynomials of degree width $4b$ for SS and CC boundary conditions, and of degree width 0 for SC and CS boundary conditions. To prove the equation, we must show that it holds for $4b + 1$ and 1 values of z , for identical and mixed boundary conditions, respectively. In Section 2.6.3, we will prove, for the identical cases, that (2.6.7) holds at $4b$ finite values of u corresponding to $4b$ distinct values of $z = e^{iu}$. The last evaluation point, needed for both the identical and mixed cases, is the braid limit $u \rightarrow i\infty$, corresponding to $z = 0$. This will be the topic of Section 2.6.4, and will then end the proof of the theorem, for all four boundary conditions.

2.6.2 Symmetries at roots of unity

In this section, we establish the periodicity and crossing properties (2.6.6) of the functions $\mathcal{P}(u)$ and $\mathcal{J}(u)$. The function $\mathcal{J}(u)$ is equal to \mathbf{I} times a function involving only simple trigonometric functions, and verifying that it satisfies the two symmetry properties is straightforward. We therefore focus on the function $\mathcal{P}(u)$. We will use repeatedly the symmetries $\mathcal{D}_{2b+k} = \mathcal{D}_k$ and $\mathcal{F}_{2b+k} = \mathcal{F}_k$. Using

(2.4.32c) with $(m, n) = (b - 2, 1)$, we express $\mathcal{P}(u)$ as

$$\begin{aligned} \mathcal{P}(u) &= \det(b, 0)_0 - \mathcal{F}_{-2}\mathcal{D}_{-1} \det(b - 2, 0)_2 + \mathcal{F}_{-4}\mathcal{F}_{-3}\mathcal{F}_{-2} \det(b - 3, 0)_2 \\ &\quad + \mathcal{F}_{-2}\mathcal{F}_{-1}\mathcal{F}_0 \det(b - 3, 0)_4 . \end{aligned} \quad (2.6.8)$$

We now show the crossing symmetry of $\mathcal{P}(u)$. It directly follows from (2.4.35a) and (2.4.35d) that $\det(b, 0)(u) = \det(b, 0)(5\lambda - 2b\lambda - u)$, so the first term in (2.6.8) is invariant under $u \mapsto 5\lambda - 2b\lambda - u$. For the second term, we have

$$\begin{aligned} \mathcal{F}(5\lambda - 2b\lambda - u - 2\lambda) &= \mathcal{F}(u - 2\lambda + 2b\lambda) = \mathcal{F}_{-2} , \\ \mathcal{D}(5\lambda - 2b\lambda - u - \lambda) &= \mathcal{D}(u - \lambda + 2b\lambda) = \mathcal{D}_{-1} , \\ \det(b - 2, 0)(5\lambda - 2b\lambda - u + 2\lambda) &= \det(b - 2, 0)(5\lambda - 2(b - 2)\lambda - (u + 2\lambda)) = \det(b - 2, 0)_2 , \end{aligned} \quad (2.6.9)$$

where we used (2.4.26c) and (2.4.26d). We thus see that this second term is also invariant. This is in contrast with the last two terms of (2.6.8), which are mapped to one another:

$$\det(b - 3, 0)(5\lambda - 2b\lambda - u + 2\lambda) = \det(b - 3, 0)(5\lambda - 2(b - 3)\lambda - (u + 4\lambda)) = \det(b - 3, 0)_4(u) . \quad (2.6.10)$$

The same is seen to apply to the prefactors, namely we have

$$\left(\mathcal{F}_{-4}\mathcal{F}_{-3}\mathcal{F}_{-2} \det(b - 3, 0)_2 \right) (5\lambda - 2b\lambda - u) = \left(\mathcal{F}_{-2}\mathcal{F}_{-1}\mathcal{F}_0 \det(b - 3, 0)_4 \right) (u) , \quad (2.6.11)$$

ending the proof of the crossing symmetry.

To prove the periodicity, we compute $\mathcal{P}_0 - \mathcal{P}_2$. The terms proportional to $\det(b - 3, 0)_4$ immediately cancel, and we are left with

$$\begin{aligned} \mathcal{P}_0 - \mathcal{P}_2 &= \det(b, 0)_0 - \mathcal{F}_{-2}\mathcal{D}_{-1} \det(b - 2, 0)_2 + \mathcal{F}_{-4}\mathcal{F}_{-3}\mathcal{F}_{-2} \det(b - 3, 0)_2 \\ &\quad - \det(b, 0)_2 + \mathcal{F}_0\mathcal{D}_1 \det(b - 2, 0)_4 - \mathcal{F}_0\mathcal{F}_1\mathcal{F}_2 \det(b - 3, 0)_6 . \end{aligned} \quad (2.6.12)$$

We now expand $\det(b, 0)_0$ using (2.4.34b). The terms proportional to $\det(b - 2, 0)_4$ and $\det(b - 3, 0)_6$ cancel, resulting in

$$\begin{aligned} \mathcal{P}_0 - \mathcal{P}_2 &= \mathcal{D}_0 \det(b - 1, 0)_2 - \mathcal{F}_{-2}\mathcal{D}_{-1} \det(b - 2, 0)_2 \\ &\quad + \mathcal{F}_{-4}\mathcal{F}_{-3}\mathcal{F}_{-2} \det(b - 3, 0)_2 - \det(b, 0)_2 = 0 , \end{aligned} \quad (2.6.13)$$

where at the last step we rewrote $\det(b, 0)_2$ using (2.4.34a). This ends the proof of the periodicity of $\mathcal{P}(u)$.

2.6.3 Evaluations at finite points

In this section, we focus on the SS and CC boundary conditions. Our goal is to prove that the closure relation holds at $4b$ distinct values of u that are real and in the interval $[0, 2\pi)$.

Let us suppose that we are able to prove it for some finite value $u = \hat{u}$. By the periodicity and crossing properties (2.6.6) of $\mathcal{P}(u)$ and $\mathcal{J}(u)$, we will also have proved the relation for $u = \hat{u} + 2k\lambda$, $\hat{u} + 2k\lambda + \pi$, $-\hat{u} + (2k + 1)\lambda$ and $-\hat{u} + (2k + 1)\lambda + \pi$, with $k = 0, \dots, b - 1$. Depending on \hat{u} and λ , these may or may not lead to a full set of $4b$ distinct values of $z = e^{iu}$. This turns out to depend on the parity of $b - a$. For $b - a$ odd, choosing $\hat{u} = \ell\lambda$ for a given $\ell \in \mathbb{Z}$ does in fact lead to $4b$ distinct values of z . In contrast, for $b - a$ even, choosing $\hat{u} = \ell\lambda$ for any $\ell \in \mathbb{Z}$ only gives $2b$ distinct values. These can then be combined to $2b$ more distinct values obtained from $\hat{u} = \ell'\lambda + \frac{\pi}{2}$ for some $\ell' \in \mathbb{Z}$, leading to a full set of $4b$ values.

Thus for the proof, we will show that the closure relation holds for $\hat{u} = (4 - b)\lambda + \frac{r\pi}{2}$ with $r \in \{0, 1\}$. The cases $b = 2$ and $b = 3$ are treated separately in Section 2.A.4. For $b \geq 4$, we keep λ generic for now and note that⁴

$$\mathbf{D}_2^{b-2,1}(\hat{u}) = \frac{\beta^2(b-2, 1, \hat{u}_2)}{\beta^1(b-2, 1, \hat{u}_2)} \mathbf{D}_{2b-1}^{1,0}(\hat{u}) \mathbf{D}_2^{b-2,0}(\hat{u}), \quad (2.6.14a)$$

$$\mathbf{D}_4^{b-3,0}(\hat{u}) = \frac{\mu^2(b-3, \hat{u}_4)}{\mu^1(b-3, \hat{u}_4)} \mathbf{D}_{2b-4}^{1,0}(\hat{u}) \mathbf{D}_4^{b-4,0}(\hat{u}). \quad (2.6.14b)$$

The three remaining fused transfer matrices, $\mathbf{D}_0^{b,0}(\hat{u})$, $\mathbf{D}_2^{b-2,0}(\hat{u})$ and $\mathbf{D}_4^{b-4,0}(\hat{u})$, are precisely of the form $\mathbf{D}_0^{m,0}(\hat{v})$ with $\hat{v} = (4 - m)\lambda + \frac{r\pi}{2}$, for $m = b, b - 2$, and $b - 4$ respectively. By (2.4.43), these tangles are all multiples of \mathbf{I} . Let us define

$$\mathbf{R}^1(u) = w^{(a)}(u_{-5/2}) f_{-1} \mathbf{D}_0^{b,0}, \quad (2.6.15a)$$

$$\mathbf{R}^2(u) = -w^{(1)}(u_{-5/2}) \mathbf{D}_2^{b-2,1}, \quad (2.6.15b)$$

$$\mathbf{R}^3(u) = w(u_{-7/2}) w(u_{-5/2}) \bar{w}(u_{-5/2}) \bar{w}(u_{-3/2}) \bar{w}(u_{-1/2}) \bar{w}^{(a)}(u_{-3/2}) \bar{w}^{(-1)}(u_{1/2}) f_{-3} \mathbf{D}_4^{b-3,0}, \quad (2.6.15c)$$

$$\mathbf{R}^4(u) = w(u_{-5/2}) U f_{-3} f_{-2} f_{-1} \mathbf{I}, \quad (2.6.15d)$$

$$\mathbf{R}^5(u) = w(u_{-5/2}) V f_{-3} f_{-2} f_{-1} \mathbf{I}. \quad (2.6.15e)$$

Using (2.6.14) and (2.4.43), we obtain simple expressions for $\mathbf{R}^1(\hat{u})$, $\mathbf{R}^2(\hat{u})$ and $\mathbf{R}^3(\hat{u})$: $\mathbf{R}^1(\hat{u})$ is proportional to \mathbf{I} , whereas $\mathbf{R}^2(\hat{u})$ and $\mathbf{R}^3(\hat{u})$ are respectively proportional to $\mathbf{D}_{2b-1}^{1,0}(\hat{u})$ and $\mathbf{D}_{2b-4}^{1,0}(\hat{u})$. This is true for all λ . Setting $\lambda = \lambda_{a,b}$, we remark that

$$\mathbf{D}_{2b-1}^{1,0}(\hat{u}) = \mathbf{D}_{2b-4}^{1,0}(\hat{u}) = \mathbf{D}_0^{1,0}((b - a + r)\frac{\pi}{2}), \quad (2.6.16)$$

4. We note that (2.6.14b) also works for $b = 4$, with $\mathbf{D}_4^{0,0} \mapsto f_1 f_2 \mathbf{I}$ and $\frac{\mu^2(b-3, \hat{u}_4)}{\mu^1(b-3, \hat{u}_4)}$ understood as $\lim_{u \rightarrow \hat{u}} \frac{\mu^2(b-3, u_4)}{\mu^1(b-3, u_4)}$.

which follows from periodicity and crossing symmetry. From (2.4.42b), we see that $D_{2b-1}^{1,0}(\hat{u})$ and $D_{2b-4}^{1,0}(\hat{u})$ are scalar multiples of \mathbf{I} at $\lambda = \lambda_{a,b}$.

The evaluation of the closure relation at \hat{u} then reads

$$\mathbf{R}^1(\hat{u}) + \mathbf{R}^2(\hat{u}) + \mathbf{R}^3(\hat{u}) = \kappa(\mathbf{R}^4(\hat{u}) - 2\mathbf{R}^5(\hat{u})). \quad (2.6.17)$$

and checking it amounts to comparing the prefactors of \mathbf{I} in $\mathbf{R}^1(\hat{u})$, $\mathbf{R}^2(\hat{u})$ and $\mathbf{R}^3(\hat{u})$ with those in $\mathbf{R}^4(\hat{u})$ and $\mathbf{R}^5(\hat{u})$. Evaluating the prefactors, one finds

$$\mathbf{R}^1(\hat{u}) = \mathbf{R}^2(\hat{u}) = \mathbf{R}^3(\hat{u}) = -\mathbf{R}^4(\hat{u}) = (-1)^{b+1}\mathbf{R}^5(\hat{u}), \quad \text{for } b \geq 4. \quad (2.6.18)$$

For $b - a$ even, each $\mathbf{R}^i(\hat{u})$ in fact vanishes, and thus the above equalities hold trivially in this case. In contrast, for $b - a$ odd, none of the $\mathbf{R}^i(\hat{u})$ vanish. For either parity of $b - a$, the proof of (2.6.17) is trivial using (2.6.18).

The proof of (2.6.18) is lengthy but straightforward. To show how it works, let us prove that $\mathbf{R}^4(\hat{u}) = (-1)^b \mathbf{R}^5(\hat{u})$. From the definition (2.6.15), we have

$$U(\hat{u}) = \prod_{j=0}^{b-1} \bar{w}_{-b+2j+9/2} w_{-b+2j+11/2}, \quad V(\hat{u}) = \prod_{j=0}^{b-1} \bar{w}_{-b+2j+11/2} w_{-b+2j+9/2}, \quad (2.6.19)$$

where we use the short-hand notation

$$w_k = w(k\lambda + \frac{r\pi}{2}), \quad \bar{w}_k = \bar{w}(k\lambda + \frac{r\pi}{2}). \quad (2.6.20)$$

The proof rests on the identities

$$w_{k+2b} = (-1)^{b-a} w_k, \quad \bar{w}_{k+2b} = (-1)^{b-a} \bar{w}_k, \quad w_{-k} \bar{w}_{-\ell} = -w_k \bar{w}_\ell, \quad (2.6.21)$$

valid for both SS and CC and all k, ℓ . The first two of these equations hold for $\lambda = \lambda_{a,b}$, whereas the last one holds for all λ . The first two identities allow us to write

$$\prod_{j=0}^{b-1} \bar{w}_{2j+x} w_{2j+y} = \prod_{j'=1}^b \bar{w}_{2(j'-1)+x} w_{2(j'-1)+y} = \prod_{j'=0}^{b-1} \bar{w}_{2j'+x-2} w_{2j'+y-2}, \quad (2.6.22)$$

for all x, y . Thus we may freely shift the indices of all functions in the products by two. For the products in (2.6.19), this yields

$$U(\hat{u}) = \prod_{j=0}^{b-1} \bar{w}_{-b+2j+1/2} w_{-b+2j+3/2}, \quad (2.6.23a)$$

$$V(\hat{u}) = (-1)^b \prod_{j=0}^{b-1} \bar{w}_{b-2j-11/2} w_{b-2j-9/2} = (-1)^b \prod_{j'=0}^{b-1} \bar{w}_{b-2(b-1-j')-11/2} w_{b-2(b-1-j')-9/2}$$

$$= (-1)^b \prod_{j'=0}^{b-1} \bar{w}_{-b+2j'-7/2} w_{-b+2j'-5/2} = (-1)^b \prod_{j'=0}^{b-1} \bar{w}_{-b+2j'+1/2} w_{-b+2j'+3/2} . \quad (2.6.23b)$$

The two products are thus equal up to the sign $(-1)^b$, confirming that $\mathbf{R}^4(\hat{u}) = (-1)^b \mathbf{R}^5(\hat{u})$. Showing that $\mathbf{R}^1(\hat{u})$, $\mathbf{R}^2(\hat{u})$ and $\mathbf{R}^3(\hat{u})$ are equal to $-\mathbf{R}^4(\hat{u})$ then follows three similar paths. For each, one can show, using the identities $f(-u) = f(u) = f(u + \pi)$ and $s(-u) = -s(u) = s(u + \pi)$, that all functions $f(u_k)$ and $s(2u_k)$ appearing in the functions $\mathbf{R}^1(\hat{u})$, $\mathbf{R}^2(\hat{u})$ and $\mathbf{R}^3(\hat{u})$ simplify up to a potential sign. A finer analysis is needed for the factors w and \bar{w} , but one can check that they always coincide with those of $\mathbf{R}^4(\hat{u})$, again up to potential signs. These lengthy checks complete the proof of (2.6.18). Finally, the fact that each $\mathbf{R}^i(\hat{u})$ vanishes for $b - a$ even follows from an analysis of the products of w, \bar{w} functions: either the argument of a sine function is an integer multiple of π or the argument of a cosine function is an odd integer multiple of $\frac{\pi}{2}$. This ends the proof of the closure relation at $4b$ separate values, for both parities of $b - a$.

2.6.4 Evaluation at infinity

This section finishes the proof of the closure relations by taking the braid limit of the four terms in (2.6.2a). These are all polynomials in $z = e^{iu}$ of the same degree. Multiplying them with a properly chosen rational function of e^{iu} gives a finite result in the limit $u \rightarrow i\infty$. This rational function will be chosen as

$$r(u) = \frac{e^{4i\lambda bN}}{w^{(a)}(u_{-5/2}) f_{-3} f_{-2} f_{-1} \prod_{j=0}^{b-1} \gamma(u_{2j})}, \quad (2.6.24)$$

where $\gamma(u)$ defined in (2.4.50). This choice ensures that the first term is

$$\lim_{u \rightarrow i\infty} r(u) w^{(a)}(u_{-5/2}) \mathbf{D}_0^{b,0}(u) = \mathbf{D}_\infty^{b,0}, \quad (2.6.25)$$

as introduced in (2.4.52a), and thus that the limit of the closure relation is non-trivial. With this rational function $r(u)$, the limit of the other terms are

$$\begin{aligned} \lim_{u \rightarrow i\infty} -r(u) w^{(1)}(u_{-5/2}) \mathbf{D}_2^{b-2,1}(u) &= -\mathbf{D}_\infty^{b-2,1}, \\ \lim_{u \rightarrow i\infty} r(u) w(u_{-7/2}) w(u_{-5/2}) \bar{w}(u_{-5/2}) \bar{w}(u_{-3/2}) \bar{w}(u_{-1/2}) \bar{w}^{(a)}(u_{-3/2}) \bar{w}^{(-1)}(u_{1/2}) f_3 \mathbf{D}_4^{b-3,0}(u) &= \mathbf{D}_\infty^{b-3,0}, \\ \lim_{u \rightarrow i\infty} r(u) w(u_{-5/2}) (U - 2V) f_{-3} f_{-2} f_{-1} \kappa \mathbf{I} &= \Delta^b = \mathbf{I} \times \begin{cases} 1 + 2(-1)^b & \text{identical,} \\ 3 & \text{mixed.} \end{cases} \end{aligned} \quad (2.6.26)$$

The computation of these limits proceeds as in the proof leading to the identities (2.4.53) for the fusion hierarchy of braid transfer tangles. The problem is thus reduced to proving that the braid transfer tangles satisfy

$$\mathbf{D}_\infty^{b,0} - \mathbf{D}_\infty^{b-2,1} + \mathbf{D}_\infty^{b-3,0} - \Delta^b = 0, \quad b \geq 2. \quad (2.6.27)$$

(For the special cases $b = 2$ and $b = 3$, this is also true with the conventions $\mathbf{D}_\infty^{0,0} = \mathbf{I}$ and $\mathbf{D}_\infty^{-1,0} = 0$.) The proof of this identity proceeds in several steps: (i) we introduce families of polynomials $p_m(x)$ and $q_m(x)$ related to Chebyshev polynomials and establish a link with the fused transfer matrices; (ii) we show that one of these polynomials is equal, up to an additive constant, to the left-hand side of (2.6.27) with the variable x set to $\mathbf{D}_\infty - \mathbf{I}$; (iii) we recall that the tangle \mathbf{D}_∞ is a central element of $\mathbf{dTL}_N(\beta)$ and discuss its minimal polynomial in the regular representation of this algebra; (iv) we show that the determinant obtained in (ii) has this minimal polynomial as a factor, thus confirming that the left-hand side of (2.6.27) is equal to zero.

Let $p_m(x)$ with $m \geq 1$ and $q_m(x)$ with $m \geq 3$ be the polynomials in x defined as the following $m \times m$ determinants:

$$p_m(x) = \begin{vmatrix} x & 1 & 0 & \dots & 0 & 0 \\ 1 & x & 1 & \dots & 0 & 0 \\ 0 & 1 & x & \dots & 0 & 0 \\ \vdots & \vdots & \vdots & \ddots & \vdots & \vdots \\ 0 & 0 & 0 & \dots & x & 1 \\ 0 & 0 & 0 & \dots & 1 & x \end{vmatrix}, \quad q_m(x) = \begin{vmatrix} x & 1 & 0 & \dots & 0 & 1 \\ 1 & x & 1 & \dots & 0 & 0 \\ 0 & 1 & x & \dots & 0 & 0 \\ \vdots & \vdots & \vdots & \ddots & \vdots & \vdots \\ 0 & 0 & 0 & \dots & x & 1 \\ 1 & 0 & 0 & \dots & 1 & x \end{vmatrix}. \quad (2.6.28)$$

By expanding the determinants along the first line, they are seen to satisfy the recurrence relations

$$p_m(x) = xp_{m-1}(x) - p_{m-2}(x), \quad q_m(x) = p_m(x) - p_{m-2}(x) - 2(-1)^m, \quad m \geq 3. \quad (2.6.29)$$

The solutions are written in terms of Chebyshev polynomials as

$$p_m(x) = U_m\left(\frac{x}{2}\right), \quad q_m(x) = 2T_m\left(\frac{x}{2}\right) - 2(-1)^m. \quad (2.6.30)$$

This then allows us to extend the definition of $q_m(x)$ to $m = 1$ and $m = 2$.

The determinant form of $q_m(x)$ was crucial in the study of the dense loop models (see Section 7 of [10]). We now relate the fused braid transfer matrices of the dilute $A_2^{(2)}$ model to the polynomials $p_m(x)$.

First, we note the matrix identity

$$\begin{pmatrix} 1 & 1 & 0 & \dots & 0 & 0 \\ 0 & 1 & 1 & \dots & 0 & 0 \\ 0 & 0 & 1 & \dots & 0 & 0 \\ \vdots & \vdots & \vdots & \ddots & \vdots & \vdots \\ 0 & 0 & 0 & \dots & 1 & 1 \\ 0 & 0 & 0 & \dots & 0 & 1 \end{pmatrix} \cdot \begin{pmatrix} x & 1 & 0 & \dots & 0 & 0 \\ 1 & x & 1 & \dots & 0 & 0 \\ 0 & 1 & x & \dots & 0 & 0 \\ \vdots & \vdots & \vdots & \ddots & \vdots & \vdots \\ 0 & 0 & 0 & \dots & x & 1 \\ 0 & 0 & 0 & \dots & 1 & x \end{pmatrix}$$

$$= \begin{pmatrix} x+1 & x+1 & 1 & 0 & \dots & 0 & 0 & 0 \\ 1 & x+1 & x+1 & 1 & \dots & 0 & 0 & 0 \\ 0 & 1 & x+1 & x+1 & \dots & 0 & 0 & 0 \\ 0 & 0 & 1 & x+1 & \dots & 0 & 0 & 0 \\ \vdots & \vdots & \vdots & \ddots & \vdots & \vdots & \vdots & \\ 0 & 0 & 0 & 0 & \dots & x+1 & x+1 & 1 \\ 0 & 0 & 0 & 0 & \dots & 1 & x+1 & x+1 \\ 0 & 0 & 0 & 0 & \dots & 0 & 1 & x \end{pmatrix}. \quad (2.6.31)$$

Except for the bottom right entry, this matrix with $x+1 \rightarrow \mathbf{D}_\infty$ is identical to matrix in the expression (2.4.54) for $\mathbf{D}_\infty^{m,0}$. Moreover, the first matrix in (2.6.31) clearly has a unit determinant. By expanding the determinants of the other two matrices along the last row, we find the simple identity

$$\mathbf{D}_\infty^{m,0} = \mathbf{D}_\infty^{m-1,0} + p_m(\mathbf{D}_\infty - \mathbf{I}). \quad (2.6.32)$$

This completes step (i).

Step (ii) aims at tying the polynomials $q_m(x)$ to the left-hand side of (2.6.27). The relation is remarkably simple:

$$\mathbf{D}_\infty^{m,0} - \mathbf{D}_\infty^{m-2,1} + \mathbf{D}_\infty^{m-3,0} - \Delta^m = q_m(\mathbf{D}_\infty^{1,0} - \mathbf{I}) + \begin{cases} 0 & \text{identical,} \\ 2((-1)^m - 1)\mathbf{I} & \text{mixed,} \end{cases} \quad m \geq 2, \quad (2.6.33)$$

where we set $\mathbf{D}_\infty^{-1,0} \mapsto 0$ for $m = 2$. This relation is easily checked for $m = 2$ and $m = 3$. The proof for $m \geq 4$ is by induction:

$$\begin{aligned} \mathbf{D}_\infty^{m,0} - \mathbf{D}_\infty^{m-2,1} + \mathbf{D}_\infty^{m-3,0} &= \mathbf{D}_\infty^{m,0} - \mathbf{D}_\infty \mathbf{D}_\infty^{m-2,0} + 2\mathbf{D}_\infty^{m-3,0} \\ &= \mathbf{D}_\infty^{m-1,0} - \mathbf{D}_\infty \mathbf{D}_\infty^{m-3,0} + 2\mathbf{D}_\infty^{m-4,0} + p_m(x) - (1+x)p_{m-2}(x) + 2p_{m-3}(x) \\ &= q_{m-1}(x) + (1 - 2(-1)^m)\mathbf{I} + p_m(x) - (1+x)p_{m-2}(x) + 2p_{m-3}(x) \\ &= q_m(x) + (1 + 2(-1)^m)\mathbf{I}, \end{aligned} \quad (2.6.34)$$

where $x = \mathbf{D}_\infty - \mathbf{I}$. The inductive hypothesis was used at the third equality, and the relations (2.6.29) at the fourth. This ends the proof of (2.6.33), and therefore of step (ii).

The first two steps translated the statement (2.6.27) into one involving only the fundamental braid transfert tangle \mathbf{D}_∞ defined in (2.4.49). Defining the polynomial

$$\mathbb{Q}_m(x) = q_m(x-1) + \begin{cases} 0 & \text{identical,} \\ 2((-1)^m - 1) & \text{mixed,} \end{cases} \quad (2.6.35)$$

we must then show that $\mathbb{Q}_b(x)$ vanishes for $x = \mathbf{D}_\infty$ with $\lambda = \lambda_{a,b}$. It will be so if this polynomial

contains, as a factor, the minimal polynomial of \mathbf{D}_∞ or, more precisely, the minimal polynomial $\mathbb{P}_{a,b}(x)$ of its action on the algebra $\mathfrak{dTL}_N(\beta)$ with $\beta = -2\cos 4\lambda_{a,b}$. In other words, we need to prove that $\mathbb{P}_{a,b} \mid \mathbb{Q}_b$. Step (iii) consists in finding all factors that can possibly appear in this minimal polynomial $\mathbb{P}_{a,b}(x)$. A key observation is that \mathbf{D}_∞ is central. A proof of this for a slightly different element of $\mathfrak{dTL}_N(\beta)$ is given in Appendix B of [21]. It rests upon relations similar to (2.4.46) and goes through without change for \mathbf{D}_∞ . Since it is central, it defines a homomorphism $d : \mathbb{M} \rightarrow \mathbb{M}$ on any module \mathbb{M} by multiplication $\mu \mapsto \mathbf{D}_\infty \mu$, for $\mu \in \mathbb{M}$. Such a homomorphism can have only one eigenvalue on an indecomposable module. Computing this eigenvalue Υ_N^d on the standard module W_N^d is then a good idea. Indeed, these standard modules are indecomposable and their quotients by their radicals give a complete family of isomorphic classes of simple modules. In other words, the eigenvalues of the action of \mathbf{D}_∞ on any module \mathbb{M} will be among those on the W_N^d with $0 \leq d \leq N$. Similar computations were done before. For example, Section 3.1 of [31] does such a computation for the action of the fundamental braid transfer matrix for the ordinary Temperley-Lieb algebra $\mathfrak{TL}_N(\beta)$ on its standard modules. The computation for \mathbf{D}_∞ is similar and gives

$$\Upsilon_N^d = \mathbf{D}_\infty|_{W_N^d} = 1 + 2\epsilon \cos(4\lambda(1+d)), \quad \epsilon = \begin{cases} -1 & \text{identical,} \\ 1 & \text{mixed.} \end{cases} \quad (2.6.36)$$

Can any of these eigenvalues have multiplicities in the minimal polynomial of \mathbf{D}_∞ in the regular representation? For roots of unity, the answer is yes [21]. For any d that is not critical, there is a non-zero nilpotent homomorphism from the block of $\mathfrak{dTL}_N(\beta)$, where \mathbf{D}_∞ has the eigenvalue Υ_N^d , to itself. The square of this homomorphism is zero and no other such homomorphisms ρ can be nilpotent of a higher order, that is, there exists no homomorphism ρ such that $\rho^i = 0$ but $\rho^{i-1} \neq 0$ with $i > 2$. For d critical, any indecomposable module on which \mathbf{D}_∞ has the eigenvalue Υ_N^d is in fact irreducible and the minimal polynomial of \mathbf{D}_∞ on these is simply $(x - \Upsilon_N^d)$. Summing up, the minimal polynomial of \mathbf{D}_∞ may only contain factors $(x - \Upsilon_N^d)^1$ for d critical and $(x - \Upsilon_N^d)^2$ for d non-critical, but none with higher powers. In conclusion, the minimal polynomial $\mathbb{P}_{a,b}$ of \mathbf{D}_∞ divides the polynomial

$$\mathbb{R}_{a,b}(x) = \prod_{d \in D} (x - \Upsilon_N^d)^{n_d}, \quad n_d = \begin{cases} 1 & d \text{ critical,} \\ 2 & d \text{ non-critical,} \end{cases} \quad (2.6.37)$$

where $\lambda = \lambda_{a,b}$ and D is a subset of $\{0, 1, \dots, N\}$ such that $\{\Upsilon_N^d \mid d \in D\}$ contains all possible eigenvalues in $\{\Upsilon_N^d \mid 0 \leq d \leq N\}$ once and only once. (For $N < 2b - 1$, the orbit of some non-critical d will only contain d . In this case, $n_d = 1$ and $\mathbb{P}_{a,b}$ divides $\mathbb{R}_{a,b}$ without being equal to it. If $N \geq 2b - 1$, then $\mathbb{P}_{a,b} = \mathbb{R}_{a,b}$.)

The goal of step (iv) is to establish whether the polynomial $\mathbb{Q}_b(x)$ specified to $\lambda = \lambda_{a,b}$ contains the polynomial $\mathbb{R}_{a,b}(x)$ as a factor. If it does, then $\mathbb{P}_{a,b} \mid \mathbb{R}_{a,b} \mid \mathbb{Q}_b$ and thus $\mathbb{P}_{a,b} \mid \mathbb{Q}_b$ as desired. We rewrite the polynomial \mathbb{Q}_b using (2.6.33) as

$$\mathbb{Q}_b(x) = 2(T_b(\frac{1}{2}(x-1)) - \epsilon^b). \quad (2.6.38)$$

We must thus check that this polynomial vanishes for x replaced by the eigenvalue Υ_N^d , and show that the multiplicity of such a zero is greater than or equal to its multiplicity n_d in $\mathbb{R}_{a,b}(x)$. Because of the expression (2.6.36) for Υ_N^d , it is natural to introduce the change of variables $x = 1 + 2\epsilon \cos \theta$, thus rewriting

$$\mathbb{Q}_b(x) = 2(T_b(\epsilon \cos \theta) - \epsilon^b) = 2\epsilon^b(T_b(\cos \theta) - 1) = -4\epsilon^b \sin^2(\frac{1}{2}b\theta). \quad (2.6.39)$$

The property $T_b(-x) = (-1)^b T_b(x)$ was used at the second equality and the trigonometric formula $T_b(\cos \theta) = \cos(b\theta)$ at the third one. The evaluation at $x = \Upsilon_N^d$, namely at $\theta = 4\lambda_{a,b}(1+d)$, gives

$$\mathbb{Q}_b(\Upsilon_N^d) = -4\epsilon^b \sin^2((b-a)(1+d)\pi), \quad (2.6.40)$$

which is clearly zero for any integer d .

The multiplicity of these zeros must be computed for $\mathbb{Q}_b(x)$ seen as a polynomial in x . Care must be taken to ensure that the change of variables $x \mapsto \theta$ has not introduced spurious multiplicities. To get the correct multiplicities, we compute

$$\frac{d}{dx} \mathbb{Q}_b(x) = \frac{d\theta}{dx} \frac{d}{d\theta} \mathbb{Q}_b(1 + 2\epsilon \cos \theta) = b\epsilon^{b-1} \frac{\sin b\theta}{\sin \theta}. \quad (2.6.41)$$

The multiplicity of a zero x_0 is larger than one if and only if $\mathbb{Q}'_b(x_0) = 0$. We see from (2.6.41) that this occurs for $\theta_0 = 4\lambda(1+d)$ if $\theta_0 \neq n\pi$ for $n \in \mathbb{Z}$. In these cases, taking the second derivative of $\mathbb{Q}_b(x)$ reveals that the multiplicity is precisely 2. In contrast, for $\theta_0 = n\pi$, $\mathbb{Q}_b(x_0)' \neq 0$ and the multiplicity of the zero is 1. Recalling that $q = e^{i(4\lambda-\pi)}$ and $\theta_0 = 2\pi(\frac{b-a}{b})(1+d)$, we see that the condition $\theta_0 = n\pi$ can be written as $q^{2(d+1)} = 1$. This is precisely the condition for criticality, for which the multiplicities n_d in (2.6.37) are also equal to one. All zeros of $\mathbb{R}_{a,b}$ are thus among those of \mathbb{Q}_b (also counting the multiplicities), and thus $\mathbb{R}_{a,b}$ divides \mathbb{Q}_b . This completes the proof of the closure relation for all four boundary conditions.

2.6.5 Closure of the Y -system

In this section, we use the closure of the fusion hierarchy to derive the closure relations of the Y -system. The first step towards this goal is to derive extra closure relations in the fusion hierarchy, satisfied by the transfer matrices $\mathbf{D}^{b,k}(u)$ and $\mathbf{D}^{k,b}(u)$, for $k = 1, \dots, b-1$. For this, it turns out to be simpler to work with the determinants. The result reads:

$$\det(b, k)_0 = \mathcal{F}_{-2} \det(b-2, k+1)_2 - \left(\prod_{j=-2}^{2k} \mathcal{F}_j \right) \det(b-3-k, 0)_{2k+4} + \mathcal{J}_0 \det(0, k)_0, \quad (2.6.42a)$$

$$\det(k, b)_0 = \mathcal{F}_{2k-1} \det(k+1, b-2)_0 - \left(\prod_{j=-3}^{2k-1} \mathcal{F}_j \right) \det(0, b-3-k)_{2k+2} + \mathcal{J}_1 \det(k, 0)_0, \quad (2.6.42b)$$

where we recall the definition (2.6.5) of $\mathcal{J}(u)$. The closure relations for $\det(b, k)_0$ are proven inductively from the same relation for $\det(b, 0)_0$ following the arguments of Proposition B.3 of [17]. The closure relations (2.6.42b) are then directly obtained by applying the crossing symmetry to (2.6.42a).

The second step is to derive the following quartic relation:

$$\begin{aligned}
& (\det(b-1, 0)_0 \det(0, b-1)_0 - \mathcal{F}_{-2} \mathcal{F}_{-3} \det(b-2, 0)_2 \det(0, b-2)_0) \\
& \times (\det(b-1, 0)_2 \det(0, b-1)_0 - \mathcal{F}_{-2} \mathcal{F}_{-1} \det(b-2, 0)_2 \det(0, b-2)_2) \\
& = \left(\prod_{j=0}^{b-2} \mathcal{F}_{2j} \right) \det^3(0, b-1)_0 + \mathcal{J}_0 \det^2(0, b-1)_0 \det(b-2, 0)_2 \\
& + \mathcal{J}_1 \mathcal{F}_{-2} \det(0, b-1)_0 \det^2(b-2, 0)_2 + (\mathcal{F}_{-2})^2 \left(\prod_{j=0}^{b-1} \mathcal{F}_{2j+1} \right) \det^3(b-2, 0)_2.
\end{aligned} \tag{2.6.43}$$

Its proof follows the same arguments as those in Proposition B.4 of [17]. This relation can be rewritten as

$$(\mathbf{I} + \mathbf{d}_0^{b-1})(\mathbf{I} + \mathbf{y}_0)(\mathbf{I} + \mathbf{y}_1) = \mathbf{I} + \frac{\mathcal{J}_0 \mathbf{x}_0}{\prod_{j=0}^{b-1} \mathcal{F}_{2j}} + \frac{\mathcal{J}_1 (\mathbf{x}_0)^2}{\prod_{j=0}^{b-1} \mathcal{F}_{2j}} + \frac{\prod_{j=0}^{b-1} \mathcal{F}_{2j+1}}{\prod_{j=0}^{b-1} \mathcal{F}_{2j}} (\mathbf{x}_0)^3 \tag{2.6.44}$$

where

$$\mathbf{x}(u) = \frac{\mathcal{F}_{-2} \det(b-2, 0)_2}{\det(b-1, 0)_1}, \quad \mathbf{y}(u) = -\mathbf{x}_{-1} \mathbf{x}_0. \tag{2.6.45}$$

To factorize the right-hand side, we recall that $\mathcal{J}_0 = \kappa \Lambda_0(U - 2V)$, with $U(u)$, $V(u)$ and κ introduced in (2.6.2c) and $\Lambda(u)$ in (2.6.4), and use the equalities

$$\prod_{j=0}^{b-1} \mathcal{F}_{2j} = \sigma \Lambda_0 U, \quad \prod_{j=0}^{b-1} \mathcal{F}_{2j+1} = \Lambda_1 V, \quad \Lambda_1 U = \sigma \Lambda_0 V, \quad \sigma = \begin{cases} (-1)^{b-a} & \text{identical,} \\ 1 & \text{mixed,} \end{cases} \tag{2.6.46}$$

and

$$\frac{V}{U} = \begin{cases} 1 & \text{SS and CC with } a \text{ odd,} \\ -\tan^2(bu + (b-a)\frac{\pi}{4}) & \text{SS with } a \text{ even,} \\ -\cot^2(bu + (b-a)\frac{\pi}{4}) & \text{CC with } a \text{ even,} \\ 1 & \text{SC and CS.} \end{cases} \tag{2.6.47}$$

With this information, we treat separately the identical and mixed boundary conditions, as well as the different parities of a and b , and find that the above equation can be nicely rewritten as

$$\mathbf{I} + \mathbf{d}_0^{b-1} = \frac{(\mathbf{I} + \mathbf{x}_0)(\mathbf{I} + \iota \frac{V}{U} \mathbf{x}_0)^2}{(\mathbf{I} + \mathbf{y}_0)(\mathbf{I} + \mathbf{y}_1)}, \quad \iota = \begin{cases} (-1)^b & \text{identical,} \\ 1 & \text{mixed,} \end{cases} \tag{2.6.48}$$

for all parities of a and b . We also have the relation

$$\frac{\mathbf{x}_0 \mathbf{x}_2}{\mathbf{x}_1} = \frac{U^2 \mathbf{I} + \mathbf{d}_2^{b-2}}{V^2 \mathbf{I} + \mathbf{d}_1^{b-1}} = \frac{U^2 (\mathbf{I} + \mathbf{d}_2^{b-2})(\mathbf{I} + \mathbf{y}_1)(\mathbf{I} + \mathbf{y}_2)}{V^2 (\mathbf{I} + \mathbf{x}_1)(\mathbf{I} + \iota \frac{U}{V} \mathbf{x}_1)^2}. \tag{2.6.49}$$

Thus the closed Y -system for $\lambda = \lambda_{a,b}$ consists of the relations (2.4.61) for $m = 1, \dots, b-2$, along with the relations (2.6.48) and (2.6.49).

2.7 Free energies

In this section, we show how the fusion hierarchy relation for $\mathbf{D}^{1,1}(u)$ can be used to compute the bulk and boundary free energies of the homogeneous transfer matrix (whereby $\xi_{(j)} = 0$), following the method of Baxter [32]. This relation reads

$$\beta^2(1, 1, u) \mathbf{D}_0^{1,0} \mathbf{D}_3^{1,0} = \beta^1(1, 1, u) \mathbf{D}_0^{1,1} + \beta^0(1, u) \beta^0(1, -u) \beta^3(1, 1, u) \mathbf{I}. \quad (2.7.1)$$

The idea consists in noticing that the function $\beta^1(1, 1, u)$ has a zero of degree $2N + 2$ at $u = 0$, thus rendering the first term on the right side exponentially negligible compared to the second in the neighbourhood of $u = 0$. The bulk and boundary free energies for the leading eigenvalues $D(u)$ of $\mathbf{D}^{1,0}(u)$ can then be computed from the relation

$$\begin{aligned} D(u)D(u+3\lambda) &\simeq \beta^0(1, u)\beta^0(1, -u)\frac{\beta^3(1, 1, u)}{\beta^2(1, 1, u)} \\ &= \left(s(u+2\lambda)s(u-2\lambda)s(u+3\lambda)s(u-3\lambda)\right)^{2N} \\ &\times \frac{s(6\lambda-2u)s(6\lambda+2u)}{s(2\lambda-2u)s(2\lambda+2u)} \frac{\bar{w}(\frac{\lambda}{2}+u)\bar{w}(\frac{\lambda}{2}-u)}{\bar{w}(\frac{3\lambda}{2}+u)\bar{w}(\frac{3\lambda}{2}-u)} w(\frac{5\lambda}{2}+u)w(\frac{5\lambda}{2}-u)w(\frac{3\lambda}{2}+u)w(\frac{3\lambda}{2}-u). \end{aligned} \quad (2.7.2)$$

Writing $\log D(u) \simeq -2N f_{\text{bulk}}(u) - f_{\text{bdy}}(u)$, we identify together the different orders in N and write

$$f_{\text{bulk}}(u) + f_{\text{bulk}}(u+3\lambda) = -\log(s(u+2\lambda)s(u-2\lambda)s(u+3\lambda)s(u-3\lambda)), \quad (2.7.3a)$$

$$\begin{aligned} f_{\text{bdy}}(u) + f_{\text{bdy}}(u+3\lambda) &= -\log \left[\frac{s(6\lambda-2u)s(6\lambda+2u)}{s(2\lambda-2u)s(2\lambda+2u)} \frac{\bar{w}(\frac{\lambda}{2}+u)\bar{w}(\frac{\lambda}{2}-u)}{\bar{w}(\frac{3\lambda}{2}+u)\bar{w}(\frac{3\lambda}{2}-u)} \right. \\ &\quad \left. \times w(\frac{5\lambda}{2}+u)w(\frac{5\lambda}{2}-u)w(\frac{3\lambda}{2}+u)w(\frac{3\lambda}{2}-u) \right]. \end{aligned} \quad (2.7.3b)$$

We may now solve these relations using Fourier transforms and assuming that the function $D(u)$ is analytic and non-zero in the strip $0 \leq \text{Re}(u) \leq 3\lambda$. For the bulk free energy, this calculation was done previously by Warnaar, Batchelor and Nienhuis [28]. For $0 < \lambda < \frac{\pi}{3}$, the final expression is

$$f_{\text{bulk}}(u) = -\log \sin(2\lambda) \sin(3\lambda) - 2 \int_{-\infty}^{\infty} dk \frac{\sinh[uk] \sinh[(3\lambda-u)k] \cosh[(\pi-5\lambda)k] \cosh[\lambda k]}{k \sinh(\pi k) \cosh(3\lambda k)}. \quad (2.7.4)$$

Let us now solve (2.7.3b) for $f_{\text{bdy}}(u)$, starting with the mixed boundary conditions for which $w(u) = \bar{w}(u) = 1$. We first study the asymptotic behavior of $\log D(u)$ as $u \rightarrow i\infty$. From the form of $D(u)$ as a

centered Laurent polynomial in e^{iu} , we deduce that its behavior for $u \rightarrow i\infty$ is given by

$$\log D(u) = \log (\alpha_{-4N} e^{-4Ni u} + \alpha_{-(4N-2)} e^{-(4N-2)iu} + \dots) \simeq -4iuN + \log \alpha_{-4N} + \dots \quad (2.7.5)$$

with the next terms going to zero in the limit. We thus find that⁵

$$\lim_{u \rightarrow i\infty} f''_{\text{bulk}}(u) = \lim_{u \rightarrow i\infty} f'_{\text{bdy}}(u) = 0. \quad (2.7.6)$$

As a next step, we define the function

$$g(y) = f_{\text{bdy}}(iy + \frac{3\lambda}{2}), \quad (2.7.7)$$

for which

$$g''(y + \frac{3i\lambda}{2}) + g''(y - \frac{3i\lambda}{2}) = \frac{4}{\sinh^2(2y + 6i\lambda)} + \frac{4}{\sinh^2(2y - 6i\lambda)} - \frac{4}{\sinh^2(2y + 2i\lambda)} - \frac{4}{\sinh^2(2y - 2i\lambda)}. \quad (2.7.8)$$

We define the Fourier transform of $g''(y)$:

$$G(k) = \frac{1}{2\pi} \int_{-\infty}^{\infty} dy e^{-iky} g''(y), \quad g''(y) = \int_{-\infty}^{\infty} dk e^{iky} G(k). \quad (2.7.9)$$

With the assumption that $f_{\text{bdy}}(u)$ has no zeros in the analyticity strip $0 \leq \text{Re}(u) \leq 3\lambda$, we find

$$\frac{1}{2\pi} \int_{-\infty}^{\infty} dy e^{-iky} g''(y \pm \frac{3i\lambda}{2}) = e^{\mp 3k\lambda/2} G(k). \quad (2.7.10)$$

As a result, we have

$$2 \cosh(\frac{3\lambda k}{2}) G(k) = \frac{1}{2\pi} \int_{-\infty}^{\infty} dy e^{-iky} \left(\frac{4}{\sinh^2(2y + 6i\lambda)} + \frac{4}{\sinh^2(2y - 6i\lambda)} - \frac{4}{\sinh^2(2y + 2i\lambda)} - \frac{4}{\sinh^2(2y - 2i\lambda)} \right). \quad (2.7.11)$$

We can compute these integrals using the identity

$$\frac{1}{2\pi} \int_{-\infty}^{\infty} dy e^{-iky} \frac{1}{\sinh^2(y - i\gamma)} = -\frac{k e^{k\gamma}}{e^{\pi k} - 1}, \quad \gamma \in (0, \pi), \quad (2.7.12)$$

which is easily obtained from the residue theorem. With $\gamma \mapsto \pi - \gamma$, we then also have

$$\frac{1}{2\pi} \int_{-\infty}^{\infty} dy e^{-iky} \frac{1}{\sinh^2(y + i\gamma)} = -\frac{k e^{k(\pi-\gamma)}}{e^{\pi k} - 1}, \quad \gamma \in (0, \pi). \quad (2.7.13)$$

5. For SS and CC boundary conditions, the lowest power of $D(u)$ as a Laurent polynomial is $e^{-(4N+2)iu}$, and in this case only the second derivative of $f_{\text{bdy}}(u)$ vanishes, with the first derivative instead given by $\lim_{u \rightarrow i\infty} f'_{\text{bdy}}(u) = 2i$.

We also give the identity

$$\frac{1}{2\pi} \int_{-\infty}^{\infty} dy e^{-iky} \frac{1}{\cosh^2(y \pm i\gamma)} = \frac{k e^{k(\frac{\pi}{2} \mp \gamma)}}{e^{\pi k} - 1}, \quad \gamma \in (-\frac{\pi}{2}, \frac{\pi}{2}), \quad (2.7.14)$$

as it is needed for the boundary conditions SS and CC. Applying this to the four terms in (2.7.11), we find after some simplifications

$$G(k) = \frac{k}{2 \cosh(\frac{3\lambda k}{2})} \frac{\cosh[(\frac{\pi}{4} - \lambda)k] - \cosh[(\frac{\pi}{4} - 3\lambda)k]}{\sinh(\frac{\pi k}{4})}. \quad (2.7.15)$$

The inverse transform is then given by

$$\begin{aligned} g''(y) &= \int_{-\infty}^{\infty} dk \frac{k e^{iky}}{2 \cosh(\frac{3\lambda k}{2})} \frac{\cosh[(\frac{\pi}{4} - \lambda)k] - \cosh[(\frac{\pi}{4} - 3\lambda)k]}{\sinh(\frac{\pi k}{4})} \\ &= \int_{-\infty}^{\infty} dk \frac{k \cos(ky)}{2 \cosh(\frac{3\lambda k}{2})} \frac{\cosh[(\frac{\pi}{4} - \lambda)k] - \cosh[(\frac{\pi}{4} - 3\lambda)k]}{\sinh(\frac{\pi k}{4})}, \end{aligned} \quad (2.7.16)$$

where we used the symmetry of the integrand under $k \rightarrow -k$. Integrating once with respect to y yields

$$g'(y) = \int_{-\infty}^{\infty} dk \frac{\sin(ky)}{2 \cosh(\frac{3\lambda k}{2})} \frac{\cosh[(\frac{\pi}{4} - \lambda)k] - \cosh[(\frac{\pi}{4} - 3\lambda)k]}{\sinh(\frac{\pi k}{4})} + C. \quad (2.7.17)$$

We fix the constant C by imposing that $\lim_{y \rightarrow \infty} g'(y) = 0$, see (2.7.6). Indeed, we have

$$\lim_{y \rightarrow \infty} g'(y) - C = \lim_{y \rightarrow \infty} \int_{-\infty}^{\infty} dk' \frac{\sin k'}{2y \cosh(\frac{3\lambda k'}{2y})} \frac{\cosh[(\frac{\pi}{4} - \lambda)\frac{k'}{y}] - \cosh[(\frac{\pi}{4} - 3\lambda)\frac{k'}{y}]}{\sinh(\frac{\pi k'}{4y})} = 0, \quad (2.7.18)$$

as the integrand behaves as y^{-2} . We thus conclude that $C = 0$. Integrating once more, we find

$$g(y) = - \int_{-\infty}^{\infty} dk \frac{\cos(ky)}{2k \cosh(\frac{3\lambda k}{2})} \frac{\cosh[(\frac{\pi}{4} - \lambda)k] - \cosh[(\frac{\pi}{4} - 3\lambda)k]}{\sinh(\frac{\pi k}{4})} + K. \quad (2.7.19)$$

The value of $g(\frac{3i\lambda}{2})$ can be read off directly from (2.4.5): $g(\frac{3i\lambda}{2}) = -\log \left[\frac{\sin(6\lambda)}{\sin(2\lambda)} \right]$. This can also be obtained from (2.7.3b) by noting that $g(\frac{3i\lambda}{2})$ and $g(-\frac{3i\lambda}{2})$ are equal due to crossing symmetry. This fixes the value of K . After simplification, this yields

$$g(y) = -\log \left[\frac{\sin(6\lambda)}{\sin(2\lambda)} \right] + \int_{-\infty}^{\infty} dk \frac{\sinh \left[(\frac{3\lambda}{2} + iy)\frac{k}{2} \right] \sinh \left[(\frac{3\lambda}{2} - iy)\frac{k}{2} \right]}{k \cosh(\frac{3\lambda k}{2})} \frac{\cosh[(\frac{\pi}{4} - \lambda)k] - \cosh[(\frac{\pi}{4} - 3\lambda)k]}{\sinh(\frac{\pi k}{4})} \quad (2.7.20)$$

and finally,

$$f_{\text{bdy}}(u) = -\log \left[\frac{\sin(6\lambda)}{\sin(2\lambda)} \right] + \int_{-\infty}^{\infty} dk \frac{\sinh \left[\frac{uk}{2} \right] \sinh \left[(3\lambda - u)\frac{k}{2} \right]}{k \cosh(\frac{3\lambda k}{2})} \frac{\cosh[(\frac{\pi}{4} - \lambda)k] - \cosh[(\frac{\pi}{4} - 3\lambda)k]}{\sinh(\frac{\pi k}{4})}. \quad (2.7.21)$$

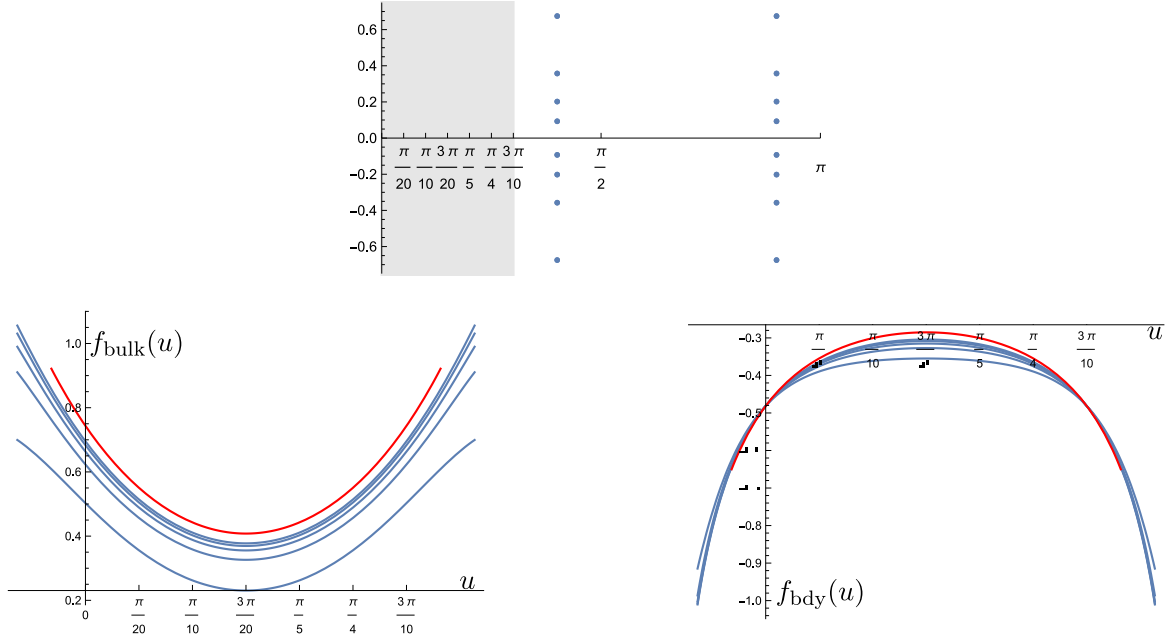


FIGURE 2.2 – Zeros and free energies for SC boundary conditions with $\lambda = \frac{\pi}{10}$. *Top*: the position of the zeros of $D(u)$ in the complex u -plane for $N = 4$, with the analyticity strip colored in gray. *Left*: the integral formula (2.7.4) for $f_{\text{bulk}}(u)$ in red and its finite-size approximations $-\frac{1}{2N} \log D(u)$ for $N = 1, \dots, 5$ in blue. *Right*: the integral formula (2.7.21) for $f_{\text{bdy}}(u)$ in red and its finite-size approximations $-\log D(u) - 2N f_{\text{bulk}}(u)$ for $N = 1, \dots, 5$ in blue.

In deriving this result, we applied (2.7.12) with $\gamma = 6\lambda$, so this result holds for $0 < \lambda < \frac{\pi}{6}$. In Figure 2.2, we compare these results with the groundstate eigenvalue $D(u)$ (namely the largest eigenvalue at $u = \frac{3\lambda}{2}$), for SC boundary conditions and with $\lambda = \frac{\pi}{10}$. We see from the pattern of zeros of $D(u)$ that it has no zeros in the strip $0 \leq \text{Re}(u) \leq 3\lambda$. We also see that the integral formulas for $f_{\text{bulk}}(u)$ and $f_{\text{bdy}}(u)$ nicely match the numerical data. We find a similar agreement numerically for the CS boundary condition.

For SS boundary conditions, the linear functional relation for $f_{\text{bdy}}(u)$ involves more terms on the right-hand side:

$$\begin{aligned}
 f_{\text{bdy}}(u) + f_{\text{bdy}}(u + 3\lambda) = & -\log \left[\frac{s(6\lambda - 2u)s(6\lambda + 2u)}{s(2\lambda - 2u)s(2\lambda + 2u)} \frac{c(\frac{\lambda}{2} + u)c(\frac{\lambda}{2} - u)}{c(\frac{3\lambda}{2} + u)c(\frac{3\lambda}{2} - u)} \right. \\
 & \left. \times s(\frac{5\lambda}{2} + u)s(\frac{5\lambda}{2} - u)s(\frac{3\lambda}{2} + u)s(\frac{3\lambda}{2} - u) \right]. \tag{2.7.22}
 \end{aligned}$$

From this expression, the steps are similar to those for the mixed boundary conditions. We provide

only the key steps. The second derivative of $g(y)$ is given by

$$g''(y) = \int_{-\infty}^{\infty} dk \frac{k \cos(ky)}{2 \cosh(\frac{3\lambda k}{2})} \left[\frac{\cosh[(\frac{\pi}{4} - \lambda)k] - \cosh[(\frac{\pi}{4} - 3\lambda)k]}{\sinh(\frac{\pi k}{4})} + \frac{\cosh(\frac{3\lambda k}{2}) - \cosh(\frac{\lambda k}{2}) - \cosh[(\frac{\pi-5\lambda}{2})k] - \cosh[(\frac{\pi-3\lambda}{2})k]}{\sinh(\frac{\pi k}{2})} \right]. \quad (2.7.23)$$

As before, the first integration on y replaces the first numerator $k \cos(ky)$ by $\sin(ky)$ and introduces a new constant of integration C which is obtained by computing

$$\lim_{y \rightarrow \infty} g'(y) - C = \lim_{y \rightarrow \infty} \int_{-\infty}^{\infty} dk' \frac{\sin k' y}{2y \cosh(\frac{3\lambda k'}{2y})} \left[\frac{\cosh[(\frac{\pi}{4} - \lambda)\frac{k'}{y}] - \cosh[(\frac{\pi}{4} - 3\lambda)\frac{k'}{y}]}{\sinh(\frac{\pi k'}{4y})} + \frac{\cosh(\frac{3\lambda k'}{2y}) - \cosh(\frac{\lambda k'}{2y}) - \cosh[(\frac{\pi-5\lambda}{2})\frac{k'}{y}] - \cosh[(\frac{\pi-3\lambda}{2})\frac{k'}{y}]}{\sinh(\frac{\pi k'}{2y})} \right] = -2. \quad (2.7.24)$$

The value of $g'(y) = i f'_{\text{bdy}}(u)$ in the limit $u \rightarrow i\infty$ is -2 by the above footnote, and C must be set to 0. The final result for these boundary conditions is thus

$$f_{\text{bdy}}(u) = -\log \left[-\frac{\sin(6\lambda) \cos(\frac{\lambda}{2}) \sin(\frac{5\lambda}{2}) \sin(\frac{3\lambda}{2})}{\sin(2\lambda) \cos(\frac{3\lambda}{2})} \right] + \int_{-\infty}^{\infty} dk \frac{\sinh(\frac{uk}{2}) \sinh[(3\lambda - u)\frac{k}{2}]}{k \cosh(\frac{3\lambda k}{2})} \left[\frac{\cosh[(\frac{\pi}{4} - \lambda)k] - \cosh[(\frac{\pi}{4} - 3\lambda)k]}{\sinh(\frac{\pi k}{4})} + \frac{\cosh(\frac{3\lambda k}{2}) - \cosh(\frac{\lambda k}{2}) - \cosh[(\frac{\pi-5\lambda}{2})k] - \cosh[(\frac{\pi-3\lambda}{2})k]}{\sinh(\frac{\pi k}{2})} \right]. \quad (2.7.25)$$

It again holds for $0 < \lambda < \frac{\pi}{6}$. As illustrated in Figure 2.3, our numerical investigations for small N confirm the analyticity assumptions for the groundstate eigenvalue $D(u)$ and show a good match between the integral formulas for the free energies and the numerical data. We also note that, for $0 < \lambda < \frac{\pi}{6}$, the logarithm on the first line of (2.7.25) has a negative argument, which implies that $f_{\text{bdy}}(u)$ has a non-zero imaginary part equal to an odd multiple of π . This is a simple artifact of our choice of normalisation for $\mathbf{D}(u)$, causing it to be negative for $0 < u < 3\lambda$ for SS boundary conditions, see for instance (2.4.5). As a result, we only plot the real part $f_{\text{bdy}}(u)$ in the right panel of Figure 2.3.

For CC boundary conditions, the functional relation (2.7.3b) is

$$f_{\text{bdy}}(u) + f_{\text{bdy}}(u + 3\lambda) = -\log \left[\frac{s(6\lambda - 2u)s(6\lambda + 2u)}{s(2\lambda - 2u)s(2\lambda + 2u)} \frac{s(\frac{\lambda}{2} + u)s(\frac{\lambda}{2} - u)}{s(\frac{3\lambda}{2} + u)s(\frac{3\lambda}{2} - u)} \times c(\frac{5\lambda}{2} + u)c(\frac{5\lambda}{2} - u)c(\frac{3\lambda}{2} + u)c(\frac{3\lambda}{2} - u) \right]. \quad (2.7.26)$$

While it is possible to solve this equation with the same arguments as before, the solution turns out not to match the numerical data. Indeed, for CC boundary conditions, our numerical explorations

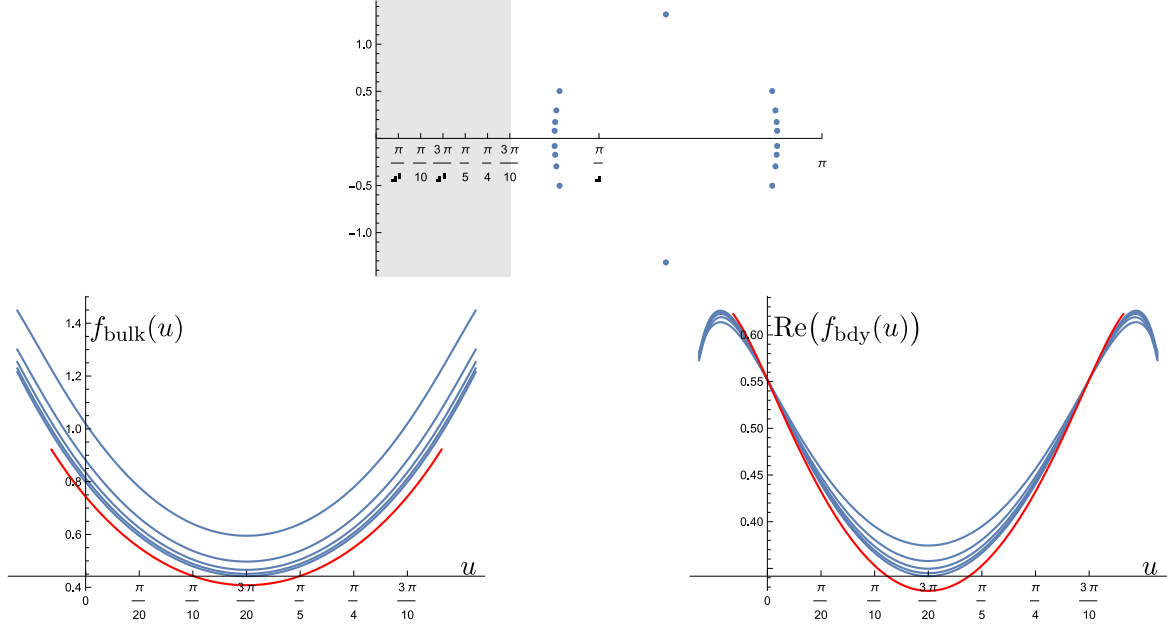


FIGURE 2.3 – Zeros and free energies for SS boundary conditions, with $\lambda = \frac{\pi}{10}$. *Top*: the position of the zeros of $D(u)$ in the complex u -plane for $N = 4$, with the analyticity strip colored in gray. *Left*: the integral formula (2.7.4) for $f_{\text{bulk}}(u)$ in red and its finite-size approximations $-\frac{1}{2N} \log D(u)$ for $N = 1, \dots, 5$ in blue. *Right*: the integral formula (2.7.25) for the real part of $f_{\text{bdy}}(u)$ in red and its finite-size approximations $-\log D(u) - 2N f_{\text{bulk}}(u)$ for $N = 1, \dots, 5$ in blue.

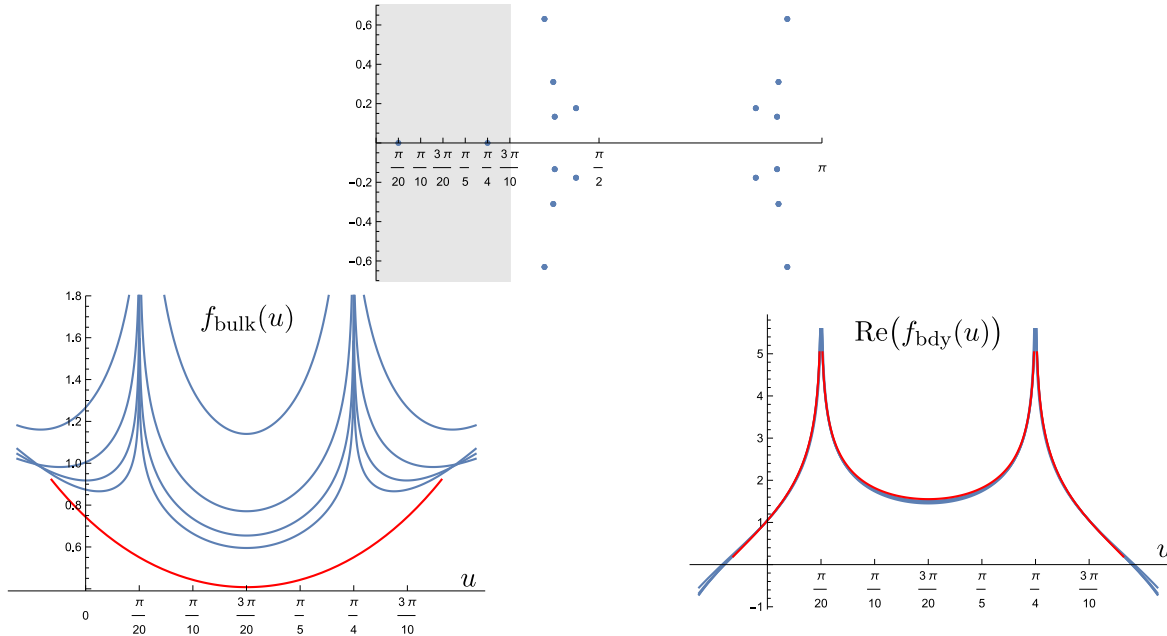


FIGURE 2.4 – Zeros and free energies for CC boundary conditions, with $\lambda = \frac{\pi}{10}$. *Top*: the position of the zeros of $D(u)$ in the complex u -plane for $N = 4$, with the analyticity strip colored in gray. *Left*: the integral formula (2.7.4) for $f_{\text{bulk}}(u)$ in red and its finite-size approximations $-\frac{1}{2N} \log D(u)$ for $N = 2, \dots, 5$ in blue. *Right*: the integral formula (2.7.30) for the real part of $f_{\text{bdy}}(u)$ in red and its finite-size approximations $-\log D(u) - 2N f_{\text{bulk}}(u)$ for $N = 2, \dots, 5$ in blue.

reveal that the groundstate eigenvalue $D(u)$ has a pair of real zeros very close to $u = \frac{\lambda}{2}$ and $u = \frac{5\lambda}{2}$. These thus lie inside the strip $0 < \text{Re}(u) < 3\lambda$, and the condition that $D(u)$ is free of zeros in this strip is violated. As a result, (2.7.9) no longer holds, as the argument leading to this identity requires that we deform the integration path across an area that is free of poles, a condition that does not hold in the present case. The position of these zeros is not exactly at $u = \frac{\lambda}{2}, \frac{5\lambda}{2}$, however they appear to converge to these positions rapidly as N is increased. To bypass this problem and compute $f_{\text{bdy}}(u)$ for CC boundary conditions, it is useful to consider the eigenvalue

$$\widehat{D}(u) = \frac{D(u)}{\sin(\frac{\lambda}{2} - u) \sin(\frac{5\lambda}{2} - u)}, \quad (2.7.27)$$

a function that has no zero in the analyticity strip, in the limit $N \rightarrow \infty$. Its corresponding boundary free energy satisfies the functional relation

$$\widehat{f}_{\text{bdy}}(u) + \widehat{f}_{\text{bdy}}(u + 3\lambda) = -\log \left[\frac{s(6\lambda - 2u)s(6\lambda + 2u) c(\frac{5\lambda}{2} + u)c(\frac{5\lambda}{2} - u)c(\frac{3\lambda}{2} + u)c(\frac{3\lambda}{2} - u)}{s(2\lambda - 2u)s(2\lambda + 2u) s(\frac{3\lambda}{2} + u)s(\frac{3\lambda}{2} - u)s(\frac{5\lambda}{2} + u)s(\frac{5\lambda}{2} - u)} \right]. \quad (2.7.28)$$

Defining $\widehat{g}(y) = \widehat{f}_{\text{bdy}}(iy + \frac{3\lambda}{2})$, we find that its second derivative is

$$\begin{aligned} \widehat{g}''(y) = \int_{-\infty}^{\infty} dk \frac{k \cos(ky)}{2 \cosh(\frac{3\lambda k}{2})} & \left[\frac{\cosh[(\frac{\pi}{4} - \lambda)k] - \cosh[(\frac{\pi}{4} - 3\lambda)k]}{\sinh(\frac{\pi k}{4})} \right. \\ & \left. + \frac{\cosh[(\frac{\pi - 5\lambda}{2})k] + \cosh[(\frac{\pi - 3\lambda}{2})k] - \cosh(\frac{5\lambda k}{2}) - \cosh(\frac{3\lambda k}{2})}{\sinh(\frac{\pi k}{2})} \right] \end{aligned} \quad (2.7.29)$$

and the integral formula for $f_{\text{bdy}}(u)$ for CC boundary conditions reads

$$\begin{aligned} f_{\text{bdy}}(u) = -\log \left[\frac{\sin(6\lambda) \cos(\frac{5\lambda}{2}) \cos(\frac{3\lambda}{2})}{\sin(2\lambda) \sin(\frac{5\lambda}{2}) \sin(\frac{3\lambda}{2})} \right] & - \log(\sin(\frac{\lambda}{2} - u) \sin(\frac{5\lambda}{2} - u)) \\ + \int_{-\infty}^{\infty} dk \frac{\sinh[\frac{uk}{2}] \sinh[(3\lambda - u)\frac{k}{2}]}{k \cosh(\frac{3\lambda k}{2})} & \left[\frac{\cosh[(\frac{\pi}{4} - \lambda)k] - \cosh[(\frac{\pi}{4} - 3\lambda)k]}{\sinh(\frac{\pi k}{4})} \right. \\ & \left. + \frac{\cosh(\frac{(\pi - 3\lambda)k}{2}) + \cosh(\frac{(\pi - 5\lambda)k}{2}) - \cosh(\frac{5\lambda k}{2}) - \cosh(\frac{3\lambda k}{2})}{\sinh(\frac{\pi k}{2})} \right] \end{aligned} \quad (2.7.30)$$

and is valid for $0 < \lambda < \frac{\pi}{6}$. One can then check that $\lim_{u \rightarrow i\infty} f'_{\text{bdy}}(u) = 2i$ as needed. The second logarithm in (2.7.30) gives rise to an imaginary part for $u \in (\frac{\lambda}{2}, \frac{5\lambda}{2})$. This is due to the presence of the poles in $\widehat{D}(u)$, see (2.7.27). Only the real part has a physical interpretation. The corresponding numerical data is given in Figure 2.4. In addition to the zeros of $D(u)$ lying inside the analyticity strip, we also see that the convergence of the numerical data for $f_{\text{bulk}}(u)$ to its integral formula is much slower in this case due to the two singularities of $f_{\text{bdy}}(u)$. The agreement for $\text{Re}(f_{\text{bdy}}(u))$ is in contrast very convincing.

2.8 Conclusion

In this paper, we studied the commuting transfer matrices of the $A_2^{(2)}$ model on the strip. The main results of the article are the fusion hierarchy relations (2.4.15) defining the fused transfer matrices, their T -system (2.4.55), and for $\lambda/\pi \in \mathbb{Q}$ the closure relation (2.6.2) for the hierarchy and the corresponding the finite Y -systems, consisting of the relations (2.4.61), (2.6.48) and (2.6.49). These formulas and their proofs turn out to have a much greater complexity than the similar results for the dense loop model or for the $A_2^{(2)}$ model with periodic boundary conditions. This can be traced back to the fact that the solutions of the boundary Yang-Baxter equation have a non-trivial dependence on the spectral parameter u , which then causes the fused transfer matrices to have polynomial degrees in e^{iu} that increase with the fusion indices. A similar feature in fact arises for the dense loop model with loop segments that can be attached to the boundaries of the strip, in the context of the two-boundary Temperley-Lieb algebra. The closure relation in this case is conjectured in Section 5.2 of [11], but remains without proof. We expect that the methods developed here will apply to this case and lead to a proof of this result.

In contrast, here we provided complete proofs for all the results. These proofs, particularly the difficult ones for the polynomiality of the fused tangles and their closure relation, indicate how tightly constrained the definition of the fusion hierarchy is. Despite the substantial length of this text, it is worth mentioning that our first versions of many proofs were even longer. For example, an alternative proof of the polynomiality of $\mathbf{D}^{m,0}(u)$ and $\mathbf{D}^{m,1}(u)$ relies on their equivalent diagrammatic definitions with the projectors $P^{m,0}$ and $P^{m,1}$ defined in [17]. Moreover, we note that, like for the periodic $A_2^{(2)}$ dilute loop models, a diagrammatic definition of $\mathbf{D}^{m,n}(u)$ for $m, n > 1$ and of the corresponding projectors $P^{m,n}$ is still missing. Finally, we note that unifying the presentation of the hierarchies for the four boundary conditions (SS, CC, SC and CS) through the notation of Table 2.1 was not an easy task. It reduced the length of the proofs significantly.

We also computed the bulk and boundary free energies using the first fusion hierarchy relations and the analyticity properties of the groundstate eigenvalues. Their agreement with numerical data, obtained for small strip lengths N , is striking. In particular, the case of CC boundary conditions featured zeros inside the analyticity strip and was resolved convincingly. This, of course, raises the question of which conformal weights arise in the continuum limit of the loop models. The method of non-linear integral equations, originally developed by Klümper and Pearce in the nineties [24–26], allows for the computation of the next leading term in the large- N expansion of the eigenvalues. This term is proportional to $1/N$ and its coefficient involves the combination $c - 24\Delta$, where c is the central charge and Δ is the conformal weight of the field that the corresponding eigenstate scales to in the limit. These techniques were recently applied to the groundstate of the loop models in the standard module with no defects, for the $A_1^{(1)}$, $A_2^{(1)}$ and $A_2^{(2)}$ models with periodic boundary conditions [27]. For $A_2^{(2)}$, these results were found to be consistent with the known values of the central charge in Regimes I and

II. The general formula is [28]

$$c = \begin{cases} 1 - \frac{3(\pi - 4\lambda)^2}{\pi(\pi - 2\lambda)}, & \text{Regime I: } 0 < \lambda < \frac{\pi}{2}, \\ -1 + \frac{6(\pi - 2\lambda)^2}{\pi(\pi - \lambda)}, & \text{Regime III: } \frac{\pi}{2} < \lambda < \frac{2\pi}{3}, \\ \frac{3}{2} - \frac{3(3\pi - 4\lambda)^2}{2\pi(\pi - \lambda)}, & \text{Regime II: } \frac{2\pi}{3} < \lambda < \pi. \end{cases} \quad (2.8.1)$$

This work should be extended to the same models on the strip, for all four choices of boundary conditions. In the representation $W_N^{d=0}$, one can expect for the mixed boundary conditions a groundstate with a non-zero conformal weight Δ , corresponding to the insertion at infinity of a field that changes the boundary condition from S to C . For identical boundary conditions, we instead expect that the groundstate has the weight $\Delta = 0$, since no boundary condition changing field must be inserted in this case. The technique of non-linear equations and Rogers dilogarithms should be applied to confirm this, and subsequently to compute the conformal weights of the groundstates in all the standard representations W_N^d . A more ambitious project would then be to apply this to the excited states of the $A_2^{(2)}$ loop model as well, and thus to compute the properly scaled transfer matrix traces and express them in terms of characters of representations of the Virasoro algebra. This program is currently being implemented for the special case of $\lambda = \frac{\pi}{3}$ corresponding to the model of critical site percolation on the triangular lattice, with the results to appear soon [33].

Acknowledgements

FB thanks the Département de physique of the Université de Montréal for its financial support during her graduate studies. AMD is supported by the EOS Research Project, project number 30889451. He also acknowledges support from the Max-Planck-Institute für Mathematik in Bonn and the Leibniz Universität Hannover, where parts of this work were done. YSA holds a grant from the Natural Sciences and Engineering Research Council of Canada. This support is gratefully acknowledged. AMD and YSA thank J. Rasmussen for collaborative investigations of the dilute $A_2^{(2)}$ loop model that predated this project.

2.A Proofs of properties of the fused transfer matrices

In this appendix, we collect the technical proofs of some of the properties of the fused transfer matrices.

2.A.1 Proof of the crossing symmetry of $D^{m,n}(u)$ and $\det(m,n)(u)$

This section is devoted to proving the crossing symmetries (2.4.17a) and (2.4.35a). We start with the proof for $D^{m,0}(u)$. Together with certain properties of the functions $\beta^i(m,n,u)$, it will imply the crossing symmetry of both $D^{m,n}(u)$ and $\det(m,n)(u)$.

The proof of the equality $D^{m,0}((4-2m)\lambda - u) = D^{0,m}(u)$ is by induction on m . The inductive argument requires that the cases $m-1$, $m-2$ and $m-3$ be already shown. We thus check the crossing symmetry for transfer tangles $D^{1,0}(u)$, $D^{2,0}(u)$ and $D^{3,0}(u)$ first. The case $m=1$ follows readily from (2.4.4a) and (2.4.11). For $m=2$, we use the definition (2.4.15a) for $D^{2,0}(u)$ and the evaluation point $\psi = (4-4)\lambda - u = -u$. We show that $D^{2,0}(\psi) = D^{2,0}(u)$ using the definitions of the weights in (2.4.15a) and (2.4.15c) and the crossing symmetry of $D^{1,0}(u)$. For $m=3$, proving the crossing symmetry for $D^{3,0}(u)$ requires that we understand the same property for $D^{1,1}(u)$. Its crossing symmetry follows from (2.4.15b), the crossing symmetry of $D^{1,0}(u)$, and the fact that the three functions $\beta^i(1,1,u)$, $i=1,2,3$, are invariant under $u \mapsto \psi = -u$. Then, the symmetry of $D^{3,0}(u)$ is checked using the same arguments as for $D^{2,0}(u)$, with the property just proved for $D^{1,1}(u)$.

We now consider $m \geq 4$, for which $\psi = (4-2m)\lambda - u$. The fusion hierarchies (2.4.15d) and (2.4.15e) respectively define $D^{m,0}(u)$ and $D^{0,m}(u)$ and involve the fused transfer matrices $D^{m-2,1}(u)$ and $D^{1,m-2}(u_2)$, to which the inductive assumption does not apply. These are replaced by their definitions (2.4.15f) and (2.4.15g):

$$D^{m-2,1}(u) = \frac{\beta^2(m-2,1,u)D_0^{m-2,0}D_{2(m-2)}^{0,1} - \beta^3(m-2,1,u)\beta^0(m-2,u)D_0^{m-3,0}}{\beta^1(m-2,1,u)}, \quad (2.A.1a)$$

$$D^{1,m-2}(u_2) = \frac{\beta^2(m-2,1,v)D_2^{1,0}D_4^{0,m-2} - \beta^3(m-2,1,v)\beta^0(m-2,v)D_6^{0,m-3}}{\beta^1(m-2,1,v)}, \quad (2.A.1b)$$

where, in the second equation, v must be computed following the prescription (2.4.15g):

$$v = (4-2-2(m-2))\lambda - u_2 = (4-2m)\lambda - u = \psi. \quad (2.A.2)$$

Equation (2.A.1b) provides an example where the operation $u \mapsto \psi$ is performed before the shift $u \mapsto u_2$. Thus, v is precisely the combination appearing in the crossing symmetry for $D^{m,0}(u)$. The expressions for $D^{m,0}(u)$ and $D^{0,m}(u)$ become

$$\begin{aligned} \alpha^1(m,u)D^{m,0}(u) &= \left[\alpha^2(m,u)D_0^{m-1,0}D_{2m-2}^{1,0} \right. \\ &\quad \left. - \frac{\alpha^3(m,u)}{\beta^1(m-2,1,u)} \left(\beta^2(m-2,1,u)D_0^{m-2,0}D_{2m-4}^{0,1} - \beta^3(m-2,1,u)\beta^0(m-2,u)D_0^{m-3,0} \right) \right], \end{aligned} \quad (2.A.3a)$$

$$\begin{aligned} \alpha^1(m,\psi)D^{0,m}(u) &= \left[\alpha^2(m,\psi)D_2^{0,m-1}D_0^{0,1} \right. \\ &\quad \left. - \frac{\alpha^3(m,\psi)}{\beta^1(m-2,1,\psi)} \left(\beta^2(m-2,1,\psi)D_2^{1,0}D_4^{0,m-2} - \beta^3(m-2,1,\psi)\beta^0(m-2,\psi)D_6^{0,m-3} \right) \right]. \end{aligned} \quad (2.A.3b)$$

In both of these equations, the fused matrices on the right-hand side are evaluated at u . We now evaluate all terms in (2.A.3a) at ψ . All weight functions become exactly equal to those of (2.A.3b). It remains to check that the transfer tangles transform correctly. Here are two examples:

$$\begin{aligned} D_0^{m-1,0}(\psi) &= D_0^{m-1,0}((4-2m)\lambda - u) = D_0^{m-1,0}((4-2(m-1))\lambda - (u+2\lambda)) = D_2^{0,m-1}(u) , \\ D_{2m-2}^{1,0}(\psi) &= D_0^{1,0}((4-2m)\lambda - u + (2m-2)\lambda) = D_0^{1,0}((4-2)\lambda - u) = D_0^{0,1}(u) . \end{aligned} \quad (2.A.4)$$

The last equality in each line uses the induction hypothesis with $m' = m-1$ and $m' = 1$ respectively. The proofs for the other matrices is similar. This completes the proof of the crossing symmetry for $D^{m,0}(u)$.

The proof of $D^{m,n}(u) = D^{n,m}((4-2m-2n)\lambda - u)$ for $m, n > 0$ rests on the following property of the functions β^i :

$$\beta^i(m, n, \psi) = \beta^i(n, m, u), \quad i = 1, 2, 3 . \quad (2.A.5)$$

(We already used this fact to prove the crossing symmetry of $D^{1,1}(u)$.) This equality requires the identity $f(u) = f(-u)$ and is clear for all the other weights, as they appear in pairs.

We give the details of the proof for (2.4.15h) wherein both $m, n \geq 2$. The manipulations are similar for (2.4.15f) or (2.4.15g). With (2.A.5), (2.4.15h) evaluated at ψ reads

$$\begin{aligned} D_0^{m,n}(\psi) &= \frac{\beta^2(m, n, \psi) D_0^{m,0}(\psi) D_{2m}^{0,n}(\psi) - \beta^3(m, n, \psi) D_0^{m-1,0}(\psi) D_{2m+2}^{0,n-1}(\psi)}{\beta^1(m, n, \psi)} \\ &= \frac{\beta^2(n, m, u) D_0^{m,0}(\psi) D_{2m}^{0,n}(\psi) - \beta^3(n, m, u) D_0^{m-1,0}(\psi) D_{2m+2}^{0,n-1}(\psi)}{\beta^1(n, m, u)} . \end{aligned} \quad (2.A.6)$$

The remaining step is to check that the fused tangles in $D_0^{m,n}(\psi)$ are identical to those appearing in the definition of $D^{n,m}(u)$. Here are two examples, the two others being obtained with similar arguments:

$$\begin{aligned} D_0^{m,0}(\psi) &= D_0^{m,0}((4-2m-2n)\lambda - u) = D_0^{m,0}((4-2m)\lambda - (u+2n\lambda)) = D_{2n}^{0,m}(u) , \\ D_{2m}^{0,n}(\psi) &= D_0^{0,n}((4-2m-2n)\lambda - u + 2m\lambda) = D_0^{0,n}((4-2n)\lambda - u) = D_0^{n,0}(u) . \end{aligned} \quad (2.A.7)$$

The last equality in each line uses $D^{m',0}((4-2m')\lambda - u) = D^{0,m'}(u)$. This ends the proof of the crossing symmetry (2.4.17a).

The proof of the crossing symmetry of the determinantal form (2.4.30a) follows easily. For $m, n \geq 1$, it consists in exchanging m and n in (2.4.31) and evaluating the result at $\psi = (4-2m-2n)\lambda - u$. Clearly the two bottom lines of the right-hand side of (2.4.31) simply get exchanged. So are all the other factors, except maybe the three factors $s(2u_{m+n-2})$, $s(2\psi_{2n-2})$ and $f(u_{2m-2})$. A direct computation shows that the latter remains invariant under the changes while the two former become $-s(2u_{m+n-2})$ and $-s(2\psi_{2m-2})$ respectively. The last step is to use the crossing symmetry of $D^{m,n}(u)$. This confirms the crossing symmetry (2.4.35a) of the determinantal form, for $m, n > 1$. Note that, by definition of

$\det(0, n)$ in (2.4.27b), the crossing symmetry when one of m and n is zero is actually built in, so nothing has to be proved. Still the relation (2.4.28) between $\det(m, 0)(u)$ and $\mathbf{D}^{m,0}(u)$ enjoys an invariance similar to that of (2.4.31) and it will play a role in the next section.

2.A.2 Proof of the conjugacy of $\mathbf{D}^{m,n}(u)$ and $\det(m, n)(u)$

This section proves the conjugacy properties (2.4.17d) and (2.4.35d). We start with the latter: $\det(0, m)(u) = \det(m, 0)(u + \lambda)$.

By definition, we have $\det(0, m)(u) = \det(m, 0)((4 - 2m)\lambda - u)$. It is thus natural to evaluate the entries in the determinant $\det(m, 0)$ at $\psi = (4 - 2m)\lambda - u$. Let k be an arbitrary shift of the spectral parameter and $v = u + \lambda$. The functions \mathcal{D}_k and \mathcal{F}_k in this determinant become

$$\begin{aligned} \mathcal{D}_k(u) \Big|_{u \rightarrow (4-2m)\lambda - u} &= \mathcal{D}((4 - 2m)\lambda - u + k\lambda) = \mathcal{D}(3\lambda - (u + (2m - k - 1)\lambda)) \\ &\stackrel{(2.4.26c)}{=} \mathcal{D}(u + (2m - k - 1)\lambda) = \mathcal{D}_{2m-2-k}(v) , \end{aligned} \quad (2.A.8)$$

and

$$\begin{aligned} \mathcal{F}_k(u) \Big|_{u \rightarrow (4-2m)\lambda - u} &= \mathcal{F}((4 - 2m)\lambda - u + k\lambda) = \mathcal{F}(\lambda - (u + (2m - k - 3)\lambda)) \\ &\stackrel{(2.4.26d)}{=} \mathcal{F}(u + (2m - k - 3)\lambda) = \mathcal{F}_{2m-4-k}(v) . \end{aligned} \quad (2.A.9)$$

It follows that

$$\det(m, 0)(4\lambda - 2m\lambda - u) = \begin{vmatrix} \mathcal{D}_0(v) & \mathcal{D}_1(v) & \mathcal{F}_1(v) & 0 & 0 \\ \mathcal{F}_0(v) & \mathcal{D}_2(v) & \mathcal{D}_3(v) & \ddots & 0 \\ 0 & \mathcal{F}_2(v) & \mathcal{D}_4(v) & \ddots & \mathcal{F}_{2m-5}(v) \\ 0 & 0 & \ddots & \ddots & \mathcal{D}_{2m-3}(v) \\ 0 & 0 & 0 & \mathcal{F}_{2m-4}(v) & \mathcal{D}_{2m-2}(v) \end{vmatrix} . \quad (2.A.10)$$

This matrix is the transpose with respect to the anti-diagonal of the one appearing in $\det(m, 0)(v)$. Their determinants are equal, and therefore

$$\det(0, m)(u) = \det(m, 0)((4 - 2m)\lambda - u) = \det(m, 0)(v) = \det(m, 0)_1(u) . \quad (2.A.11)$$

We now argue that the previous result implies the conjugacy property for the fused matrix, namely $\mathbf{D}^{m,0}(u + \lambda) = \mathbf{D}^{0,m}(u)$. From (2.A.11), we have

$$\det(m, 0)((5 - 2m)\lambda - u) = \det(m, 0)(u) . \quad (2.A.12)$$

The product of weights in the expression (2.4.28) for $\det(m, 0)_0(u)$ is invariant under $u \mapsto (5-2m)\lambda - u$. (This fact can be verified by direct computation. Some signs appear during this computation, but they all cancel at the end. This invariance is the property alluded to at the end of the previous section.) From (2.A.12), the identity $\mathbf{D}^{m,0}((5-2m)\lambda - u) = \mathbf{D}^{m,0}(u)$ follows and, by the crossing symmetry (2.4.17a), the desired conjugacy property: $\mathbf{D}_1^{m,0}(u) = \mathbf{D}_0^{0,m}(u)$.

2.A.3 Proof of the T -system relations

The proof of the T -system relations (2.4.55) presented in this section is completely analogous to the same proof given for the periodic case in [17]. The proof is inductive on m and requires that we first check the seed cases $m = 1, 2, 3$ separately, for all the allowed values of k , namely for $k = 0, \dots, m-1$. For the proof, we will repeatedly use (2.4.32) as well as the relations

$$\det(m, n)_0 = \mathcal{D}_0 \det(m-1, n)_2 - \mathcal{F}_0 \mathcal{D}_1 \det(m-2, n)_4 + \mathcal{F}_0 \mathcal{F}_1 \mathcal{F}_2 \det(m-3, n)_6, \quad (2.A.13a)$$

$$\begin{aligned} \det(m, n)_0 &= \mathcal{D}_{2m+2n-1} \det(m, n-1)_0 - \mathcal{F}_{2m+2n-3} \mathcal{D}_{2m+2n-2} \det(m, n-2)_0 \\ &\quad + \mathcal{F}_{2m+2n-5} \mathcal{F}_{2m+2n-4} \mathcal{F}_{2m+2n-3} \det(m, n-3)_0. \end{aligned} \quad (2.A.13b)$$

These are obtained by expanding the determinant (2.4.30a) along the first row and the last column, respectively. We also recall that $\det(1, 0)_k = \mathcal{D}_k$ and $\det(0, 0)_k = \mathbf{I}$.

It is easy to see that the T -system relation for $(m, k) = (m, m-1)$ is directly equivalent to the fusion hierarchy relation (2.4.32a) with $m \mapsto m+1$. As a result, for the seed cases, we need only check $(m, k) = (2, 0)$, $(3, 0)$ and $(3, 1)$. For $(m, k) = (2, 0)$, we have

$$\begin{aligned} \det(2, 0)_0 \det(2, 0)_2 &= (\mathcal{D}_0 \mathcal{D}_2 - \mathcal{D}_1 \mathcal{F}_0) \det(2, 0)_2 = \mathcal{D}_0 \mathcal{D}_2 \det(2, 0)_2 - \mathcal{D}_1 \mathcal{F}_0 (\mathcal{D}_2 \mathcal{D}_4 - \mathcal{D}_3 \mathcal{F}_2) \\ &= \mathcal{D}_2 (\mathcal{D}_0 \det(2, 0)_2 - \mathcal{F}_0 \mathcal{D}_1 \mathcal{D}_4) + \mathcal{F}_0 \mathcal{F}_2 (\mathcal{D}_1 \mathcal{D}_3) \\ &= \mathcal{D}_2 (\mathcal{D}_0 \det(2, 0)_2 - \mathcal{F}_0 \mathcal{D}_1 \mathcal{D}_4 + \mathcal{F}_0 \mathcal{F}_1 \mathcal{F}_2) + \mathcal{F}_0 \mathcal{F}_2 \det(2, 0)_1 \\ &= \mathcal{D}_2 \det(3, 0)_0 + \mathcal{F}_0 \mathcal{F}_2 \det(0, 2)_0, \end{aligned} \quad (2.A.14)$$

which is the desired result. For $(m, k) = (3, 0)$, we use (2.A.13a) and find

$$\begin{aligned} \det(3, 0)_0 \det(3, 0)_2 &= (\mathcal{D}_0 \det(2, 0)_2 - \mathcal{F}_0 \mathcal{D}_1 \mathcal{D}_4 + \mathcal{F}_0 \mathcal{F}_1 \mathcal{F}_2) \det(3, 0)_2 \\ &= \det(2, 0)_2 \mathcal{D}_0 \det(3, 0)_2 - \mathcal{F}_0 \mathcal{D}_1 \mathcal{D}_4 \det(3, 0)_2 + \mathcal{F}_0 \mathcal{F}_1 \mathcal{F}_2 \det(3, 0)_2. \end{aligned} \quad (2.A.15)$$

Here we rewrite $\mathcal{D}_4 \det(3, 0)_2$ using the T -system relation for $(m, k) = (2, 0)$ already proven above, and

use (2.4.32a) for $\det(3, 0)_2$ in the last term. This yields

$$\begin{aligned} \det(3, 0)_0 \det(3, 0)_2 &= \det(2, 0)_2 (\mathcal{D}_0 \det(3, 0)_2 - \mathcal{F}_0 \mathcal{D}_1 \det(2, 0)_4 + \mathcal{F}_0 \mathcal{F}_1 \mathcal{F}_2 \mathcal{D}_6) \\ &\quad + \mathcal{F}_0 \mathcal{F}_2 \mathcal{F}_4 (\mathcal{D}_1 \det(0, 2)_2 - \mathcal{F}_1 \det(1, 1)_2) \\ &= \det(2, 0)_2 \det(4, 0)_0 + \mathcal{F}_0 \mathcal{F}_2 \mathcal{F}_4 \det(0, 3)_0, \end{aligned} \quad (2.A.16)$$

which ends the proof in this case. For $(m, k) = (3, 1)$, we have

$$\det(3, 0)_0 \det(2, 0)_4 = (\mathcal{D}_0 \det(2, 0)_2 - \mathcal{F}_0 \mathcal{D}_1 \mathcal{D}_4 + \mathcal{F}_0 \mathcal{F}_1 \mathcal{F}_2) \det(2, 0)_4. \quad (2.A.17)$$

We rewrite the first term using the T -system for $(m, k) = (2, 0)$ proven above, and the second term using the fusion hierarchy relation (2.4.32a) for $\det(2, 0)_4$:

$$\begin{aligned} \det(3, 0)_0 \det(2, 0)_4 &= \mathcal{D}_0 (\mathcal{D}_4 \det(3, 0)_2 + \mathcal{F}_2 \mathcal{F}_4 \det(0, 2)_2) - \mathcal{F}_0 \mathcal{D}_1 \mathcal{D}_4 \det(2, 0)_4 \\ &\quad + \mathcal{F}_0 \mathcal{F}_1 \mathcal{F}_2 (\mathcal{D}_4 \mathcal{D}_6 - \mathcal{D}_5 \mathcal{F}_4) \\ &= \mathcal{D}_4 (\mathcal{D}_0 \det(3, 0)_2 - \mathcal{F}_0 \mathcal{D}_1 \det(2, 0)_4 + \mathcal{F}_0 \mathcal{F}_1 \mathcal{F}_2 \mathcal{D}_6) \\ &\quad + \mathcal{F}_2 \mathcal{F}_4 (\mathcal{D}_0 \det(0, 2)_2 - \mathcal{F}_0 \mathcal{F}_1 \mathcal{D}_5) \\ &= \mathcal{D}_4 \det(4, 0)_0 + \mathcal{F}_2 \mathcal{F}_4 \det(1, 2)_0, \end{aligned} \quad (2.A.18)$$

ending the proof.

Having proven all the seed cases, we now move on to the general case (m, k) . We thus assume that (2.4.55) holds for $m - 1, m - 2, m - 3$ and all corresponding values of k . We expand $\det(m, 0)$ using (2.A.13a) and find

$$\begin{aligned} \det(m, 0) \det(m - k, 0)_{2k+2} &= \mathcal{D}_0 \det(m - 1, 0)_2 \det(m - k, 0)_{2k+2} \\ &\quad - \mathcal{D}_1 \mathcal{F}_0 \det(m - 2, 0)_4 \det(m - k, 0)_{2k+2} + \mathcal{F}_0 \mathcal{F}_1 \mathcal{F}_2 \det(m - 3, 0)_6 \det(m - k, 0)_{2k+2} \\ &= \mathcal{D}_0 (\det(m - 1, 0)_0 \det((m - 1) - (k - 1), 0)_{2(k-1)+2})_2 \\ &\quad - \mathcal{D}_1 \mathcal{F}_0 (\det(m - 2, 0)_0 \det((m - 2) - (k - 2), 0)_{2(k-2)+2})_4 \\ &\quad + \mathcal{F}_0 \mathcal{F}_1 \mathcal{F}_2 (\det(m - 3, 0)_0 \det((m - 3) - (k - 3), 0)_{2(k-3)+2})_6. \end{aligned} \quad (2.A.19)$$

For each of the three terms, we use the induction hypothesis and apply the T -system relation for $(m, k) \mapsto (m - 1, k - 1)$, $(m - 2, k - 2)$ and $(m - 3, k - 3)$, respectively. To avoid negative indices, we first consider the case $k \geq 3$. In this case, we find

$$\begin{aligned} \det(m, 0) \det(m - k, 0)_{2k+2} &= \mathcal{D}_0 \left(\det(k - 1, m - k)_0 \prod_{j=k-1}^{m-2} \mathcal{F}_{2j} + \det(m, 0)_0 \det(m - k - 1, 0)_{2k} \right)_2 \\ &\quad - \mathcal{D}_1 \mathcal{F}_0 \left(\det(k - 2, m - k)_0 \prod_{j=k-2}^{m-3} \mathcal{F}_{2j} + \det(m - 1, 0)_0 \det(m - k - 1, 0)_{2k-2} \right)_4 \end{aligned}$$

$$\begin{aligned}
& + \mathcal{F}_0 \mathcal{F}_1 \mathcal{F}_2 \left(\det(k-3, m-k)_0 \prod_{j=k-3}^{m-4} \mathcal{F}_{2j} + \det(m-2, 0)_0 \det(m-k-1, 0)_{2k-4} \right)_6 \\
& = \det(k, m-k)_0 \prod_{j=k}^{m-1} \mathcal{F}_{2j} + \det(m+1, 0)_0 \det(m-k-1, 0)_{2k+2} . \tag{2.A.20}
\end{aligned}$$

At the last step, we applied (2.A.13a) with $(m, n) \mapsto (k, m-k)$ to combine the first, third and fifth term, and the same equation with $(m, n) \mapsto (m+1, 0)$ for the other three.

It thus remains to check the cases $k=0$, $k=1$ and $k=2$. For $k=2$, we find

$$\begin{aligned}
& \det(m, 0)_0 \det(m-2, 0)_6 = \mathcal{D}_0 \det(m-1, 0)_2 \det(m-2, 0)_6 \\
& - \mathcal{D}_1 \mathcal{F}_0 \det(m-2, 0)_4 \det(m-2, 0)_6 + \mathcal{F}_0 \mathcal{F}_1 \mathcal{F}_2 \det(m-3, 0)_6 \det(m-2, 0)_6 \\
& = \mathcal{D}_0 \left(\det(1, m-2)_0 \prod_{j=1}^{m-2} \mathcal{F}_{2j} + \det(m, 0)_0 \det(m-3, 0)_4 \right)_2 - \mathcal{D}_1 \mathcal{F}_0 \left(\det(0, m-2)_0 \prod_{j=0}^{m-3} \mathcal{F}_{2j} \right. \\
& \left. + \det(m-1, 0)_0 \det(m-3, 0)_2 \right)_4 + \mathcal{F}_0 \mathcal{F}_1 \mathcal{F}_2 \det(m-3, 0)_6 \det(m-2, 0)_6 \\
& = \prod_{j=2}^{m-1} \mathcal{F}_{2j} \left(\mathcal{D}_0 \det(1, m-2)_2 - \mathcal{D}_1 \mathcal{F}_0 \det(0, m-2)_4 \right) + \det(m+1, 0)_0 \det(m-3, 0)_6 , \tag{2.A.21}
\end{aligned}$$

which is the announced result. The only difference with the general case is that we only used two T -system relations inductively at the second equality. For $k=1$, we have

$$\begin{aligned}
& \det(m, 0)_0 \det(m-1, 0)_4 = \mathcal{D}_0 \det(m-1, 0)_2 \det(m-1, 0)_4 \\
& - \mathcal{D}_1 \mathcal{F}_0 \det(m-2, 0)_4 \det(m-1, 0)_4 + \mathcal{F}_0 \mathcal{F}_1 \mathcal{F}_2 \det(m-3, 0)_6 \det(m-1, 0)_4 \\
& = \mathcal{D}_0 \left(\det(0, m-1)_0 \prod_{j=0}^{m-2} \mathcal{F}_{2j} + \det(m, 0)_0 \det(m-2, 0)_2 \right)_2 - \mathcal{D}_1 \mathcal{F}_0 \det(m-2, 0)_4 \det(m-1, 0)_4 \\
& + \mathcal{F}_0 \mathcal{F}_1 \mathcal{F}_2 \left(\det(m-2, 0)_4 \det(m-2, 0)_6 - \det(0, m-2)_4 \prod_{j=2}^{m-1} \mathcal{F}_{2j} \right) , \tag{2.A.22}
\end{aligned}$$

where we applied the T -system relation (2.4.55) inductively for the first and last terms, with $(m, n) \mapsto (m-1, 0)$ and $(m-2, 0)$ respectively. Collecting the second, third and fourth terms, we apply (2.A.13a) and find

$$\begin{aligned}
\det(m, 0)_0 \det(m-1, 0)_4 & = \prod_{j=1}^{m-1} \mathcal{F}_{2j} \left(\mathcal{D}_0 \det(0, m-1)_2 - \mathcal{F}_0 \mathcal{F}_1 \det(0, m-2)_4 \right) \\
& + \det(m+1, 0)_0 \det(m-2, 0)_4 \\
& = \det(1, m-1)_0 \prod_{j=1}^{m-1} \mathcal{F}_{2j} + \det(m+1, 0)_0 \det(m-2, 0)_4 , \tag{2.A.23}
\end{aligned}$$

ending the proof for this case.

Finally, for $k = 0$, we first use (2.A.13a) and find

$$\begin{aligned}
\det(m, 0) \det(m, 0)_2 &= \mathcal{D}_0 \det(m-1, 0)_2 \det(m, 0)_2 - \mathcal{D}_1 \mathcal{F}_0 \det(m-2, 0)_4 \det(m, 0)_2 \\
&+ \mathcal{F}_0 \mathcal{F}_1 \mathcal{F}_2 \det(m-3, 0)_6 \det(m, 0)_2 \\
&= \mathcal{D}_0 \det(m-1, 0)_2 \det(m, 0)_2 \\
&- \mathcal{D}_1 \mathcal{F}_0 \left(\det(m-1, 0)_2 \det(m-1, 0)_4 - \det(0, m-1)_2 \prod_{j=1}^{m-1} \mathcal{F}_{2j} \right) \\
&+ \mathcal{F}_0 \mathcal{F}_1 \mathcal{F}_2 \left(\det(m-1, 0)_2 \det(m-2, 0)_6 - \det(1, m-2)_2 \prod_{j=2}^{m-1} \mathcal{F}_{2j} \right). \quad (2.A.24)
\end{aligned}$$

At the last equality, we used inductively the T -system relation for $(m, n) \mapsto (m-1, 0)$ and $(m-1, 1)$ to reexpress the second and third terms, respectively. Collecting the first, second and fourth terms, which all have a factor of $\det(m-1, 0)_2$, we use (2.A.13a) and find

$$\begin{aligned}
\det(m, 0) \det(m, 0)_2 &= \det(m+1, 0)_0 \det(m-1, 0)_2 + \prod_{j=0}^{m-1} \mathcal{F}_{2j} (\mathcal{D}_1 \det(0, m-1)_2 - \mathcal{F}_1 \det(1, m-2)_2) \\
&= \det(m+1, 0)_0 \det(m-1, 0)_2 + \det(0, m)_0 \prod_{j=0}^{m-1} \mathcal{F}_{2j}, \quad (2.A.25)
\end{aligned}$$

ending the proof.

2.A.4 Closure relations for $b = 2$ and $b = 3$

In this section, we give more details on the closure relations and their proofs, for $b = 2$ and $b = 3$ with identical boundary conditions. We show that these relations hold at $u = \hat{u} = (4-b)\lambda + \frac{r\pi}{2}$, thus completing the work of Section 2.6.3 where the proof is presented for $b \geq 4$. The arguments are given separately for (i) $b = 2$, (ii) $b = 3$ with a odd, and (iii) $b = 3$ with a even.

The case $b = 2$. In this case, a is an odd integer and the loop weight is $\beta = 2$. Following the same idea as in (2.6.15), we denote the four terms in the closure relation (2.6.2b) as $\mathbf{S}^1(u), \dots, \mathbf{S}^4(u)$ in such a way that it reads

$$\mathbf{S}^1(u) + \mathbf{S}^2(u) = \kappa(\mathbf{S}^3(u) - 2\mathbf{S}^4(u)), \quad \kappa = 3. \quad (2.A.26)$$

At $\lambda = \lambda_{a,2}$, the various functions have the symmetries

$$\mathbf{D}^{m,n}(u) = \mathbf{D}^{m,n}(u_4) = \mathbf{D}^{m,n}(u_2 + \frac{\pi}{2}) \quad f(u) = f(-u) = f(u_4) = f(u_2 + \frac{\pi}{2}), \quad (2.A.27a)$$

$$w(u) = -w(u_4), \quad \bar{w}(u) = \zeta \varrho w(u_2), \quad (2.A.27b)$$

$$w^{(1)}(u) = \zeta w(u_2), \quad \bar{w}^{(1)}(u) = -\varrho w(u), \quad (2.A.27c)$$

$$w(-u) = -\varrho w(u), \quad \bar{w}(-u) = \varrho \bar{w}(u), \quad (2.A.27d)$$

where

$$\zeta = (-1)^{(a-1)/2}, \quad \varrho = \begin{cases} 1 & \text{SS,} \\ -1 & \text{CC.} \end{cases} \quad (2.A.28)$$

We use this information to evaluate each term of the closure relation at $\hat{u} = 2\lambda + \frac{r\pi}{2}$. Using the notation (2.6.20), we find

$$\mathbf{S}^1(\hat{u}) = 2\mathbf{S}^2(\hat{u}) = -2\mathbf{S}^3(\hat{u}) = -2\mathbf{S}^4(\hat{u}) = (-1)^{r+1} 2\varrho w_{1/2}^3 w_{3/2}^2 f(\frac{r\pi}{2}) f(\lambda + \frac{r\pi}{2}) \mathbf{I}, \quad (2.A.29)$$

which we use to confirm that (2.A.26) holds at $u = \hat{u}$. In particular, to compute $\mathbf{S}^1(\hat{u})$, one must carefully use the result (2.4.43) for generic λ and then take the limit $\lambda \rightarrow \lambda_{a,2}$. Finally, we note that the closure relation for $b = 2$ can be rewritten as the quadratic functional relation in $\mathbf{D}(u)$

$$\begin{aligned} 0 &= w(u_{1/2})w(u_{5/2})\mathbf{D}_0\mathbf{D}_2 + \varrho w(u_{3/2})^4 f_1 f_2 \mathbf{D}_1 - \varrho w(u_{7/2})^4 f_0 f_3 \mathbf{D}_3 \\ &+ 3w(u_{1/2})w(u_{3/2})^2 w(u_{5/2})w(u_{7/2})^2 f_0 f_1 f_2 f_3 \mathbf{I}. \end{aligned} \quad (2.A.30)$$

The case $b = 3$ with a odd. In this case, the loop weight is $\beta = 1$ and the functions entering the closure relation (2.6.2) have the symmetries

$$\mathbf{D}^{m,n}(u) = \mathbf{D}^{m,n}(u_3), \quad f(u) = f(-u) = f(u_3), \quad (2.A.31a)$$

$$w(u) = -\zeta w(u_3), \quad \bar{w}(u) = -\zeta \bar{w}(u_3), \quad (2.A.31b)$$

$$w^{(1)}(u) = \varrho \bar{w}(u), \quad \bar{w}^{(1)}(u) = -\varrho w(u), \quad (2.A.31c)$$

$$w(-u) = -\varrho w(u), \quad \bar{w}(-u) = \varrho \bar{w}(u), \quad (2.A.31d)$$

where ζ and ϱ are as in (2.A.28). Using this information, we find that all five terms in the closure relation vanish at $\hat{u} = \lambda + \frac{r\pi}{2}$ with $r \in \{0, 1\}$:

$$\mathbf{R}^i(\hat{u}) = 0, \quad i = 1, \dots, 5. \quad (2.A.32)$$

To show this, we first note that exactly one of $w(\frac{3\lambda}{2})$ or $\bar{w}(\frac{3\lambda}{2})$ vanishes at $\lambda = \lambda_{a,3}$ with a odd. Then, depending of the values of λ and r and the choice of boundary conditions, the fact that $\mathbf{R}^i(\hat{u}) = 0$ may be easy to check due to the vanishing of one of the factors arising explicitly in the definition of

this function. If this factor is $w^{(a)}(u_{-5/2})$ or $w^{(1)}(u_{-5/2})$, then one must use the symmetries (2.A.31) to show that it indeed vanishes. In fact, $\mathbf{R}^3(\hat{u})$, $\mathbf{R}^4(\hat{u})$ and $\mathbf{R}^5(\hat{u})$ are always easy to compute in this sense. For $\mathbf{R}^1(\hat{u})$, when it is not easy to compute, one must instead rewrite $\mathbf{D}^{3,0}(\hat{u})$ with (2.4.43) to show that it vanishes. Similarly, in the cases where $\mathbf{R}^2(\hat{u})$ is not straightforward to compute, showing that it vanishes requires that we carefully apply the limit $\lambda \rightarrow \lambda_{a,3}$ to the fusion hierarchy relation (2.4.15b) for $\mathbf{D}^{1,1}(\hat{u}_2)$.

Note that, for $b = 3$ and a odd, the face operator (2.3.1) vanishes at $u = 0, \pi$. Moreover, the weights $\delta(u + \frac{3\lambda}{2})$ and $\delta(u - \frac{3\lambda}{2})$ that define the boundary operator in (2.3.4) are equal up to a sign. This implies that the renormalised transfer matrix

$$\widehat{\mathbf{D}}(u) = \frac{\mathbf{D}(u)}{f(u)w(u_{3/2})^2} \quad (2.A.33)$$

is a Laurent polynomial in e^{iu} . Its maximal power is $2N$. In terms of this matrix, the closure relation is equivalent to the simple cubic functional relation for $\widehat{\mathbf{D}}(u)$

$$0 = \varrho \widehat{\mathbf{D}}_0 \widehat{\mathbf{D}}_1 \widehat{\mathbf{D}}_2 - f_0 \widehat{\mathbf{D}}_0^2 - f_1 \widehat{\mathbf{D}}_1^2 - f_2 \widehat{\mathbf{D}}_2^2 + 4f_0 f_1 f_2 \mathbf{I}. \quad (2.A.34)$$

This is precisely the functional relation studied in [33] for $\lambda = \frac{\pi}{3}$ corresponding to critical site percolation on the triangular lattice.

The case $b = 3$ with a even. In this case, the loop weight is also $\beta = 1$. We see from (2.4.5) that $\mathbf{D}(u)$ vanishes at $u = 0, \frac{\pi}{2}$. We therefore define the renormalised transfer matrix

$$\widehat{\mathbf{D}}(u) = \frac{\mathbf{D}(u)}{\sin 2u}. \quad (2.A.35)$$

It is a Laurent polynomial in e^{iu} of maximal power $4N$. Of course, these zeroes are particular to $b = 3$ with a even and, in the computations below, the evaluation on λ must thus precede that on u . (This observation turns out to be crucial for the computation of $\mathbf{R}^2(\hat{u})$.) The various functions in (2.6.2) have the symmetries

$$\mathbf{D}^{m,n}(u) = \mathbf{D}^{m,n}(u_6), \quad f(u) = f(-u) = f(u_6), \quad (2.A.36a)$$

$$w(u) = -w(u_6), \quad \bar{w}(u) = -\varrho \zeta w(u_3), \quad (2.A.36b)$$

$$w^{(1)}(u) = -\zeta w(u_3), \quad \bar{w}^{(1)}(u) = -\varrho w(u), \quad (2.A.36c)$$

$$w(-u) = -\varrho w(u), \quad \bar{w}(-u) = \varrho \bar{w}(u), \quad (2.A.36d)$$

where

$$\zeta = (-1)^{a/2}, \quad \varrho = \begin{cases} 1 & \text{SS,} \\ -1 & \text{CC.} \end{cases} \quad (2.A.37)$$

Using the short-hand notation (2.6.20), we find

$$\mathbf{R}^1(\hat{u}) = -\mathbf{R}^4(\hat{u}) = \mathbf{R}^5(\hat{u}) = (-1)^r \zeta w_{1/2}^2 w_{3/2}^3 w_{5/2}^2 f\left(\frac{r\pi}{2}\right) f\left(\lambda + \frac{r\pi}{2}\right) f\left(2\lambda + \frac{r\pi}{2}\right) \mathbf{I}, \quad (2.A.38a)$$

$$\mathbf{R}^2(\hat{u}) = \zeta w_{3/2} \mathbf{D}^{1,1}(3\lambda + \frac{r\pi}{2}) = \frac{(-1)^{r+1} \zeta w_{3/2}^3}{f(3\lambda + \frac{r\pi}{2})} \left(s(2\lambda)^2 \widehat{\mathbf{D}}(0) \widehat{\mathbf{D}}\left(\frac{\pi}{2}\right) - w_{1/2}^4 f\left(\frac{r\pi}{2}\right)^2 f\left(\lambda + \frac{r\pi}{2}\right)^2 \mathbf{I} \right), \quad (2.A.38b)$$

$$\mathbf{R}^3(\hat{u}) = (-1)^r \zeta w_{3/2}^3 w_{5/2}^4 f\left(2\lambda + \frac{r\pi}{2}\right)^2 f\left(3\lambda + \frac{r\pi}{2}\right) \mathbf{I}. \quad (2.A.38c)$$

Here we used (2.4.43) for $\mathbf{R}^1(\hat{u})$ and simplified the terms. Likewise the product of factors for $\mathbf{R}^3(\hat{u})$, $\mathbf{R}^4(\hat{u})$ and $\mathbf{R}^5(\hat{u})$ were simplified using (2.A.36). Only $\mathbf{R}^2(\hat{u})$ is not yet in its final form. In Lemma 2.A.1 below, we show that $\widehat{\mathbf{D}}(0)$ and $\widehat{\mathbf{D}}(\frac{\pi}{2})$ are equal and proportional to the unit \mathbf{I} , and we compute the corresponding prefactor. Inserting these results in (2.6.17), we find that the identity indeed holds, ending the proof of the closure relation at $u = \hat{u}$. Finally, we note that the closure relation in this case is equivalent to the cubic functional relation

$$0 = \varrho s(2u_0) s(2u_1) s(2u_2) \widehat{\mathbf{D}}_0 \widehat{\mathbf{D}}_2 \widehat{\mathbf{D}}_4 \quad (2.A.39)$$

$$+ s(2u_0) s(2u_2) w(u_{5/2})^2 f_2 f_3 \widehat{\mathbf{D}}_1 \widehat{\mathbf{D}}_4 - s(2u_1) s(2u_2) w(u_{9/2})^2 f_4 f_5 \widehat{\mathbf{D}}_0 \widehat{\mathbf{D}}_3$$

$$- s(2u_0) s(2u_1) w(u_{1/2})^2 f_0 f_1 \widehat{\mathbf{D}}_2 \widehat{\mathbf{D}}_5 + w(u_{1/2})^2 w(u_{3/2})^2 w(u_{5/2})^2 f_0 f_1^2 f_2^2 f_3 \mathbf{I}$$

$$+ w(u_{5/2})^2 w(u_{7/2})^2 w(u_{9/2})^2 f_2 f_3^2 f_4^2 f_5 \mathbf{I} + w(u_{1/2})^2 w(u_{9/2})^2 w(u_{11/2})^2 f_0^2 f_1 f_4 f_5^2 \mathbf{I} \quad (2.A.40)$$

$$- \left[\prod_{j=0}^5 f_j \right] \left(w(u_{3/2})^2 w(u_{7/2})^2 w(u_{11/2})^2 + 2 w(u_{1/2})^2 w(u_{5/2})^2 w(u_{9/2})^2 \right) \mathbf{I}.$$

LEMMA 2.A.1. *The renormalized transfer matrix satisfies*

$$\widehat{\mathbf{D}}(0) = \widehat{\mathbf{D}}\left(\frac{\pi}{2}\right) = \frac{\varrho}{s(2\lambda)} \left(w\left(\frac{\lambda}{2}\right)^2 f(0) f(\lambda) - w\left(\frac{5\lambda}{2}\right)^2 f(2\lambda) f(3\lambda) \right) \mathbf{I}. \quad (2.A.41)$$

PROOF. We give the proof for $\widehat{\mathbf{D}}(0)$, noting that the result will also hold for $\widehat{\mathbf{D}}(\frac{\pi}{2})$ because of crossing symmetry. To compute $\widehat{\mathbf{D}}(0)$, we use L'Hôpital's rule to write

$$\widehat{\mathbf{D}}(0) = \frac{1}{2} \frac{d}{du} \mathbf{D}(u) \Big|_{u=0} = -\frac{1}{2} \frac{d}{du} \tilde{\mathbf{D}}(u) \Big|_{u=0} \quad (2.A.42)$$

where $\tilde{\mathbf{D}}(u)$ is defined in (2.4.1). Let us then define

$$\boxed{v'} = \frac{d}{du} \boxed{u} \Big|_{u=v}, \quad \triangleleft v' = \frac{d}{du} \triangleleft u \Big|_{u=v}. \quad (2.A.43)$$

For $\lambda = \lambda_{a,3}$ with a even, we have

$$\begin{aligned} \begin{array}{c} \text{---} \\ \diagup \\ 0 \\ \diagdown \\ \text{---} \end{array} &= \delta\left(\frac{3\lambda}{2}\right) \begin{array}{c} \text{---} \\ \diagup \\ \text{---} \\ \diagdown \\ \text{---} \end{array}, & \begin{array}{c} \text{---} \\ \diagup \\ 0' \\ \diagdown \\ \text{---} \end{array} &= -\varrho\zeta \delta\left(\frac{3\lambda}{2}\right) \begin{array}{c} \text{---} \\ \diagup \\ \square \\ \diagdown \\ \text{---} \end{array}, \end{aligned} \quad (2.A.44a)$$

$$\begin{aligned} \begin{array}{c} \text{---} \\ \diagup \\ 3\lambda \\ \diagdown \\ \text{---} \end{array} &= \varrho \delta\left(\frac{3\lambda}{2}\right) \begin{array}{c} \text{---} \\ \diagup \\ \square \\ \diagdown \\ \text{---} \end{array}, & \begin{array}{c} \text{---} \\ \diagup \\ 3\lambda' \\ \diagdown \\ \text{---} \end{array} &= \zeta \delta\left(\frac{3\lambda}{2}\right) \begin{array}{c} \text{---} \\ \diagup \\ \text{---} \\ \diagdown \\ \text{---} \end{array}. \end{aligned} \quad (2.A.44b)$$

There are two push-through properties. The first, given in (2.3.13b), has dashed arcs that propagate to the left. The second, specific to $\lambda = \lambda_{a,3}$, involves a dashed arc with a gauge operator which is moved to the right:

$$\begin{array}{c} \text{---} \\ \diagup \\ \square \\ \diagdown \\ \text{---} \end{array} \begin{array}{c} u_3 \\ \hline u_0 \end{array} = s(u_{-1})s(u_1)s(u_0)^2 \begin{array}{c} \text{---} \\ \diagup \\ \square \\ \diagdown \\ \text{---} \end{array}. \quad (2.A.45)$$

This relation is derived from (2.3.13b) using (2.3.15) and the fact that $6\lambda = \pi \pmod{2\pi}$. We apply the derivative to the right side of (2.4.1) and use the product rule. The derivative must be applied to each of the face and boundary operators, so this produces a total of $2N + 2$ terms: two boundary terms and $2N$ bulk terms. For each, we use the two push-through properties repeatedly. This yields

$$\begin{aligned} \widehat{D}(0) &= \frac{1}{2} \left(f(2\lambda)f(3\lambda) \begin{array}{c} \text{---} \\ \diagup \\ 3\lambda' \\ \diagdown \\ \text{---} \end{array} \begin{array}{c} \text{---} \\ \diagup \\ 0 \\ \diagdown \\ \text{---} \end{array} - f(0)f(\lambda) \begin{array}{c} \text{---} \\ \diagup \\ 3\lambda \\ \diagdown \\ \text{---} \end{array} \begin{array}{c} \text{---} \\ \diagup \\ 0' \\ \diagdown \\ \text{---} \end{array} \right) \mathbf{I}_N \\ &\quad - \frac{1}{2} \sum_{j=1}^N \left[\prod_{k=1}^{j-1} s(\xi_{(k)} + \lambda)s(\xi_{(k)} - \lambda)s(\xi_{(k)})^2 \right] \left[\prod_{\ell=j+1}^N s(\xi_{(\ell)} + 2\lambda)s(\xi_{(\ell)} - 2\lambda)s(\xi_{(\ell)} + 3\lambda)s(\xi_{(\ell)} - 3\lambda) \right] \\ &\quad \times \mathbf{I}_{j-1} \otimes \left(\begin{array}{c} \text{---} \\ \diagup \\ 3\lambda \\ \diagdown \\ \text{---} \end{array} \begin{array}{c} \xi'_{(j)} \\ \hline -\xi_{(j)} \end{array} \begin{array}{c} \text{---} \\ \diagup \\ 0 \\ \diagdown \\ \text{---} \end{array} + \begin{array}{c} \text{---} \\ \diagup \\ 3\lambda \\ \diagdown \\ \text{---} \end{array} \begin{array}{c} \xi_{(j)} \\ \hline -\xi'_{(j)} \end{array} \begin{array}{c} \text{---} \\ \diagup \\ 0 \\ \diagdown \\ \text{---} \end{array} \right) \otimes \mathbf{I}_{N-j}, \end{aligned} \quad (2.A.46)$$

where, to get the correct signs, one must remember the sign in (2.A.42) and another coming from the derivative of the left boundary triangle. Moreover, we use the notation \mathbf{I}_N to denote the identity in $\text{dTL}_N(\beta)$, and $c_1 \otimes c_2$ to denote the horizontal juxtaposition of two elements of $\text{dTL}_{N_1}(\beta)$ and $\text{dTL}_{N_2}(\beta)$ that forms an element of $\text{dTL}_{N_1+N_2}(\beta)$. The remaining diagrams are evaluated as

$$\begin{array}{c} \text{---} \\ \diagup \\ 3\lambda' \\ \diagdown \\ \text{---} \end{array} \begin{array}{c} \text{---} \\ \diagup \\ 0 \\ \diagdown \\ \text{---} \end{array} = - \begin{array}{c} \text{---} \\ \diagup \\ 3\lambda \\ \diagdown \\ \text{---} \end{array} \begin{array}{c} \text{---} \\ \diagup \\ 0' \\ \diagdown \\ \text{---} \end{array} = \zeta \delta\left(\frac{3\lambda}{2}\right)^2 (1 + \beta) = \zeta, \quad (2.A.47a)$$

$$\begin{array}{c} \text{---} \\ \diagup \\ 3\lambda \\ \diagdown \\ \text{---} \end{array} \begin{array}{c} \xi' \\ \hline -\xi \end{array} \begin{array}{c} \text{---} \\ \diagup \\ 0 \\ \diagdown \\ \text{---} \end{array} + \begin{array}{c} \text{---} \\ \diagup \\ 3\lambda \\ \diagdown \\ \text{---} \end{array} \begin{array}{c} \xi \\ \hline -\xi' \end{array} \begin{array}{c} \text{---} \\ \diagup \\ 0 \\ \diagdown \\ \text{---} \end{array} = \frac{\varrho}{s(2\lambda)} (s(\xi_{-3})s(\xi_{-2})s(\xi_2)s(\xi_3) - s(\xi_{-1})s(\xi_0)^2s(\xi_1)) \mathbf{I}_1. \quad (2.A.47b)$$

These two relations lead to a straightforward check of (2.A.41) for $N = 1$. To show this, we use

$$\frac{\varrho\zeta}{2}s(2\lambda) + \frac{1}{2} = w\left(\frac{\lambda}{2}\right)^2, \quad \frac{\varrho\zeta}{2}s(2\lambda) - \frac{1}{2} = -w\left(\frac{5\lambda}{2}\right)^2. \quad (2.A.48)$$

For $N > 1$, inserting (2.A.47b) into (2.A.46), we find that all terms in the sum cancel pairwise, except for one contribution from $j = 1$ and another from $j = N$. This yields

$$\widehat{\mathbf{D}}(0) = \frac{\zeta}{2}(f(2\lambda)f(3\lambda) + f(0)f(\lambda))\mathbf{I} - \frac{\varrho}{2s(2\lambda)}(f(2\lambda)f(3\lambda) - f(0)f(\lambda))\mathbf{I}, \quad (2.A.49)$$

which is found to be equal to (2.A.41) after simplification. ■

Chapitre 3

Conclusion

Dans ce mémoire, le modèle de boucles diluées sur le ruban a été étudié à partir de la méthode de Klümper et Pearce. Le but était d'obtenir les équations fonctionnelles analogues à celles de [17] pour ce modèle sur la géométrie du cylindre. La hiérarchie de fusion et les systèmes T et Y ont été calculés directement dans l'algèbre de Temperley-Lieb diluée. Leur structure est similaire à celle du modèle sur le cylindre : la définition de $\mathbf{D}^{m,n}(u)$ fait intervenir les mêmes produits de fonctions $f(u)$ et de matrices fusionnées d'indices plus bas. Les coefficients sont cependant beaucoup plus compliqués dû aux contributions des conditions frontières.

Pour λ générique, ces systèmes d'équations sont infinis. Cependant, lorsque $e^{i\lambda}$ est une racine de l'unité, la hiérarchie de fusion et le système Y obéissent à une relation de fermeture et ne contiennent plus qu'un nombre fini d'équations. Notons que la méthode polynomiale utilisée pour la preuve de la fermeture en Section 2.6 est la même que celle utilisée dans [17]. Finalement, de nouveaux résultats quant aux énergies libres de surface ont été obtenus.

Les matrices de transfert étudiées dans ce mémoire sont définies pour diverses conditions frontières. L'article réussit cependant à présenter les résultats, et leurs preuves, uniformément pour toutes ces conditions frontières. Cette présentation uniforme est une de mes contributions.

Au cours de ce projet, des outils calculatoires spécifiques à la géométrie du ruban ont été développés. Les propriétés diagrammatiques pour les opérateurs frontières des Équations (2.3.23) à (2.3.31) sont de nouveaux résultats. Les relations de réduction (2.4.40) et l'utilisation de la symétrie de croisement dans le contexte des preuves présentées en Sections 2.5 et 2.6 sont aussi nouveaux et font également partie de mes contributions.

Rappelons que la méthode développée par Klümper et Pearce permet d'obtenir un développement en $1/N$ des plus grandes valeurs propres de la matrice de transfert, les corrections de taille finie, directement à partir de celle-ci. La première étape est d'obtenir les équations mentionnées plus haut (hiérarchie de fusion, systèmes T et Y et relations de fermeture). La deuxième étape est de transformer les relations de fermeture en équations intégrales non-linéaires. Il est alors possible, toujours en suivant la méthode initiée par Klümper et Pearce, de résoudre ces équations et d'obtenir certaines informations

conformes à propos du modèle.

Ce travail a été effectué dans [27] pour les modèles de boucles denses, *fully packed* et dilués sur le cylindre, lorsque λ correspond aux séries principales et duales¹. La suite naturelle de l'article présenté au Chapitre 2 est donc d'obtenir les résultats analogues pour la géométrie du ruban. Un des thèmes récurrent de ce projet est la complexité des calculs suite à l'ajout des poids frontières. De tels problèmes sont donc à prévoir pour cette deuxième étape. Un autre aspect intéressant est que les outils calculatoires mentionnés plus haut et spécifiques à la géométrie du ruban pourraient être appliqués à d'autres modèles. Cela pourrait être le cas, par exemple, pour une relation de fermeture dans [11] qui était conjecturée, mais non démontrée.

1. Par exemple, pour le modèle de boucles dilués sur le cylindre, les séries principale et duale sont respectivement $a = b - 1$ et $a = 1 - b$ avec la même notation qu'en (2.6.1).

Bibliographie

- [1] J.L. Jacobsen, *Conformal field theory applied to loop models*, Lect. Notes Phys. **775** (2009) 347–424.
- [2] R.J. Baxter, *Exactly solved models in statistical mechanics*, Academic Press, London (1982).
- [3] V. Gurarie, *Logarithmic operators in conformal field theory*, Nucl. Phys. **B410** (1993) 535–549, [arXiv:hep-th/9303160](#).
- [4] P.A. Pearce, J. Rasmussen, J.-B. Zuber, *Logarithmic minimal models*, J. Stat. Mech. **0611** (2006) P11017, [arXiv:hep-th/0607232](#).
- [5] A. Gainutdinov, D. Ridout, I. Runkel (Guest Editors), *Special issue on logarithmic conformal field theory*, J. Phys. A : Math. Theor. **46(49)** (2013).
- [6] V.V. Bazhanov, *Trigonometric solutions of triangle equations and classical Lie algebras*, Phys. Lett. **B159** (1985) 321–324.
- [7] M. Jimbo, *Quantum R matrix for the generalized Toda system*, Comm. Math. Phys. **102** (1986) 537–547.
- [8] Y.K. Zhou, P.A. Pearce, *Solution of functional equations of restricted $A_{n-1}^{(1)}$ fused lattice models*, Nucl. Phys. **B446** (1995) 485–510, [arXiv:hep-th/9502067](#).
- [9] V.V. Bazhanov, V.V. Mangazeev, *Analytic theory of the eight-vertex model*, Nucl. Phys. **B775** (2007) 225–282, [arXiv:hep-th/0609153](#).
- [10] A. Morin-Duchesne, P.A. Pearce, J. Rasmussen, *Fusion hierarchies, T-systems, and Y-systems of logarithmic minimal models*, J. Stat. Mech. **0514** (2014) P05012, [arXiv:1401.7750 \[math-ph\]](#).
- [11] H. Frahm, A. Morin-Duchesne, P.A. Pearce, *Extended T-systems, Q matrices and T-Q relations for $sl(2)$ models at roots of unity*, J. Phys. A : Math. Theor. **52** (2019) 285001, [arXiv:1812.01471 \[hep-th\]](#).
- [12] B. Nienhuis, *Critical and multicritical $\mathcal{O}(n)$ models*, Physica A **163** (1990) 152–157.
- [13] A.G. Izergin, V.E. Korepin, *The inverse scattering method approach to the quantum Shabat-Mikhailov model*, Comm. Math. Phys. **79** (1981) 303–316.
- [14] E. Vernier, J.L. Jacobsen, H. Saleur, *Non compact conformal field theory and the $a_2^{(2)}$ (Izergin-Korepin) model in regime III*, J. Phys. A **47** (2014) 285202, [arXiv:1404.4497 \[math-ph\]](#).

- [15] C.M. Yung, M.T. Batchelor, *Integrable vertex and loop models on the square lattice with open boundaries via reflection matrices*, Nucl. Phys. **B435** (1995) 430–462, [arXiv:hep-th/9410042](#); *$O(n)$ model on the honeycomb lattice via reflection matrices : Surface critical behaviour*, Nucl. Phys. **B453** (1995) 552–580, [arXiv:hep-th/9506074](#); *Surface critical behaviour of the honeycomb $O(n)$ loop model with mixed ordinary and special boundary conditions*, J. Phys. A **28** (1995) L421–L426, [arXiv:cond-mat/9507010](#)
- [16] J. Dubail, J.L. Jacobsen, H. Saleur, *Conformal boundary conditions in the critical $\mathcal{O}(n)$ model and dilute loop models*, Nucl. Phys. B **827** (2010) 457–502, [arXiv:0905.1382 \[math-ph\]](#).
- [17] A. Morin-Duchesne, P.A. Pearce, *Fusion hierarchies, T -systems and Y -systems for the dilute $A_2^{(2)}$ loop models*, J. Stat. Mech. **1909** (2019) 094007, [arXiv:1905.07973 \[math-ph\]](#).
- [18] U. Grimm, P.A. Pearce, *Multi-colour braid monoid algebras*, J. Phys. A **26** (1993) 7435–7459, [arXiv:hep-th/9303161](#).
- [19] P.A. Pearce, *Recent progress in solving A - D - E lattice models*, Physica A **205** (1994) 15–30.
- [20] U. Grimm, *Dilute algebras and solvable lattice models*, Statistical Models, Yang-Baxter Equation and Related Topics, Proc. of the satellite meeting of STATPHYS-19, World Scientific (1996) 110–117, [arXiv:q-alg/9511020](#).
- [21] J. Belletête, Y. Saint-Aubin, *The principal indecomposable modules of the dilute Temperley-Lieb algebra*, J. Math. Phys. **55** (2014) 111706, [arXiv:1310.4791 \[math-ph\]](#).
- [22] H. Temperley, E. Lieb, *Relations between the “percolation” and “colouring” problem and other graph-theoretical problems associated with regular planar lattices : Some exact results for the “percolation” problem*, Proc. Roy. Soc. London Ser. **A322** (1971) 251–280.
- [23] V.F.R. Jones, *Planar algebras I*, [arXiv:math/9909027 \[math.QA\]](#).
- [24] P.A. Pearce, A. Klümper, *Finite-size corrections and scaling dimensions of solvable lattice models : An analytic method*, Phys. Rev. Lett. **66** (1991) 974–977.
- [25] A. Klümper, P.A. Pearce, *Analytic calculation of scaling dimensions : Tricritical hard squares and critical hard hexagons*, J. Stat. Phys. **64** (1991) 13–76.
- [26] A. Klümper, P.A. Pearce, *Conformal weights of RSOS lattice models and their fusion hierarchies*, Physica A **183** (1992) 304–350.
- [27] A. Morin-Duchesne, A. Klümper, P.A. Pearce, *Groundstate finite-size corrections and dilogarithm identities for the twisted $A_1^{(1)}$, $A_2^{(1)}$ and $A_2^{(2)}$ loop models*, J. Stat. Mech. **2103** (2021) 033105, [arXiv:2006.08233 \[math-ph\]](#).
- [28] S.O. Warnaar, M.T. Batchelor, B. Nienhuis, *Critical properties of the Izergin-Korepin and solvable $O(n)$ models and their related quantum chains*, J. Phys. A **25** (1992) 3077–3095.
- [29] A. Morin-Duchesne, P.A. Pearce, J. Rasmussen, *Fusion hierarchies, T -systems and Y -systems for the $A_2^{(1)}$ models*, J. Stat. Mech. **1901** (2019) 013101, [arXiv:1809.07868 \[math-ph\]](#).
- [30] R.E. Behrend, P.A. Pearce, D.L. O’Brien, *Interaction-Round-A-Face Models with Fixed Boundary Conditions : The ABF Fusion Hierarchy*, J. Stat. Phys. **84** (1996) 1–48, [arXiv:hep-th/9507118](#).

- [31] A. Morin-Duchesne, Y. Saint-Aubin, *The Jordan structure of two-dimensional loop models*, J. Stat. Mech. **1104** (2011) P04007, [arXiv:1101.2885 \[math-ph\]](https://arxiv.org/abs/1101.2885).
- [32] R.J. Baxter, *The inversion relation method for some two-dimensional exactly solved models in lattice statistic*, J. Stat. Phys. **28** (1982) 1–41.
- [33] A. Morin-Duchesne, A. Klümper, P.A. Pearce, *Critical site percolation on the triangular lattice : from integrability to conformal partition functions*, in preparation.
- [34] E. Ising, *Contribution to the Theory of Ferromagnetism*, Z. Phys. **31** (1925) 253–258.
- [35] C.J. Thompson, *Mathematical statistical mechanics*, Macmillan, New York (1972).
- [36] B. Simons, *Phase Transitions and Collective Phenomena*, Cambridge (1997), <http://www.tcm.phy.cam.ac.uk/~bds10/phase.html>.
- [37] D. Ridout, Y. Saint-Aubin, *Standard Modules, Induction and the Temperley-Lieb Algebra*, Advances in theoretical and mathematical physics **18.5** (2014), [arXiv:1204.4505v4 \[math-ph\]](https://arxiv.org/abs/1204.4505v4).
- [38] A. Morin-Duchesne, *La structure de Jordan des matrices de transfert des modèles de boucles et la relation avec les hamiltoniens XXZ*, Thèse de doctorat, Université de Montréal (2012).
- [39] R.J. Baxter, P.A. Pearce, *Hard hexagons : interfacial tension and correlation length*, J. Phys. A : Math. Gen. **15** (1982) 897–910.
- [40] R.J. Baxter, P.A. Pearce, *Hard squares with diagonal attractions*, J. Phys. A : Math. Gen. **16** (1983) 2239–2255.
- [41] H.W.J. Blöte, J.L. Cardy, M.P. Nightingale, *Conformal invariance, the central charge, and universal finite-size amplitudes at criticality*, Phys. Rev. Lett. **56** (1986) 742–745.
- [42] I. Affleck, *Universal Term in the Free Energy at a Critical Point and the Conformal Anomaly*, Phys. Rev. Lett. **56** (1986) 746–748.
- [43] V.V. Bazhanov, N. Reshetikhin, *Critical RSOS models and conformal field theory*, Int. J. Mod. Phys. **A4** (1989) 115–142.
- [44] A. Klümper, M.T. Batchelor, *An analytic treatment of finite-size corrections in the spin-1 antiferromagnetic XXZ chain*, J. Phys. A : Math. Gen. **23** (1990) L189.
- [45] D.L. O’Brien, P.A. Pearce, S. Ole Warnaar, *Finitized conformal spectrum of the Ising model on the cylinder and torus*, Physica A **228** (1996) 63–77.
- [46] A.B. Zamolodchikov, *On the thermodynamic Bethe ansatz equations for reflection less ADE scattering theories*, Phys. Lett. **B253** (1991) 391–394.
- [47] A.B. Zamolodchikov, *Thermodynamic Bethe ansatz for RSOS scattering theories*, Nucl. Phys. **B358** (1991) 497–523.
- [48] A. Morin-Duchesne, A. Klümper, P.A. Pearce, *Conformal partition functions of critical percolation from D_3 Thermodynamic Bethe Ansatz equations*, J. Stat. Mech. **1708** (2017) 083101, [arXiv:1701.08167 \[cond-mat.stat-mech\]](https://arxiv.org/abs/1701.08167).